The role of cytosolic calcium in potentiation of mouse lumbrical muscle

by

Ian Curtis Smith

A thesis
presented to the University of Waterloo
in fulfillment of the
thesis requirement for the degree of
Doctor of Philosophy
in
Kinesiology

Waterloo, Ontario, Canada, 2014

Author's Declaration

This thesis consists of material all of which I authored or co-authored: see Statement of Contributions included in the thesis. This is a true copy of the thesis, including any required final revisions, as accepted by my examiners.

I understand that my thesis may be made electronically available to the public.

Ian Curtis Smith

Statement of Contributions

Chapter II of this thesis was a joint effort of several co-authors, and this chapter is presented largely as published in:

> ©Smith I.C., Gittings W., Huang J., McMillan E.M., Quadrilatero J., Tupling A.R., Vandenboom R., 2013. Potentiation in mouse lumbrical muscle without myosin light chain phosphorylation: is resting calcium responsible? *Journal of General Physiology* 141(3):297-308. doi: 10.1085/jgp.201210918.

with only the following notable exceptions: 1) increased methodological detail 2) the addition of a figure depicting the cancellation of motion artifact 3) expanded description and depiction of the methods and results of the indo-1 experiments 4) the addition of supplementary data in the form of appendices. The inclusion of this article as part of this thesis is in accordance with the provisional license to publish signed with Rockefeller University Press (see Appendix 7). This study was conceived and designed by Ian Smith, William Gittings, Dr. Russell Tupling, and Dr. Rene Vandenboom. William Gittings, in the lab of Dr. Rene Vandenboom, collected extensor digitorum longus samples for myosin regulatory light chain phosphate content analysis. Dr. Jian Huang performed the analysis of myosin regulatory light chain phosphate content. Elliott McMillan, in the lab of Dr. Joe Quadrilatero, stained the muscle cross sections for fiber type analysis. Ian Smith, in the lab of Dr. Russell Tupling, performed all sample collection and data analysis not listed above. Drafting of the manuscript was performed by Dr. Rene Vandenboom and Ian Smith. Editing was performed by Ian Smith, William Gittings, Dr. Rene Vandenboom, and Dr. Russell Tupling.

Western blotting for sarcolipin and phospholamban, as found in Appendix 4, was performed by Val Fajardo.

All aspects of this thesis not listed above were authored by myself, Ian Smith.

Abstract

Following contractile activity, fast twitch skeletal muscle exhibits increases in submaximal force known as potentiation. Although there is no consensus on the purpose of potentiation, it is known to enhance power during rapid dynamic contractions and counteract the early stages of peripheral fatigue. Potentiation is primarily attributed to phosphorylation of the myosin regulatory light chain (RLC) through a calcium-mediated process which results in increased calcium-sensitivity of crossbridge formation. However, there is a growing body of evidence showing that potentiation can be achieved in the absence of RLC phosphorylation, albeit to a lesser degree. A secondary characteristic of the potentiated contraction is an acceleration of relaxation properties, which could be teleologically beneficial to enhance the cycling rate of rapid motions (e.g. running). However, accelerated relaxation is inconsistent with elevations in calcium-sensitivity as this would tend to slow the time course and slow relaxation. Therefore there are multiple mechanisms involved in potentiation, some of which enhance crossbridge formation, and some of which enhance crossbridge detachment. A possible explanation for these events involves contraction-induced changes in the intracellular cytosolic calcium signal that triggers muscle contraction. For example, elevations in submaximal force could be achieved by increasing the amplitude of the calcium signal while enhanced relaxation speed could be achieved by a shorter duration of the calcium signal. Thus the main objective of this thesis was to investigate the contribution of changes in cytosolic Ca^{2+} to force potentiation.

To achieve this objective, intact lumbrical muscles were extracted from the hind feet of C57BL/6 mice for use as the experimental model. The first study in this thesis examined cytosolic calcium signals during posttetanic potentiation using high (AM-fura-2 and AM-indo-1) and low (AM-furaptra) affinity calcium-sensitive fluorescent indicators to monitor resting

and peak calcium respectively, both before and after a potentiating stimulation protocol of 2.5 s of 20 Hz stimulation at 37^{o}C. This protocol resulted in an immediate 17±3% increase in twitch force (n=10; P<0.05), though this potentiation dissipated quickly, lasting only 30 s. Resting cytosolic Ca^{2+} was also increased following the potentiating stimulus as indicated by increases of 11.1 ± 1.3% and 8.1 ± 1.3% in the fura-2 and indo-1 fluorescence ratios respectively. Like the force potentiation, these increases were short lived, lasting 20-30 s. No changes were detected in either the amplitude or kinetics of the Ca^{2+} transients following the potentiating stimulus. Western blotting analysis of the myosin heavy chain isoforms which determine the contractile phenotype of lumbrical muscle revealed predominance of fast type IIX fibres, while immunohistochemical analysis of proteins important for relaxation, namely parvalbumin, sarco-endoplasmic reticulum Ca^{2+} ATPase (SERCA) 1a and SERCA2a, revealed that the expression of these proteins in lumbrical moderated those found in the soleus (slow) and EDL (fast) archetypes. Surprisingly, despite the fast phenotype of the lumbrical, it exhibited low expression of the skeletal muscle isoform of myosin light chain kinase, the enzyme responsible for phosphorylating the myosin RLC, and high expression of myosin targeting phosphatase subunit 2, the enzyme responsible for dephosphorylating the myosin RLC. These data were corroborated by a complete lack of myosin RLC phosphorylation in either the rested or potentiated states. It was thus concluded that elevations in resting cytosolic calcium concentration, in the absence of changes in the intracellular calcium transient and RLC phosphorylation, can potentiate twitch force.

The next objective of this thesis was to determine if there are changes in the cytosolic calcium transient during staircase potentiation, defined as a stepwise increase in twitch force during low frequency stimulation (<10 Hz). Staircase potentiation has been repeatedly

demonstrated to exhibit more robust potentiation than posttetanic potentiation in the absence of RLC phosphorylation. It was hypothesized that while the calcium transient is not altered during posttetanic potentiation, it may be an important potentiating factor in staircase due to the lower rest intervals between successive contractions. The effects of temperature on the intracellular calcium transient during staircase potentiation were also examined as part of this investigation. Here, lumbricals were loaded with AM- furaptra and then subjected to stimulation at 8 Hz for 8.0 s to induce staircase potentiation at either 30 or 37^{o}C. This stimulation protocol resulted in a 26.8 ± 3.2 % increase in twitch force at 37^{o}C ($P<0.05$) and a 6.8 ± 1.9 % decrease in twitch force at 30^{o}C ($P<0.05$) at the 8 s mark. Both the peak amplitude and the calcium-time integral of the calcium transient decreased during the first 2.0 s of the protocol ($P<0.05$), however these decreases were greater at 30^{o}C than 37^{o}C ($P<0.05$ amplitude; $P=0.09$ area). While peak amplitude remained low throughout the duration of the protocol, the calcium-time integral began to increase after the 2 s time point ($P<0.05$), a change reflective of the progressive increases in the 50% decay time and full width at half maximum of the calcium transient ($P<0.05$). Regression analysis of raw furaptra fluorescence ratios revealed a progressive decline in the peak amplitude of the calcium transients throughout the protocol which was not present at 37^{o}C. The increases in the duration of the calcium transient were mirrored by increases in the half relaxation time of the twitch contractions at both 30 and 37^{o}C, which had initially been reduced by ~20 and 9 % at 30 and 37^{o}C during the first 2 s of the protocol. Therefore the degree of staircase potentiation depends, in part, on the magnitude of the decline in the amplitude and the degree of slowing of the cytosolic calcium transient.

The declines in calcium transient amplitude noted above occurred simultaneously with increased rates of relaxation and abbreviated contraction times. To determine if there was a

causal relationship between the reduced amplitude and the faster contractions, AM-furaptra-loaded lumbrical muscles were stimulated at 8 Hz for 2 s in the presence and absence of caffeine, an agonist of the calcium release channel. Caffeine treatment attenuated the decline of the calcium transient amplitude ($P<0.05$), and was associated with greater potentiation at 37^{o}C ($P<0.05$), and attenuated force loss at 30^{o}C ($P<0.05$). Despite the increases in calcium and force, the relaxation times and rates of relaxation exhibited a greater acceleration following caffeine treatment ($P<0.05$). Therefore the relaxation-enhancing factor during potentiated twitches cannot be attributed to the calcium transient, and must be localized to changes on the myofilament. The case for inorganic phosphate as the effector is made.

Similar to the findings of the posttetanic potentiation study, the resting cytosolic calcium concentration was elevated during staircase potentiation, as revealed by fura-2 ratio signals. The largest increase occurring immediately following the first twitch of the protocol. This coincided with the largest increases in force potentiation at both 30 and 37^{o}C. This finding is in accordance with the initial conclusion that elevations in resting calcium can enhance twitch force and contribute to potentiation, though the mechanism of action is unclear. One possibility is that increases in resting calcium, sub-threshold for force production, can enhance the number of attached but non-force producing crossbridges, thereby accelerating the transition of crossbridges to force-producing states upon calcium-release following stimulation. To test this hypothesis, the resting stiffness, a measure of crossbridge attachment, of lumbrical muscles was examined before and after a potentiating stimulus of 20 Hz 2.5 s. Resting stiffness was assessed using sinusoidal length oscillations, ~0.5 nm per half sarcomere in amplitude and ranging in frequency from 10-200 Hz. Subsequent analysis revealed decreases in the elastic stiffness ($P<0.05$) that lasted for ~20 s which were greater in magnitude ($P<0.05$) than

increases in viscous stiffness which only lasted for ~5 s. This finding is consistent with the disappearance of short range elastic component (SREC) upon stretch or muscle activation which is commonly attributed to a population of stable, bound crossbridges in resting muscle. Subsequent analysis using imposed length changes to eliminate the SREC prior to contraction had no effect on the amplitude or duration of a subsequent twitch or tetanic contraction, and the changes in elastic and viscous stiffness of resting muscle were identical whether SREC was ablated by a contraction or imposed length change. Therefore it appears that potentiation occurs without an associated increase in bound crossbridges at rest, and may actually occur with fewer bound crossbridges at rest than the unpotentiated state. The lack of effect may be related to the relaxation-enhancing factor discussed above, and be an important feature of skeletal muscle serving to protect against damage via an involuntary eccentric contraction.

This thesis describes potentiation as a complex and important biological function which is the sum of factors that serve to enhance and oppose force production.

Acknowledgements

First and foremost, I thank my wife, Leslie Conlon, for keeping me grounded, being my sounding board, questioning my sanity, making me laugh, and so much more as I worked through this degree.

I also thank my supervisor, Dr. Russ Tupling for giving me the opportunity, freedom, encouragement, and support to broaden and advance my skill set. I am truly grateful for his mentorship and sage advice.

I must also acknowledge the hard work of others who contributed to the making of this thesis. William Gittings, for his insights into the design of the study in Chapter II, collecting EDL samples for myosin regulatory light chain phosphate content analysis, and for lending me his headlamp (for 3 years). Elliott McMillan and Dr. Joe Quadrilatero, for their help staining the cross-sections for fibre type analysis. Dr. Rene Vandenboom, for his contributions to the manuscript included in Chapter II, along with his guidance, expertise, and the opportunities he has helped me seize over the years. It is unfortunate that we have not yet met, but I thank Dr. Jian Huang and Dr. James Stull for their integral work measuring the myosin regulatory light chain phosphate content presented within this thesis; without these data, the rest of this work would be unintelligible. Val Fajardo, for his expertise in Western blotting for sarcolipin and phospholamban as found in Appendix 4.

Thank you to my co-workers and fellow students in the physiology department: to Dr. Eric Bombardier, Chris Vigna, Daniel Gamu and Val Fajardo for your frequent and timely support, criticism, advice, and help; and thank you to Andrew Mitchell, Elliott McMillan, Darin Bloemberg, Marie-France Pare, Rachelle Mariani, Anton Trinh, Karlee Hall, and Khanh Tran for letting me bounce ideas off you. More importantly, I thank you all for your friendship.

Marg Burnett, Jing Ouyang, Jeff Rice, Dawn McCutcheon, Nancy Gibson, Denise Hay, Ruth Gooding, Jenny Crowley, and Wendel Prime, I thank you all for your help and support in many different capacities. Dr. Howie Green, thank you for the many opportunities, and even more for your genuine enthusiasm for science and physiology. You are an inspiration.

Thank you to my family, Ron, Bernadette, Jennifer, and Pamela for your never-ending love and support.

Dedication

This work is dedicated to my wife, Leslie. She makes good cookies.

Table of Contents

List of Figures

List of Tables

List of Abbreviations

ADP – Adenosine diphosphate

α*Fs* – Fraction of crossbridges in the force producing state

AM – Acetoxymethyl

AMP – Adenosine monophosphate

ANOVA – Analysis of variance

ATP – Adenosine triphosphate

BDM - 2,3-butanedione monoxime

BIAM - Biotinylated-iodoacetamide

Ca^{2+} - Calcium

Ca_{50} – Ca^{2+} concentration required to achieve 50% of maximum enzyme activity

CaM – Calmodulin

CaMKII– Calcium/calmodulin dependent protein kinase type II

cAMP – Cyclic adenosine monophosphate

$[Ca^{2+}]_i$ –Intracellular cytosolic free Ca^{2+} concentration

Δ*F* – Force ripple – the change in force from peak to valley during unfused tetanus

-df/dt – Rate of force decay/relaxation

+df/dt – Rate of force production

DCLP – Dichroic long pass

DF – Discriminating filter

DLRP – Dichroic reflecting long pass

DMSO - Dimethyl sulfoxide

ECC – Excitation-contraction coupling

EDL – Extensor digitorum longus

EDTA - Ethylenediaminetetraacetic acid

f_{app} – Rate constant of the transition from the non-force producing state to the force producing state

FWHM – Full width at half maximum – a measure of Ca^{2+} transient duration

g_{app} - Rate constant of the transition from the force producing state to the non-force producing state

HEK – Human embryonic kidney

HRC - histidine rich Ca^{2+}-binding protein

HRP – Horse radish peroxidase

HSD – Honestly significant difference

IMP – Inosine monophosphate

ICT – Intracellular Ca^{2+} transient

K_d - Dissociation constant of the dye in an intact muscle preparation

kDa - kiloDalton

KO – Knock out

L_o – Optimum length for twitch force production

Lum – Lumbrical

LV – Left ventricle

Mg^{2+} - Magnesium

MHC – Myosin heavy chain

MYPT2 – Myosin phosphatase targeting subunit 2

NADPH - Nicotinamide adenine dinucleotide phosphate

Nox4 – NADPH oxidase 4

PAGE – Poly acrylamide gel elecrophoresis

PBS – Phosphate buffered saline

Pi – Inorganic phosphate

PCr - Phosphocreatine

PLN – Phospholamban

PKA – Protein kinase A

PKC – Protein kinase C

PMA - phorbol-12-myristate-13-acetate

PMT – Photomultiplier tube

PP1 – Protein phosphatase 1

PS – Potentiating stimulus

PTP – Posttetanic potentiation

RLC – Myosin regulatory light chain

1/2RT – 50 % relaxation time

90%RT – 90% relaxation time

Q_{10} – Temperature coefficient

S – Stimulation

S/R-L – Slack/re-lengthening protocol

SDS – Sodium dodecyl sulfate

SEM – Standard error of the mean

SERCA – Sarco/endoplasmic reticulum calcium adenosine triphosphatase

skMLCK – Skeletal muscle isoform of myosin light chain kinase

SLN – Sarcolipin

Sol - Soleus

SR – Sarcoplasmic reticulum

SREC – Short range elastic component

TnC – Troponin C

TPT – Time to peak tension

UV – Ultraviolet

V_{max} – Maximum rate of enzyme activity

WB – Wide band

WT – Wild type

XBr - Crossbridge

Chapter I - Introduction, review of the literature and statement of the problem

Introduction and review of the literature

Cytosolic calcium (Ca^{2+}) is a key regulator of mechanical events in skeletal muscle. Precise control over the force, duration and speed of a contraction in striated skeletal muscle is dependent on controlling the size and duration of the Ca^{2+} signal as well as the sensitivity of the contractile proteins to this signal. In skeletal muscle, force is thick filament based but thin filament regulated (reviewed in Gordon *et al.*, 2001;Gordon *et al.*, 2000). In the absence of Ca^{2+}, tropomyosin blocks strong binding sites on actin in the thin filament (McKillop & Geeves, 1993). The troponin complex anchors tropomyosin in place through binding of troponin I to two adjacent actin proteins (Gordon *et al.*, 2000). Depolarization of the sarcolemma activates voltage-gated Ca^{2+} channels which are mechanically coupled to calcium channels in the membrane of the sarcoplasmic reticulum (SR), causing these channels to open and release Ca^{2+} (Meissner & Lu, 1995). When Ca^{2+} binds to the two low-affinity Ca^{2+} binding sites on troponin C (TnC), the interaction between TnC and troponin I (TnI) becomes stronger, which weakens the interaction between TnI and actin, and the position of tropomyosin becomes more dynamic, periodically exposing strong binding sites on actin (Gordon *et al.*, 2001;Potter & Gergely, 1975). Myosin heads protruding from the thick filament are then able to bind to actin and undergo the powerstroke, thereby producing mechanical force and displacement (Gordon *et al.*, 2000). In the absence of fatigue, the force per crossbridge can be considered relatively constant, while the number of crossbridges formed determines the force actively produced within a single muscle fibre (Sweeney & Stull, 1990). Since tropomyosin is flexible, the binding of a single myosin head increases the likelihood of other myosin heads binding by pushing tropomyosin away from binding sites on neighbouring actin proteins, resulting in cooperativity of force production (Maytum *et al.*, 1999). The presence of strongly

bound myosin also enhances Ca^{2+} binding to the TnC. This has been demonstrated during rapid shortening experiments performed by Vandenboom *et al.* (1998) who report increases in cytosolic Ca^{2+} at the onset of rapid shortening which are followed by decreases in cytosolic Ca^{2+} at the cessation of shortening, the amplitude of each was related to the shortening amplitude. In contractions with rapid shortening, the rate limiting step in crossbridge cycling is the dissociation of adenosine diphosphate (ADP) following the power stroke (Siemankowski *et al.*, 1985). As the rate constant for this step is relatively fast, shortening contractions are associated with a low number of crossbridges in force producing states even at saturating concentrations of cytosolic Ca^{2+} (Vandenboom *et al.*, 2002), thus allowing rapid cycling of Ca^{2+} on and off of TnC. However, in a loaded contraction the rate limiting step is the strain sensitive isomerization of the myosin head as it transforms from the pre to post power stroke position (Huxley, 1957;Goldman, 1987;Gordon *et al.*, 2001). The external load resists filament motion necessary to complete this isomerization, resulting in a large proportion of myosin heads in force producing states and greater force production, and Ca^{2+} remains bound to TnC as TnI is prevented from anchoring to actin, thereby slowing the cycling of Ca^{2+} on and off of TnC (Gordon *et al.*, 2000).

During rapid contractions, i.e. those of short duration such as a twitch contraction, the release of Ca^{2+} from the SR does not fully activate the thin filament, nor does it allow for full tetanic contraction. Thus the force produced by a twitch contraction is sensitive to the speed of crossbridge formation as faster crossbridge formation takes advantage of the cooperative mechanisms discussed earlier. Fast-twitch skeletal muscle has developed regulatory mechanisms that allow it to increase the rate of crossbridge binding, allowing either more force

production if the activating Ca^{2+} signal is unchanged, or force to be maintained with a lower activating Ca^{2+} signal. This process is known as force potentiation.

Force potentiation and myosin regulatory light chain phosphorylation

Potentiation of force refers to an increase in twitch force following previous non-fatiguing activity. Physiologically, the potentiation is thought to play a role in delaying the symptoms of fatigue (Gittings *et al.*, 2011;Gordon *et al.*, 1990;Stull *et al.*, 2011), and enhancing contractile performance during dynamic contractions (Caterini *et al.*, 2011;Vandenboom *et al.*, 1997;Sweeney *et al.*, 1993;Grange *et al.*, 1993), but may also increase the energetic costs of contractile activity (Abbate *et al.*, 2001). The best characterized mechanism causing potentiation of force is the introduction of a phosphate group on the regulatory light chain (RLC) found on the neck region of the myosin head (reviewed in Stull *et al.*, 2011;Sweeney *et al.*, 1993). In striated muscle of vertebrates, and some invertebrates RLC phosphorylation acts as a molecular switch serving to enhance contractility (Sweeney *et al.*, 1993;Stull *et al.*, 2011;Vandenboom *et al.*, 2013;Brito *et al.*, 2011;Tohtong *et al.*, 1995). In contrast, in vertebrate smooth muscle, some invertebrate striated muscle, and non-muscle cells, force regulation occurs at the thick filament and RLC phosphorylation is required for crossbridge activation (Stull *et al.*, 1996). In vertebrate skeletal muscle, RLC phosphorylation is a Ca^{2+} mediated process in which Ca^{2+} released from the sarcoplasmic reticulum (SR) binds to calmodulin (CaM), activating it and allowing it to bind to the skeletal muscle isoform of myosin light chain kinase (skMLCK). The binding of Ca^{2+}-CaM to skMLCK relieves autoinhibition, freeing up the catalytic site on skMLCK allowing entry of the N-terminus of the RLC (Gao *et al.*, 1995). Serine 15 of the RLC is then phosphorylated in an adenosine triphosphate (ATP)-dependent reaction (Gao *et al.*, 1995). The introduction of the phosphate

group on the RLC causes a shift in the average position of the myosin heads closer to the thin filament (Levine *et al.*, 1996;Yang *et al.*, 1998). This increases the chances of the myosin head interacting with the myosin binding sites on the thin filament, allows crossbridges to form more quickly, and results in higher forces at submaximal levels of Ca^{2+}-dependent thin filament activation (Sweeney & Stull, 1990).

The two state mathematical model of force asserts that force is proportional to the fraction of crossbridges in force producing states (αFs), which is calculated according to Equation 1 (Huxley, 1957;Brenner & Eisenberg, 1986;Brenner, 1988).

Equation 1:

$$\alpha Fs = f_{app} / (f_{app} + g_{app})$$

Here, f_{app} is the rate of transition of a crossbridge from a non-force-producing state to a force producing state, while g_{app} is the rate of transition of a crossbridge from a force-producing state to a non-force producing state. For example, at rest, f_{app} is very low as tropomyosin blocks access to myosin binding sites, thus αFs and force are very low. During an isometric tetanic contraction, TnC is near fully bound by Ca^{2+}, freeing up myosin binding sites on the thin filament and increasing f_{app}. The tension on the crossbridges slows the rate of crossbridge detachment, reducing g_{app}. Thus αFs and force are high due to the dominance of f_{app} over g_{app} in the denominator of Equation 1.

The freedom of motion in the myosin heads caused by RLC phosphorylation increases f_{app} but has no effect on g_{app}, resulting in enhancements in αFs and force with the greatest effects seen at low forces (Sweeney & Stull, 1990). This occurs because at high forces, the

RLC-phosphate mediated increase in f_{app} is insignificant due to the already high value for f_{app} relative to g_{app}. However, as force and αFs decrease, the ratio of g_{app} to f_{app} increases, and the increase in f_{app} caused by RLC phosphorylation become a progressively more important determinant of αFs and force, resulting in force potentiation (Sweeney & Stull, 1990).

RLC phosphorylation is reversed in skeletal muscle by myosin phosphatase (Morgan *et al.*, 1976;Stull *et al.*, 2011), which consists of myosin phosphatase-targeting subunit 2, the catalytic domain of protein phosphatase 1C and a small 20 kDa subunit (Moorhead *et al.*, 1998;Grassie *et al.*, 2011;Stull *et al.*, 2011). The peak rate of RLC phosphorylation is 70% slower than the peak rate of contraction, while the peak rate of RLC dephosphorylation is less than 10% of the peak rate of relaxation and 25% of the peak rate of RLC phosphorylation (reviewed in Stull *et al.*, 2011;Sweeney *et al.*, 1993). This slow rate of dephosphorylation provides the biochemical memory which allows RLC phosphorylation to continue building even after the muscle has relaxed, which can lead to potentiation building over time of muscle inactivity (reviewed in Stull *et al.*, 2011).

Temperature dependency of potentiation

The duration of potentiation is temperature dependent, with potentiated twitch force lasting up to 10 minutes at 25^{o}C (Smith *et al.*, 2010;Moore *et al.*, 1990), and 2 minutes or less at 35^{o}C (Moore *et al.*, 1990). The magnitude of potentiation is also temperature dependent, with greater potentiation seen at higher temperatures (Moore *et al.*, 1990;Krarup, 1981). This effect can also be explained using equation 1, as twitch force decreases as temperature increases with no effect seen on tetanic force (Moore *et al.*, 1990). This means that αFs is lower during the twitch at high temperatures, and by using the same rationale as above, the

twitch represents a lower state of activation at high temperatures and potentiation has a greater effect.

Length dependency of potentiation

Potentiation is also a length dependent process (Rassier & MacIntosh, 2002) which is related to spacing between the thick and thin filaments (Levine *et al.*, 1996;Yang *et al.*, 1998;Rassier & MacIntosh, 2002). As the length of the fibre increases, the spacing between the filaments decreases (reviewed in Millman, 1998). Since the mechanism of RLC phosphorylation is a movement of the myosin head closer to the thin filament, decreasing lattice spacing is mechanistically redundant with RLC phosphorylation, as their contribution to f_{app} is non-additive. Similar results have been found using osmotic compression of the myofilament lattice using dextran (Yang *et al.*, 1998).

Fibre type dependency of potentiation

There are distinct differences in potentiation seen between fast and slow twitch fibre types. The most notable difference is that slow twitch fibres exhibit very little potentiation (Ryder *et al.*, 2007;Moore *et al.*, 1985;Moore & Stull, 1984) and can exhibit post-tetanic depression of twitch force (Buller *et al.*, 1981). Slow twitch muscle requires more intense stimulation for longer periods of time to induce noticeable RLC phosphorylation (Crow & Kushmerick, 1982;Moore & Stull, 1984), they have higher expression and activity of myosin phosphatase (Ryder *et al.*, 2007;Moore & Stull, 1984), and they have lower skMLCK expression (Ryder *et al.*, 2007;Moore & Stull, 1984). Ryder *et al.* (2007) have shown that over-expression of skMLCK in mouse soleus, which is predominantly type I and IIA fibres (Augusto *et al.*, 2004;Bloemberg & Quadrilatero, 2012), results in robust RLC

phosphorylation, but this yielded only 23% potentiation of force versus 11% in wild type soleus. In contrast, EDL muscle, which is predominantly IIX and IIB fibres (Smith *et al.*, 2010;Gittings *et al.*, 2011;Augusto *et al.*, 2004;Bloemberg & Quadrilatero, 2012), exhibited over 50% potentiation in both the skMLCK over-expressing and wild type lines (Ryder *et al.*, 2007). Parry and DiCori (1990) suggest that the differences in potentiation between fast and slow muscle may lie in the specific isoform of the RLC expressed. EDL contains only the fast light chain isoform, but in soleus, virtually all fibres that exclusively expressed the MHC IIa isoform expressed a combination of fast and slow RLC isoforms. Their functional measures support this idea as stimulation of isolated motor units of mouse EDL via the dorsal root results in a linear relationship where lower time to peak tension results in a greater degree of potentiation, but in soleus, 75% of motor units did not potentiate at all, despite only 50% of fibres being classified as type I (Parry & DiCori, 1990).

Methods of studying potentiation in isometric contractions

While any contraction lasting longer than a single twitch will have some degree of potentiation, protocols have been developed for research purposes which maximize the quantifiable effects of potentiation, as it can be easily masked by fatigue (Rassier & MacIntosh, 2000;Fowles & Green, 2003;MacIntosh & Gardiner, 1987;Vandenboom & Houston, 1996). The most common of these are posttetanic potentiation (PTP) and staircase potentiation. PTP protocols involve measurement of single twitches after a prolonged period of inactivity or very low duty cycles (<1%) followed by a conditioning stimulus, usually consisting of a single or series of brief tetanic contractions that elicit as little fatigue as possible. Twitches in the seconds and minutes following the tetanic contraction(s) are potentiated and exhibit higher force, increased peak rates of force production, faster time to

peak tension as well as faster relaxation times and peak rates of relaxation (Smith *et al.*, 2010;Vandenboom *et al.*, 1995). Staircase potentiation involves a series of twitches given in rapid succession, usually at a stimulation rate of 5-10 Hz, such that there is sufficient time for full relaxation of force between successive twitches. In these protocols there is typically an increase in force production (Zhi *et al.*, 2005;MacIntosh *et al.*, 2008;Ryder *et al.*, 2007), and the same kinetic changes as those seen in PTP (Krarup, 1981).

Potentiation without regulatory light chain phosphorylation

While the magnitudes of both PTP (Vandenboom *et al.*, 1997;Tubman *et al.*, 1997) and staircase potentiation (Tubman *et al.*, 1996) are typically graded to the proportion of phosphorylated RLC, it is apparent that there are separate but complimentary mechanisms working in staircase protocols that are unseen during PTP protocols. It is well established that staircase potentiation can occur under treatments where PTP is entirely absent , and that staircase potentiation can occur without an associated increase in RLC phosphorylation (Zhi *et al.*, 2005;MacIntosh *et al.*, 2008;Rassier *et al.*, 1999;Rassier *et al.*, 1997;Gittings *et al.*, 2011). Using skMLCK null mice generated through disruption of the encoding *MYLK2* gene, Zhi *et al.* (2005) found that PTP was entirely absent, but attributed ~55% of staircase potentiation (15s at 10 Hz) in EDL to RLC phosphorylation, with the remaining 45% attributable to other mechanisms which are currently unknown but may be attributable to changes in Ca^{2+} signaling. However, it is known that this mechanism is more effective at low levels of acto-myosin activation (i.e. low αFs), as Rassier *et al.* (1997;1999) demonstrated that tetrodotoxin-denervated and atrophied rat gastrocnemius muscles do not exhibit increases in RLC phosphorylation, exhibit a high twitch to tetanus ratio (i.e. a high αFs), have no staircase response. However, when Ca^{2+}-release was attenuated in these animals using dantrolene,

staircase potentiation became evident (Rassier *et al.*, 1999;Rassier *et al.*, 1997). MacIntosh *et al.* (2008) also report that following spinal hemisection, staircase potentiation in rat gastrocnemius is normal, but PTP is absent following a conditioning stimulus of 200 Hz for either 100 or 500 ms and PTP is attenuated by 75% following a 1 s potentiating stimulus at 200 Hz, all without RLC phosphorylation. Therefore there must be mechanisms which can potentiate force in the absence of RLC phosphorylation, though none have been empirically examined.

Clues to the nature of the mechanism(s) may come from observations of small, though non-significant, increases in twitch force seen in the twitch tracings and averaged data of several papers (Zhi *et al.*, 2005;Gittings *et al.*, 2011;Stull *et al.*, 2011) examining PTP in skMLCK-null mice, along with noticeably faster contraction times in the potentiated state, reminiscent of those seen during the typical potentiation response caused by RLC phosphorylation. It is therefore possible that the time between the conditioning stimulus and measurement of potentiated twitch is a very important factor, where the RLC-P independent pathway has a faster inactivation time than the RLC-P dependent pathway, making it effectively invisible during PTP, which is typically measured 20 s following the potentiating stimulus, but plain to see during staircase protocols where the twitch stimulations are themselves the potentiating stimuli.

Potential alternative mechanism(s) of potentiation

Potential explanations for potentiation and the associated faster twitch kinetics occurring in the absence of RLC phosphorylation must involve one or both of a change in the Ca^{2+} signal triggering contraction and a non-RLC phosphorylation- mediated sensitization of

the contractile proteins. Increasing the rate of Ca^{2+} uptake could explain the faster relaxation times seen in potentiated muscle, but this would result in lower force and should therefore be a secondary but important effect. Increased resting cytosolic Ca^{2+} could also be playing a role to increase force as cytosolic Ca^{2+} buffers would become more saturated resulting in greater Ca^{2+} binding to TnC, resulting in faster rates of force production and elevated force. Recent evidence (published after Chapter II of this thesis) demonstrates that resting Ca^{2+} is indeed elevated above basal levels for tens of seconds following a contraction via the Ca^{2+}-sequestering activities of parvalbumin maintaining Ca^{2+} in the cytosol for extended periods of time (Hollingworth & Baylor, 2013). However, an increase in resting Ca^{2+} cannot be the lone factor as this should cause an increase in force with each and every consecutive twitch, rather than the progressive decline in twitch force seen during the first 1 s of stimulation before twitch force begins to rise (see Zhi *et al.*, 2005;Krarup, 1981). This drop is independent of the effects of RLC-P, as it appears almost identical between wild type (WT) and skMLCK null animals (Zhi *et al.*, 2005). This force declining phase is characterized by a progressive decline in the time to half relaxation (1/2RT) until reaching a plateau, and then reversing course and becoming longer (Krarup, 1981). Furthermore, reductions in 1/2RT following a potentiating stimulus are not correlated with the degree of posttetanic potentiation (Hamada *et al.*, 2000). This lends credence to the idea that mechanisms causing potentiation without RLC phosphorylation is most likely regulated via Ca^{2+} or metabolite accumulation and affects both Ca^{2+} uptake rates and Ca^{2+} release rates, as 1/2RT should not decrease without a corresponding increase in Ca^{2+} uptake. If there is faster uptake, then there should also be greater Ca^{2+} release or an increase in resting Ca^{2+} as a countermeasure to maintain or potentiate force. There is evidence that peak cytosolic Ca^{2+} increases during repetitive tetanic contractions in both mouse

(Westerblad & Allen, 1991;Dahlstedt *et al.*, 2000) and amphibian muscle (Allen *et al.*, 1989). However, this appears to only occur in fast twitch muscle and may be mediated by inorganic phosphate (Pi) as soleus muscle and fast-twitch flexor digitorum brevis of creatine kinase-null mice, neither of which exhibit increases in Pi during repeated contraction, do not exhibit such increases in tetanic concentrations of cytosolic Ca^{2+} (Bruton *et al.*, 2003;Dahlstedt *et al.*, 2000). It has been suggested that the elevations in cytosolic Ca^{2+} during repeated tetani may be more related to inhibition of Ca^{2+} pumping than increased Ca^{2+} release (reviewed in Allen *et al.*, 2008).Thus the potentiation and changes in twitch kinetics seen in slow twitch muscle with repeated activation (Ryder *et al.*, 2007;Buller *et al.*, 1981;Tupling, 2009) must either be caused by another mechanism, or the observations of changes in tetanic Ca^{2+} are fundamentally different than those caused by single twitch contractions.

Regulation of the action potential

Ca^{2+} release during a contraction protocol is ultimately triggered by the action potential. Ca^{2+}-CaM dependent activity of protein kinase C (PKC) can phosphorylate the voltage-gated Ca^{2+} channel *in vitro* (O'Callahan *et al.*, 1988;Ma *et al.*, 1992), but it appears that neither PKC nor any other Ca^{2+}-activated kinase phosphorylates this channel in intact muscle (Mundiña-Weilenmann *et al.*, 1991). Consistent with this, action potentials are characteristically similar during bouts of repetitive stimulation in isolated skeletal muscle, particularly over short durations (Hanson, 1974) and an ionic cause of potentiation has already been ruled out (reviewed in Vandenboom *et al.*, 2013). Therefore the mechanism must be a change in a downstream signal.

Regulation of Ca^{2+} release

The Ca^{2+} release channel of skeletal muscle is a 560 kDa homotetramer and is often referred to as the ryanodine receptor type 1 (RyR) (Meissner, 2004) . It is normally bound to the SR proteins, triadin, junctin, and calsequestrin which together serve as a luminal Ca^{2+} sensor (Györke *et al.*, 2004). While the amount of Ca^{2+} released per stimulus can decrease when luminal Ca^{2+} loads are low, the amount of Ca^{2+} release per stimulus is not known to increase if the Ca^{2+} load is increased above normal values (Posterino & Lamb, 2003), as the elevated levels of Ca^{2+} in the junctional gap inactivate the release channel, abbreviate the action potential, and deactivate the voltage gated ion channels (Allen *et al.*, 2008;Meissner, 1984;Franzini-Armstrong & Protasi, 1997;Schneider & Simon, 1988;Simon *et al.*, 1991). This causes the Ca^{2+} released during repeated, closely spaced contractions to decrease in skinned fibre preparations (Posterino & Lamb, 2003;Barclay, 2012).

Ca^{2+} can bind directly to the Ca^{2+}-release channel (Prosser *et al.*, 2011), an effect which modifies the affinity of the Ca^{2+}-release channel for the Ca^{2+} binding proteins CaM and S100A1which compete for the same binding sites located adjacent to sites of RyR subunit-subunit interactions (Prosser *et al.*, 2011;Fuentes *et al.*, 1994;Tripathy *et al.*, 1995;Cornea *et al.*, 2009;Zhang *et al.*, 2003). However, CaM and S1001A are thought to have the same effect, but with greater binding of CaM when it is Ca^{2+} bound and greater binding of S1001A when it is Ca^{2+}-free. Ca^{2+}-free CaM and S100A1 bound to the RyR exert an activating influence on Ca^{2+} release (Tripathy *et al.*, 1995;Prosser *et al.*, 2011). At high cytosolic concentrations of Ca^{2+}, Ca^{2+} binds to S1001A and CaM, and their effect becomes inhibitory to Ca^{2+} release (Fuentes *et al.*, 1994;Prosser *et al.*, 2011). This inhibition can occur without dissociation of either CaM or S1001A from the binding site (Tripathy *et al.*, 1995;Cornea *et al.*, 2009) with

the differences in RyR activation being caused by subtle changes in the CaM-RyR interactions upon Ca^{2+} binding (Cornea *et al.*, 2009). Regardless of the mechanism, the one thing that is clear is that high cytosolic Ca^{2+} has an inhibitory influence on RyR Ca^{2+} release, though this may only be important during the course of each transient, and have minimal effect on repeated contractions.

Similarly, many of the metabolic effects associated with repetitive activity, including ATP depletion and increased cytosolic concentrations of magnesium (Mg^{2+}), Pi, adenosine monophosphate (AMP), ADP and inosine monophosphate (IMP), have an inhibitory effect on Ca^{2+} release (reviewed in Tupling, 2004;Allen *et al.*, 2008). This would lead to progressively lower Ca^{2+} release with each contraction as ATP is utilized and Mg^{2+} concentrations increase. It is noteworthy that both AMP and ADP are actually activators of the Ca^{2+}-release channel, but they are less potent activators than ATP and compete for the same binding sites, resulting in a net inactivation (Meissner, 1984;Allen *et al.*, 2008).

The RyR is normally stabilized by a small cytosolic protein known as FK506 binding protein, or FKBP12 which is not known to dissociate from the RyR outside of immunosuppression treatment with FK506 (Franzini-Armstrong & Protasi, 1997). FKBP12 is a target of the quickly activated Ca^{2+}-CaM-dependent phosphatase, calcineurin, in cardiac muscle. This interaction has an inhibitory effect on Ca^{2+} channel opening (Bandyopadhyay *et al.*, 2000). It is not clear if this calcineurin effect also occurs in skeletal muscle, but if so, it would lead to progressive reductions in Ca^{2+} release.

SR Ca^{2+}-release is activated by the SR-bound enzyme NADPH oxidase 4 (Nox4). Nox4 is an oxygen sensing enzyme that produces superoxide in proportion to cellular oxygen levels,

which is then converted to hydrogen peroxide, which activates the Ca^{2+}-release channel (Sun *et al.*, 2011). However, oxygen levels decrease during stimulation, which would result in less Nox4 activity and inactivation of the release channel. Mitochondrial production of hydrogen peroxide via xanthine oxidase activation is not an effective activator of the Ca^{2+} release channel (Sun *et al.*, 2011).

The Ca^{2+}-release channel needs to be phosphorylated to function with even resting levels of Mg^{2+} in the cytosol (Franzini-Armstrong & Protasi, 1997;Hain *et al.*, 1994). Herrmann-Frank and Varsánya (1993) reported phosphorylation of RyR by a protein kinase that is not Ca^{2+}-CaM dependent protein kinase II (CaMKII) that enhances the open probability. However, the source of this phosphorylation is the cause of great controversy. Wang and Best (1992) reported phosphorylation of the RyR by what they stated was probably but not definitively CaMKII reducing the open probability of the channel. Since then multiple studies have disproven the theory that CaMKII was the effecting enzyme, as endogenous CaMKII cannot directly phosphorylate the RyR of skeletal muscle (reviewed in Sacchetto *et al.*, 2005). It can, however, phosphorylate the cytosolic domain of triadin and further enhance its inhibitory effect on RyR in a Ca^{2+} dependent manner (Colpo *et al.*, 2001). CaMKII may also phosphorylate the histidine rich Ca^{2+}-binding protein (HRC) (Sacchetto *et al.*, 1999), which interacts with triadin (Sacchetto *et al.*, 1999) and inhibits both Ca^{2+} release and Ca^{2+} uptake (Arvanitis *et al.*, 2011). However, evidence is mounting against a role of CaMKII in phosphorylating HRC due to localization of HRC to the lumen and CaMKII to the cytosol (reviewed in Arvanitis *et al.*, 2011). The function of HRC phosphorylation has not been established (Arvanitis *et al.*, 2011).

Studies using inhibitors of CaMKII offer support that CaMKII is important for the maintenance of Ca^{2+} release during exercise. Cardiac myocytes treated with the CaMKII inhibitor KN-93 during β-adrenergic stimulation results in an increased time to peak Ca^{2+} as well as decreased amplitude of the Ca^{2+} transient (Roof *et al.*, 2011;Curran *et al.*, 2007). In isolated single fibres of mouse flexor digitorum brevis, a fast twitch muscle, repetitive 70 Hz contractions leads to ~50% increases in peak Ca^{2+} concentrations within 10-15 contractions at contraction intervals between 0.1 and 2 s (Aydin *et al.*, 2007). KN-93 treatment of these same fibres led to reductions in the peak Ca^{2+} concentration of ~40% over this same interval. Force development over this period was reduced by ~20% in control and 60% in KN-93 treated fibres (Aydin *et al.*, 2007). Similar results were found when they used an inhibitory peptide which mimics CaMKII substrate (Aydin *et al.*, 2007). Therefore it seems that maintenance of force in fast twitch muscle fibres during repetitive contractions is dependent on CaMKII activation and subsequent activation of Ca^{2+} release proteins via some unidentified pathway which is more potent than the inhibitory pathways described above and thus CaMKII activity may enhance Ca^{2+} release during repetitive contractions and contribute to potentiation. Further supporting this idea, Aydin *et al.* (2007) found no differences in either Ca^{2+} or force during the first four contractions seen when muscles were treated with KN-93, or during contractions with long intervals between successive stimuli (70 Hz for 350 ms at 5 s intervals). Consistent with this finding, the protocol used by Gittings *et al.* (2011) to induce PTP in skMLCK KO mice was a series of 4 150 Hz stimulations lasting 400 ms each, spaced 4.5 s apart. This is just slightly more intense than the rough threshold established by Aydin *et al.* (2007) where there was no CaMKII activation between successive contractions (70 Hz 350 ms tetani spaced 5 s

apart), thus it is possible that the potentiation occurring without RLC phosphorylation is mediated by CaMKII.

Regulation of Ca^{2+} Uptake

A common, but non-essential and frequently disregarded component of the potentiated twitch response is the increase in relaxation rate and reduction in relaxation time that coincides with the elevations in force. This enhancement of relaxation seen in repeated contractions has been attributed to an increase in the rate of Ca^{2+}-uptake (Tupling, 2009;Vøllestad *et al.*, 1997), though this hypothesis has never been tested. Consistent with this hypothesis, there are myriad exercise dependent factors which could enhance the rate of Ca^{2+} uptake by the sarco/endoplasmic reticulum Ca^{2+}-ATPase (SERCA).

SERCA is a 110 kDa protein that transports Ca^{2+} from the cytosol to the lumen of the SR, at an optimal pumping ATP cost of 2 Ca^{2+}/1 ATP (reviewed in Tupling, 2009). It serves as the primary means of maintaining Ca^{2+} homeostasis in skeletal muscle and an important facilitator of muscle relaxation (MacLennan *et al.*, 1997), in conjunction with parvalbumin in fast twitch muscle (Carroll *et al.*, 1997;Hollingworth *et al.*, 1996;Hou *et al.*, 1993). Two isoforms predominate in skeletal muscle; SERCA1a in fast-twitch muscle and SERCA2a in slow twitch muscle (Wu & Lytton, 1993). Although SERCA is necessary for reloading the SR following Ca^{2+} release in all fibre types, it is not the primary means of relaxation in the fast twitch muscle of the mouse or rat. This role belongs to the cytosolic Ca^{2+}-binding protein parvalbumin (Carroll *et al.*, 1997). Electrical stimuli applied in quick succession results in progressively decreasing rates of Ca^{2+} signal decay as parvalbumin and other cytosolic Ca^{2+} buffers become saturated and the rate of decline starts to more closely match the rate of Ca^{2+}

uptake by SERCA, making parvalbumin an important consideration when measuring the rate of Ca^{2+} decline in intact fast twitch muscles (Hollingworth *et al.*, 1996).

During repetitive stimulation SERCA can be activated to increase its rate of Ca^{2+} transport. There is, however, little evidence that SERCA proteins are a direct target of Ca^{2+}/CaM mediated regulation. Although CaMKII cannot directly phosphorylate SERCA1a, it has been shown to directly phosphorylate and increase the maximum rate of Ca^{2+} uptake of SERCA2a (Hawkins *et al.*, 1994), though this could not be confirmed in SERCA2a expressing HEK-293 cells and remains controversial (Odermatt *et al.*, 1996). Similarly the activation of SERCA is not due to metabolite accumulation, as Ca^{2+} uptake is inhibited by Pi and ADP (Stienen *et al.*, 1993;MacDonald & Stephenson, 2001;Duke & Steele, 2001b;Dawson *et al.*, 1980), though high levels of IMP and Mg^{2+} have no effect (Blazev & Lamb, 1999a). Rather, SERCA can be activated through phosphorylation of the accessory proteins phospholamban and sarcolipin, or through redox regulation (reviewed in Tupling, 2009).

Phospholamban

Phospholamban (PLN) is a small 6.1 kDa transmembrane protein of the SR, 52 amino acids long (Fujii *et al.*, 1987). Amino acids 31-52 make up the transmembrane domain which serves as the inhibitory region of PLN while amino acids 1-30 project into the cytosol and contain the regulatory sites of the enzyme (MacLennan & Kranias, 2003). PLN reversibly inhibits Ca^{2+} transport by both SERCA1a and SERCA2a by reducing the apparent affinity of SERCAs for Ca^{2+} (i.e. a higher Ca_{50}) while having little effect on the maximum activity (V_{max}) of the enzymes (Mahaney *et al.*, 2000). Although PLN interacts with both fast and slow isoforms of SERCA (Toyofuku *et al.*, 1993), and it is expressed ubiquitously in mouse skeletal

muscle, it is more highly expressed in slow twitch muscle than fast twitch muscle (Tupling lab; unpublished observations). PLN expression is higher in human muscle than mouse muscle, but like mice, it is more highly expressed in type I and IIA fibres than type IIX fibres (Fajardo *et al.*, 2013). Under normal resting conditions, PLN is found bound to SERCA in the dephosphorylated state (James *et al.*, 1989). When PLN is phosphorylated, or Ca^{2+} is bound to SERCA, the inhibitory effect of PLN on SERCA activity is relieved (Toyoshima *et al.*, 2003). PLN which is not bound to SERCA is primarily phosphorylated and forms homopentamers which do not interact with SERCA (Fujii *et al.*, 1987). PLN can be phosphorylated by two different pathways, one via β-adrenergic stimulation and the other via activity dependent CaMKII activation, while PLN dephosphorylation is caused by protein phosphatase 1 (PP1) and calcineurin (MacLennan & Kranias, 2003).

While β-agonist-mediated phosphorylation of PLN is not expected to be a factor in the isolated muscle preparations typically used to study potentiation, it has important implications *in vivo*. This pathway is initiated by stimulation of the β_1-adrenergic receptors, but can also occur with β_2-adrenergic stimulation in cardiac muscle (Slack *et al.*, 1997). Upon activation of the β-adrenergic receptor, G-α_s protein is activated which in turn activates adenylate cyclase, inducing the formation of cAMP. Protein kinase A (PKA) is activated by cAMP and PKA phosphorylates serine 16 on the cytosolic domain of phospholamban, freeing SERCA from its inhibitory influence and increasing the effective rate of Ca^{2+} uptake (reviewed in MacLennan & Kranias, 2003).

The activity dependent pathway of PLN phosphorylation occurs through activation of CaMKII. Here, Ca^{2+} enters the cytosol from the SR and binds to calmodulin which in turn binds to and activates CaMKII, which can then phosphorylate other CaMKII subunits leading

to further activation (Chin, 2005). Activated CaMKII phosphorylates threonine 17 on the cytosolic domain of PLN. However, phosphorylation of serine 16 on PLN in hearts may be a necessary prerequisite as substituting serine with alanine in the 16 position results in no phosphorylation of threonine 17 during activity in heart muscle, but replacing threonine 17 with alanine results in normal responses to β-adrenergic stimulation by isoproterenol (MacLennan & Kranias, 2003). Conversely, Hagemann *et al.* (2000) report phosphorylation of threonine 17 in electrically paced myocytes independent of serine 16 phosphorylation, thus an alternative interpretation of these findings could be that a negative charge at the 16 position is necessary for CaMKII phosphorylation of threonine 17.

Ca^{2+}-CaM-dependent protein kinase C (PKC) activity may also be important in regulation of PLN. Although mechanisms of PKC activity in skeletal muscle excitation-contraction coupling are not well established, current literature from both cardiac and skeletal muscle suggests that PKC inhibits Ca^{2+} uptake (Duhamel, 2007;Braz *et al.*, 2004;Capogrossi *et al.*, 1990), while having no direct effect on Ca^{2+}-release (Herrmann-Frank & Varsánya, 1993). Supporting the idea that PKC activity inhibits SR Ca^{2+}-uptake, hearts of PKC-α null mice exhibit enhanced Ca^{2+} transients, hyperphosphorylation and reduced expression of PLN and greater SR Ca^{2+} load (Braz *et al.*, 2004). Similarly PKC-α over-expressing mice exhibit impaired contractility and high levels of PLN with little phosphorylation (Braz *et al.*, 2004). In skeletal muscle, enriched SR fractions from rat skeletal muscles of varying fibre types with the PKC activator phorbol-12-myristate-13-acetate (PMA) exhibit a left shift in the Ca_{50}, and a reduction in the Hill slope (Duhamel, 2007). Contrary to a role in Ca^{2+} uptake inhibition, PKC has been demonstrated to phosphorylate serine 10 on PLN *in vitro* (Movsesian *et al.*, 1984;Koss & Kranias, 1996;Duhamel, 2007;Colyer, 1998) which would relieve SERCA

inhibition and improve Ca^{2+} handling (Toyoshima *et al.*, 2003), however, this has not been supported *in vivo* (Wegener *et al.*, 1989). The α, β, and λ isoforms of PKC can be activated by Ca^{2+}-CaM binding (Richter *et al.*, 2004). However, the effects of Ca^{2+}-CaM-dependent PKC activity on Ca^{2+} uptake are indirect and inhibitory, as they are mediated through activation of PP1(Braz *et al.*, 2004;Sahin *et al.*, 2006). Sahin *et al.* (2006) suggest that PKC phosphorylates serine 65 on the inactive form protein phosphatase inhibitor 1 (I-1), which then becomes phosphorylated on serine 67 by cyclin-dependent kinase 5, protecting serine 65 from dephosphorylation by PP1. This diphosphorylated enzyme is a poor substrate for PKA which would normally phosphorylate threonine 35 to activate I-1, and later be dephosphorylated by calcineurin. Thus by inhibiting the inhibitor of PP1, PKC activity leads to increased phosphatase activity, reduced PLN phosphorylation, and an inhibitory effect on Ca^{2+} uptake during repetitive contractions.

PLN-phosphorylation is dependent on both the intensity and duration of exercise. Repeated bouts of activity lasting 10 minutes each at 35%, 60% and 85% of VO_2 peak resulted in progressive increases in phosphorylation of threonine 17on PLN (Rose *et al.*, 2006). These increases in phosphorylation could be detected within 1 minute of the onset of exercise, with a plateau occurring by 10 minutes of exercise (Rose *et al.*, 2006).

In summary, PLN is expressed in fast-twitch muscle and its basal-state inhibition of Ca^{2+}-uptake by SERCA can be relieved by a Ca^{2+}-sensitive pathway which could contribute to the enhancements in relaxation seen during potentiated twitches.

Sarcolipin

Sarcolipin (SLN) is functionally homologous to PLN as a membrane-bound inhibitor of SERCA activity (Odermatt *et al.*, 1997). SLN decreases the apparent affinity of SERCA for Ca^{2+}, reducing the Ca_{50} of Ca^{2+} transport *in vitro* (Odermatt *et al.*, 1998) and can interact with both SERCA1a and SERCA2a (Odermatt *et al.*, 1998;Gramolini *et al.*, 2006). However, the expression pattern of SLN is less clear, though it appears that expression is greatest in the soleus, atria, left ventricle and diaphragm (Bombardier *et al.*, 2013b;Schneider *et al.*, 2013;Tupling Lab, unpublished observations) i.e. only those muscles which are constantly active.

As with PLN, the inhibitory function of SLN on SERCA can be relieved by kinase activity. Phosphorylation of threonine 5 by serine/threonine kinase 16 relieves its inhibitory effect on SERCA, resulting in greater Ca^{2+} sensitivity of Ca^{2+} uptake *in vitro* (Gramolini *et al.*, 2006). SLN may also be a mediator of β-adrenergic stimulation as isoproteranol treatment of SLN OE/PLN null mouse hearts leads to greater peak amplitude of cytosolic Ca^{2+} transients and greater rates of Ca^{2+} decay from the cytosol (Gramolini *et al.*, 2006) Phosphorylation of threonine 5 of SLN *in vitro* by CaMKII has been shown to mediate β-adrenergic stimulation induced activation of SERCA function, as ventricular myocytes over-expressing SLN pre-incubated with the CaMKII inhibitory peptide, autocamtide inhibitor peptide (AIP), lost isoproterenol sensitivity of threonine 5 phosphorylation (Bhupathy *et al.*, 2009). However, there is little support for a Ca^{2+}-mediated pathway leading to the relief of SERCA inhibition by SLN. Unlike PLN, SLN remains bound to SERCA at high concentrations of Ca^{2+} and throughout the pump cycle (Sahoo *et al.*, 2013;Bal *et al.*, 2012). Consistent with this, Bombardier et al (2013a) have recently shown that ablation of SLN leads to reductions in

whole body metabolic rate during periods of activity, which is consistent with the inhibitory mechanism of SLN uncoupling ATP hydrolysis from Ca^{2+} transport (Bombardier *et al.*, 2013b;Bal *et al.*, 2012). However, in support of an activity-dependent pathway, wild type soleus muscles have been shown to exhibit increases in the rates of relaxation during repeated tetanic stimulations, while soleus from SLN null mice have initially faster rates of relaxation than those of wild type mice, though these do not increase with repetitive tetanic contractions (Tupling *et al.*, 2011). Similarly, slow twitch specific over-expression of SLN by plasmid injection and electro transfer resulted in reduced twitch and tetanic force, lower rates of force production and relaxation, as well as lower maximum Ca^{2+}-ATPase activity (Tupling *et al.*, 2002). Conversely, soleus from SLN null mice exhibits faster relaxation times at submaximal contraction frequencies, as well as lower peak force during twitch and 10 Hz contraction in SLN null soleus (Tupling *et al.*, 2011). Additionally, the Ca^{2+}-sensitivity of SERCA ATPase activity is higher in homogenates prepared from soleus and red gastrocnemius muscles of SLN null mice, but no such increases occur in the EDL or white gastrocnemius homogenates (Tupling *et al.*, 2011). However, 1/2RT was reduced in both soleus and EDL muscle of SLN null mice (Tupling *et al.*, 2011). Finally, as CaMKII has already been shown to phosphorylate SLN during β-adrenergic stimulation (Bhupathy *et al.*, 2009), it is quite possible that CaMKII mediates a Ca^{2+}-dependent pathway as well. Therefore, SLN could be affecting the rate of relaxation, and be a factor in increases in relaxation speed in slow twitch muscle, though the inhibitory effects of SLN are unlikely to influence any contractions taking place in fast-twitch skeletal muscle.

Redox modulation of SERCA activity

There is evidence to suggest that redox signaling may be able to increase the activity of SERCA in exercise induced pathways. For example, both SERCA2a and SERCA2b can be activated by a peroxynitrite-mediated S-glutathiolation of cysteine 674 (Lancel *et al.*, 2009;Adachi *et al.*, 2004;Qin *et al.*, 2013). It is currently unknown if SERCA1a, the dominant isoform in skeletal muscle, can similarly be glutathiolated and activated. However, it has been demonstrated that a fatiguing stimulation protocol in strips of rat diaphragm results in enhanced Ca^{2+}-uptake and Ca^{2+}-dependent ATPase activity in homogenized samples of these diaphragms (Tupling *et al.*, 2007). Similarly, it has been recently demonstrated that a reduction in free cysteine residues in SERCA1a in fatigued rat diaphragm as indicated by biotinylated-iodoacetamide (BIAM) binding (Tupling lab, unpublished data), which preferably binds to cysteine 674 in SERCA2a and SERCA2b (Adachi *et al.*, 2004;Lancel *et al.*, 2009), though it is unknown if it behaves the same in SERCA1a. The reductions in BIAM binding coincide with increases in glutathiolation of SERCA1a (Tupling lab, unpublished data). Likewise, when rats are treated with buthionine sulfoximine in their drinking water, which reduces both total glutathione and the ratio of reduced to oxidized glutathione in the diaphragm, they do not exhibit the exercise-induced increases in Ca^{2+}-uptake, Ca^{2+}-dependent ATPase activity (Tupling *et al.*, 2007), or reductions in SERCA1a BIAM binding (Tupling lab, unpublished data). This experimental evidence suggests a role for redox signaling in increasing the rate of relaxation during potentiated twitches by increasing the rate of Ca^{2+}-uptake by SERCA.

Physiological relevance of force potentiation and enhanced relaxation

Teleologically, the changes occurring during potentiation are important as the speed and power at which an animal is able to undergo a cyclic motor pattern, such as sprinting, is fundamentally linked to its ability to survive. The force-enhancing effect of potentiation increases the power of rapid concentric contractions (Gittings *et al.*, 2012), while the increased rates of relaxation prevent increases in Ca^{2+} sensitivity from reducing the rate of motor pattern cycling by extending the active time and providing resistance to antagonistic muscles. Similarly, enhancements in force and relaxation can help counteract the effects of fatigue by accumulation of metabolites such as ADP and Pi. Thus by enhancing submaximal force, as is inherent in any concentric contraction, and rates of relaxation, the sprinting animal is better equipped to evade predation or successfully capture prey. In modern human use, force potentiation appears to be most beneficial to high intensity, low duration sports performances, though optimization has proven to be challenging.

Statement of the problem

This literature review has highlighted several features of the potentiated twitch which do not have a firm mechanistic explanation. First, there is the existence of potentiation, staircase potentiation in particular, in the absence of myosin RLC phosphorylation (Zhi *et al.*, 2005;MacIntosh *et al.*, 2008;Rassier *et al.*, 1999;Rassier *et al.*, 1997;Gittings *et al.*, 2011). Second there is an increase in the rate of relaxation and a decrease in the relaxation time associated with potentiated contractions (Krarup, 1981). To date, there has been no attempt to experimentally determine a mechanism for these phenomena, though both may be attributable to changes in cytosolic Ca^{2+} signaling. For example, increased force without RLC

phosphorylation may be the result of either an increase in Ca^{2+} release leading to a higher pCa value and greater crossbridge activation. Alternatively, an increase in resting Ca^{2+} at the onset of stimulation could increase the saturation level of high affinity Ca^{2+} buffers, leading to greater TnC activation via reduced competition for Ca^{2+}, thereby enhancing crossbridge attachment and force. The evidence to suggest that Ca^{2+} release may be enhanced by a CaMKII-mediated pathway has been described in the above text. Likewise the presence of parvalbumin has been demonstrated to maintain elevated levels of Ca^{2+} in the cytosol following contractions (Hollingworth & Baylor, 2013) (Note that this was published after the publication of Chapter II in this thesis). Increases in the rate of relaxation during potentiation may be the result of the increased rate of Ca^{2+}-sequestering by SERCA, for which there is a great deal of evidence in support of activity-mediated SERCA activation, though this has never been tested on the brief time scale of potentiation. This thesis sought to test the hypothesis that changes in cytosolic Ca^{2+} can contribute to these unresolved effects of the potentiation response.

The main objectives of this thesis included:

1. Characterize the contractile properties, and the expression of the proteins primarily responsible for determining the contractile, relaxation, and potentiation properties of the mouse lumbrical muscle.

2. Characterize the cytosolic Ca^{2+} transient and resting cytosolic Ca^{2+} during both posttetanic potentiation and staircase potentiation.

3. If any changes in cytosolic Ca^{2+} are found, determine if they can be reconciled with the enhancements in force or relaxation seen during potentiation.

4. Determine how any changes in cytosolic Ca^{2+} found may exert their influence on force or relaxation.

These four objectives are addressed in the following Chapters, though much work remains for the fourth objective to be fully realized.

The main hypotheses (and outcomes) of this thesis were:

1) The cytosolic Ca^{2+} transient would be larger in the potentiated state, thereby explaining enhanced force in the absence of myosin RLC phosphorylation.

(This hypothesis was correct during staircase potentiation, as Ca^{2+} transients were longer in duration and larger in area, though lower in amplitude. These effects were not observed during posttetanic potentiation).

2) Increases in resting cytosolic Ca^{2+} concentration can contribute to potentiation.

(This hypothesis was correct, though the precise mechanism is still unclear).

3) Enhancement of relaxation is caused by abbreviation of the cytosolic Ca^{2+} transient.

(This hypothesis was incorrect. Enhanced relaxation was localized to the myofilament).

Chapter II - Potentiation in mouse lumbrical muscle without myosin light chain phosphorylation: is resting calcium responsible?

Outline

The increase in isometric twitch force observed in fast-twitch rodent muscles during or after activity, known universally as potentiation, is normally associated with myosin regulatory light chain (RLC) phosphorylation. Interestingly, fast muscles from mice devoid of detectable skeletal myosin light chain kinase (skMLCK) retain a reduced ability to potentiate twitch force, indicating the presence of a secondary origin for this characteristic feature of the fast muscle phenotype. The purpose of this study was to assess changes in intracellular cytosolic free Ca^{2+} concentration ($[Ca^{2+}]_i$) after a potentiating stimulus in mouse lumbrical muscle (37°C). Lumbricals were loaded with the Ca^{2+}-sensitive fluorescent indicators fura-2 or furaptra to detect changes in resting and peak, respectively, intracellular Ca^{2+} levels caused by 2.5 s of 20-Hz stimulation. Although this protocol produced an immediate increase in twitch force of 17 ± 3% (all data are n = 10) ($P<0.01$), this potentiation dissipated quickly and was absent 30 s afterward. Fura-2 fluorescence signals at rest were increased by 11.1 ± 1.3% ($P<0.01$) during potentiation, indicating a significant increase in resting $[Ca^{2+}]_i$. Interestingly, furaptra signals showed no change to either the amplitude or the duration of the intracellular Ca^{2+} transients (ICTs) that triggered potentiated twitches during this time ($P<0.50$). Immunofluorescence work showed that 77% of lumbrical fibres expressed myosin heavy chain isoform IIx and/or IIb, but with low expression of skMLCK and high expression of myosin phosphatase targeting subunit 2. As a result, lumbrical muscles displayed no detectable RLC phosphorylation either at rest or after stimulation. It is concluded that stimulation-induced elevations in resting $[Ca^{2+}]_i$, in the absence of change in the ICT, are responsible for a small-magnitude, short-lived potentiation of isometric twitch force. If operative in other fast-twitch muscles, this mechanism may complement the potentiating influence of myosin RLC phosphorylation.

Introduction

Excitation–contraction coupling (ECC) of vertebrate striated muscle is the process by which changes in membrane potential are translated into mechanical force by contractile proteins (Gordon *et al.*, 2000). Seminal work by Ebashi and Endo (1968) established that calcium release from the sarcoplasmic reticulum with subsequent binding of Ca^{2+} ion to regulatory proteins resident on the thin filament was the key intermediate step in this process. Subsequent work has provided evidence that the activation of the contractile apparatus, and resultant force, work, and power, is a complex process involving both Ca^{2+}-dependent and Ca^{2+}-independent activation of the thin filament, including several inter- and intrafilament cooperative interactions (Lehrer, 2011).

During ECC, muscle force may be modulated via changes in the amplitude of the Ca^{2+} signal delivered to the contractile apparatus or by the Ca^{2+} sensitivity of the contractile apparatus. In this simple two-compartment model, an augmented Ca^{2+} signal may be achieved via an augmented release from the voltage-sensitive Ca^{2+} release channels or reduced Ca^{2+} buffering such as that performed via the sarcoplasmic–endoplasmic reticulum Ca^{2+} ATPase pumps, either of which could potentiate twitch contractions by increasing the Ca^{2+} occupancy of TnC and thus increasing the probability of “open” states on the regulated thin filament(McKillop & Geeves, 1993;Maytum *et al.*, 1999). An increased Ca^{2+} sensitivity, on the other hand, may be mediated at the level of the myofilaments by muscle length and attendant variations in myofilament spacing, as first demonstrated by Endo (1972) in skinned and later confirmed by Claflin *et al.* (1998) in intact skeletal fibres.

In addition to these geometric factors, posttranslational modifications of contractile proteins, such as the phosphorylation of the myosin regulatory light chains(RLCs), have been

demonstrated to increase the Ca^{2+} sensitivity of both skeletal and cardiac muscle cells (Persechini *et al.*, 1985;Sweeney & Kushmerick, 1985;Sweeney & Stull, 1986). Thus, it seems clear that the ECC process of vertebrate striated muscle is subject to myriad influences that modulate the Ca^{2+} response of the myofilament assembly.

Close and Hoh (1968) were among the first to propose that stimulation-induced alterations to ECC could account for a classical characteristic of the mammalian fast-twitch muscle phenotype, that of posttetanic potentiation, defined as the increase in isometric twitch force observed after brief tetanic stimulation. In this regard, studies using isolated fast-twitch rodent skeletal muscle have shown quantitative associations between phosphorylation of the RLC and isometric twitch force potentiation (Klug *et al.*, 1982;Manning & Stull, 1982;Moore & Stull, 1984;Vandenboom *et al.*, 1997). Indeed, more recent studies using mouse extensor digitorum longus (EDL) muscle devoid of the enzymatic apparatus for phosphorylating the RLC show that, although posttetanic potentiation is completely absent, staircase potentiation, the gradual increase noted in isometric twitch force during low frequency stimulation, was still evident albeit reduced compared with wild-type responses (Zhi *et al.*, 2005;Gittings *et al.*, 2011). Thus, although a universal mechanism is often assumed, evidence exists to suggest that alterations in the Ca^{2+} signal delivered to the myofilament proteins may account for some aspects of potentiation phenomena. This conclusion is in fact consistent with results from rat hind limb disuse models demonstrating staircase potentiation when RLC phosphorylation is absent or reduced (Rassier *et al.*, 1999;MacIntosh *et al.*, 2008).

Although a myosin RLC phosphorylation-mediated increase in the Ca^{2+} sensitivity of force development maybe the prevalent mechanism, few studies have examined the contribution of altered Ca^{2+} signals on twitch force potentiation. Thus, the purpose of this study

was to assess how stimulation-induced alterations to ECC may contribute to potentiation using the mouse lumbrical muscle model (in vitro at 37°C). To this end, lumbrical muscles were loaded with either a high or low affinity Ca^{2+}-sensitive fluorescent indicator to determine resting and peak intracellular cytosolic free Ca^{2+} concentration ($[Ca^{2+}]_i$), respectively, before and after a tetanic stimulus that potentiated the twitch contractions. It was hypothesized that the mechanism for this persistent twitch force potentiation is the influence of repetitive stimulation on either resting or peak $[Ca^{2+}]_i$. Immunofluorescence and immunohistochemical characterization of the mouse lumbrical provide a comprehensive model with far-reaching implications for understanding this fundamental property of mammalian fast-twitch skeletal muscle.

Methods

All procedures used in this study received ethical approval from the University of Waterloo Committee for Animal Care as well as from the Brock University Animal Care and Use Committee. The basic methods and procedure for obtaining and mounting lumbrical muscles were based on those described by Claflin and Brooks (2008). Adult male C57BL/6 mice (28.0 ± 0.6 g) (The Jackson Laboratory) were killed by cervical dislocation, after which the hind paws were removed and placed in a dish which was based with silicon elastomer (Sylgard 184, Dow Corning) to allow immobilization of the feet using dissecting pins, and contained a Tyrode's dissecting solution (mM: 136.5 NaCl, 5.0 KCl, 11.9 $NaHCO_3$, 1.8 $CaCl_2$, 0.40 NaH_2PO_4, 0.10 EDTA, and 0.50 $MgCl_2$, pH 7.5; on ice), and the lumbrical muscles from both hind paws were subsequently removed. Isolated muscles were suspended horizontally between the arms of a high speed length controller (model 322C; Aurora Scientific Inc.) and a force transducer (model 400A; Aurora Scientific Inc.), affixed with four surgeon's knots on

each end using monofilament nylon thread (10-0). Muscles were aligned within the chamber such that motion in the y and z planes during contraction was minimized. Muscles were immersed in an oxygenated Tyrode's experimental solution (mM: 121.0 NaCl, 5.0 KCl, 24.0 $NaHCO_3$, 1.8 $CaCl_2$, 0.40 NaH_2PO_4, 5.50 glucose, 0.10 EDTA, and 0.50 $MgCl_2$, pH 7.3) circulating at a rate of ~4 mL/min (~5 bath changes per minute). Based on the binding affinity of EDTA to the constituent metal ions, free concentrations of Ca^{2+} and Mg^{2+} were estimated at 1.7 and 0.5 mM, respectively, in the Tyrode's solutions. Bath temperature was maintained at 37°C throughout the experiment by a Peltier heater. 0.2-ms stimulus pulses were delivered via imbedded platinum plate field stimulus electrodes using a stimulator (model 701C; Aurora Scientific Inc.). The stimulus voltage at which twitch force plateaued was found and then increased to 1.25 times this level for the duration of each experiment on each muscle. After a 15-min equilibration period, muscles were set to optimal length (L_o) for isometric twitch force development using a software-controlled procedure. Force data were collected online at 10,000 Hz and stored for analysis. Emitted fluorescence signals were collected by a microscope photometer system (D-104; Photon Technology International) affixed with photomultiplier tubes (PMTs; model 814; Photon Technology International) in analogue mode at 10,000 Hz and stored for subsequent analysis. Experimental procedures were both controlled and recorded using four channel digital control software (ASI).

Experimental model and protocol

The mouse lumbrical muscle model has been used previously to study ECC (e.g., Månsson *et al.*, 1989;Wang & Kerrick, 2002;Claflin & Brooks, 2008). A key advantage is that, in addition to providing a stable preparation for study at high temperatures (Barclay, 2005), the

small size of the lumbrical makes it highly amenable to loading with membrane-permeant acetoxymethyl (AM) forms of dyes. The principal measurements of $[Ca^{2+}]_i$ reported in this study were made using the excitation shifted ratioable fluorescent indicators furaptra and fura-2, although a subset of experiments was performed using the emission-shifted ratioable fluorescent indicator indo-1 (Molecular Probes). Loading of AM-furaptra or AM–fura-2 was accomplished by soaking mounted muscles in ~1 ml Tyrode's experimental solution containing 20 μM dye for 60 min at 32°C, replacing the solution after 30 min. After 60 min of loading, the dye-containing solution was washed out several times and ultimately replaced with normal Tyrode's experimental solution, and the temperature was raised to 37°C. See Appendix 1 for detailed information. Background fluorescence was obtained before and after loading to verify adequate dye loading and to control for the contribution of autofluorescence to records. The correction for autofluorescence was achieved by illuminating the muscle for 1.0 s using the same excitation and detection conditions which were to be used in the experimental measurements for that muscle. The fluorescence signals over the 1.0 s data collection were averaged to obtain a single value which was then subtracted from all subsequent measurements with that muscle. The timeline and experimental procedure for assessing $[Ca^{2+}]_i$ during potentiation is shown schematically in Figure II-1. After dye loading and preliminary procedures were completed, the muscles received a single stimulus pulse every 30 s until a steady-state isometric twitch force was repeatedly observed. The fluorescence ratio representing resting or peak $[Ca^{2+}]_i$ in the unpotentiated state was obtained from the last three twitches in this series. The regular interval of stimulus pacing was then stopped, and a potentiating stimulus (PS) consisting of 20 Hz for 2.5 s was applied. Thereafter, all muscles received single stimulus pulses to elicit potentiated twitches at 2.5, 5, 7.5, 10, 20, and 30 s after

PS. Additional twitches were elicited at 30-s intervals over the next 3 min, a time sufficient to dissipate all potentiation before the protocol was repeated. Each of these repeat sequences took ~5 min to complete and were performed eight times per muscle.

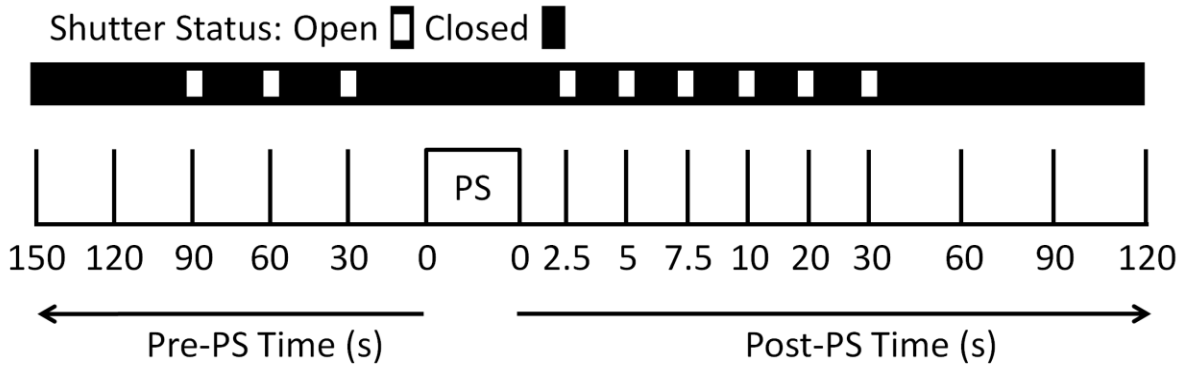

Figure II-1 - Scheme showing stimulation protocol and fluorescent ratio measurements
This schematic illustrates the experimental protocol for simultaneous collection of mechanical and fluorescent light data from lumbricals. Muscles were loaded with either a high affinity (fura-2 or indo-1) or a low affinity (furaptra) Ca^{2+}-sensitive fluorescent indictor before the start of these procedures; thus, all contractile data were obtained from muscles loaded with indicator dye. The scheme shows the timing of shutter opening and closing; each twitch (marked as a vertical line) was framed by a 1-s window of excitation light. This minimized exposure to UV light and thus the loss of light signal during each experiment. In the cases of fura-2 and furaptra, each sequence of 380- and 344-nm excitation was alternated eight times, producing four ratio signals (380/344 nm) per twitch per muscle. For indo-1 the protocol was repeated four to five times at 355 nm excitation and 485 and 405 nm emission, producing four to five ratios. Fluorescence signals from all runs were averaged for formation of representative ratio signals for resting and peak (fura-2/indo-1 and furaptra, respectively). Because each muscle was only loaded with one of the dyes, the derivation of resting and of peak Ca^{2+} intracellular concentrations ($[Ca^{2+}]_i$) always came from different muscles. Note that the last twitch in the post-potentiating stimulus (PS) period occurred 30 s prior to the first pre-PS twitch in the next sequence.

Fluorescent data collection

The excitation and emission light paths for indo-1 is shown in Figure II-2 while the light path for fura-2 and furaptra are shown in Figure II-3.The muscle chamber was mounted on the stage of an inverted microscope (Axiovert 200; Carl Zeiss) fitted with a 20× objective (NA of 0.40 and WD of 1.5 mm; LD Plan-Neofluar; Carl Zeiss). Excitation light from the monochromator (Photon Technology International) was deflected by a dichroic beam splitter (fura-2/furaptra: 415 nm; DCLP; Omega Optical, Inc.; indo-1: 390 nm DRLP; Omega Optical Inc.) housed in a filter cube in the base of the microscope before being focused on the muscle via the objective and through the transparent quartz panel in the base of the chamber in the

1500A system (Aurora Scientific Inc.) which allows the transmission of both UV and visible light.

Fluorescent light emitted from the muscle by fura-2 and furaptra was collected by the objective and passed through the dichroic long pass (DCLP) to an emission filter (510 nm; WB40; Omega Optical, Inc.) before deflection toward and detection by a photomultiplier tube (PMT) housed within a detection system (D-104; Photon Technology International). Excitation light was monitored in each experiment via a beam-splitting mirror housed within the monochromator, collected using a PMT and stored for later correction of variability of the excitation light caused by room vibrations and/or electrical instabilities.

During experiments using indo-1, emitted fluorescent light was collected by the objective and passed through the dichroic reflecting long pass (DRLP) to a second dichroic cube (450 nm DCLP; Omega Optical Inc.). Light reflected by the cube was passed through a 405 nm DF43 optical filter followed by detection by a PMT, while light passing through the cube was passed through a 495 DF20 optical filter prior to collection by a separate PMT. The simultaneous collection of two wavelengths afforded by the emission shifts of indo-1 made correction for variation of excitation light unnecessary in these experiments.

The analogue mode was used for all experiments, and the PMT was set to 600–800-V gain with a time constant of 0.5 ms for furaptra and 5.0 ms for fura-2 and indo-1. The time constant provides a means of data filtering using the PMT which introduces delays (~5x the time constant) between Ca^{2+} measurements and what is happening real time, but has the benefit of reducing noise in the signal. The time constants used in this experiment achieved the optimum balance between signal fidelity and temporal accuracy.

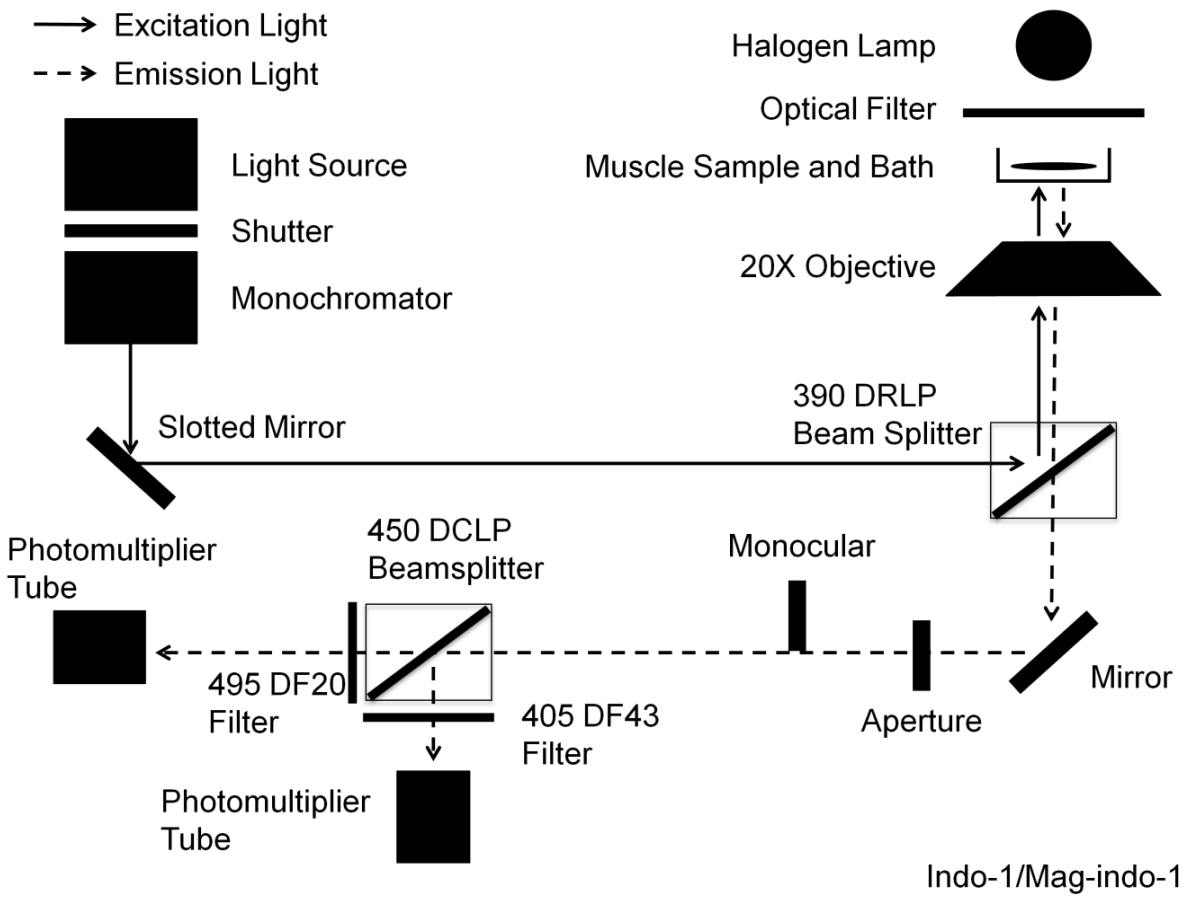

Figure II-2 – Optical configuration for indo-1 experiments
During experiments, the monochromator sent out excitation light at 355 nm to illuminate the muscle and excite indo-1during twitch contractions (slit width 0.5 mm). Excitation light was deflected by the dichroic beam splitter through the objective and onto the muscle. Emitted light was collected by the objective and passed through the dichroic beam splitter and through a second dichroic beam splitter which separated the emitted light into the Ca^{2+}-bound (405 nm) and Ca^{2+}-free (485 nm) signals which were passed through emission filters prior to collection by photomultiplier tubes. DRLP: Dichroic reflecting long pass; DCLP: Dichroic long pass; DF: Discriminating filter. Numbers preceding filter annotations refer to the center wavelength (in nm) of the light allowed to pass through the filter. The bandwidth of this light is described by the number succeeding the filter annotation. Numbers preceding the beam splitter annotation refer to the maximum wavelength (in nm) reflected by the dichroic surface.

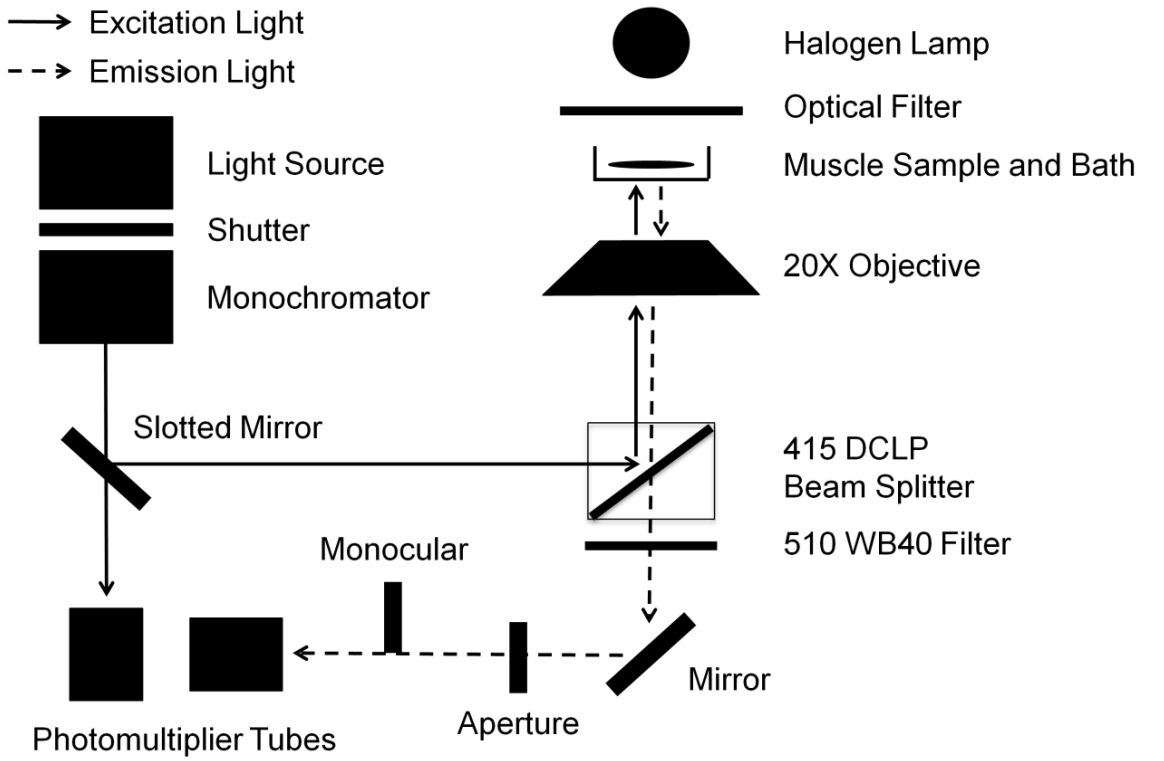

Figure II-3 – Optical path for excitation and emission light during experiments with fura-2 and furaptra

During experiments with excitation-shifted dyes, the monochromator sent out excitation light at 344 and 380 nm for both fura-2 and furaptra to illuminate the muscle and excite dye fluorescence during isometric twitch contractions. Excitation light was simultaneously sampled and collected for later correction of variable excitation intensity. In all cases, slit width was 0.5 mm. Excitation light was deflected by the dichroic beam splitter through the objective and onto the muscle. Emitted light was collected by the objective and passed through the dichroic beam splitter and through an emission filter before being bent 90° by a mirror and directed toward the photomultiplier tube for detection centered at 510 nm. The mask or aperture was adjusted to focus on a section of the muscle with minimum movement in either the y or z planes; thus, mask area did not leave the muscle at any time during contraction. Lumbrical length and width were ~4.0 × 0.6 mm, respectively, and mask size was 0.7 × 0.3 mm, which was large enough to accommodate light emission from 10–12 individual surface muscle fibres. DRLP: Dichroic reflecting long pass; WB: Wide band. Numbers preceding filter annotations refer to the center wavelength (in nm) of the light allowed to pass through the filter. The bandwidth of this light is described by the number succeeding the filter annotation. Numbers preceding the beam splitter annotation refer to the maximum wavelength (in nm) reflected by the dichroic surface.

Fluorescent dye properties

Each of the excitation- and emission-shifted dyes used in these experiments has been widely used to study $[Ca^{2+}]_i$ in both amphibian and mammalian muscle fibres (Baylor & Hollingworth, 2003;Baylor & Hollingworth, 2011;Baylor & Hollingworth, 2012;Claflin *et al.*, 1994;Hollingworth *et al.*, 1996;Hollingworth *et al.*, 2012;Konishi *et al.*, 1991;Konishi *et al.*, 1993;Morgan *et al.*, 1997;Vandenboom *et al.*, 1998;Westerblad & Allen, 1993;Zhao *et al.*, 1996;Zhao *et al.*, 1997). Although both furaptra and fura-2 share the same chromophore, i.e., excitation at 344 and/or 380 nm and emission at 510 nm, the characteristics of the emitted fluorescence intensity at different $[Ca^{2+}]_i$ vary considerably between these two dye types; fura-2 fluorescence change is most sensitive to low $[Ca^{2+}]_i$, whereas furaptra fluorescence change is most sensitive to higher $[Ca^{2+}]_i$. These properties are reflected by in vitro *K*d values of 224 nM and 44 μM (Grynkiewicz *et al.*, 1985;Konishi *et al.*, 1991;Raju *et al.*, 1989). This feature allows low affinity dyes such as furaptra to precisely track, with high fidelity, the amplitude and dynamics of the intracellular Ca^{2+} transient (ICT) at most temperatures (e.g., Claflin *et al.*, 1994;Baylor & Hollingworth, 2000). On the other hand, the use of fura-loaded lumbricals to track basal $[Ca^{2+}]_i$ avoids the limitations of furaptra for this purpose and provides a comparison point to previous work. The emitted fluorescence characteristics of indo-1 to different $[Ca^{2+}]_i$ resemble that of fura -2 (Westerblad & Allen, 1993) with an *in vitro* Kd value of 250 (Grynkiewicz *et al.*, 1985), albeit with a different chromophore (i.e. 355 nm excitation, emission at 485 and 410 nm). For all dyes, the ratio technique minimizes contamination of the signal of interest by factors such as motion artifact and/or loss of dye or dye signal by bleaching (see Morgan *et al.*, 1997;Baylor & Hollingworth, 2000;Baylor & Hollingworth, 2011). This assumption was tested by applying sinusoidal length changes to muscles during

fluorescent light collection and found no evidence of fibre motion in the resulting ratio signals (Figure II-4). (See also Morgan *et al.*, 1997).

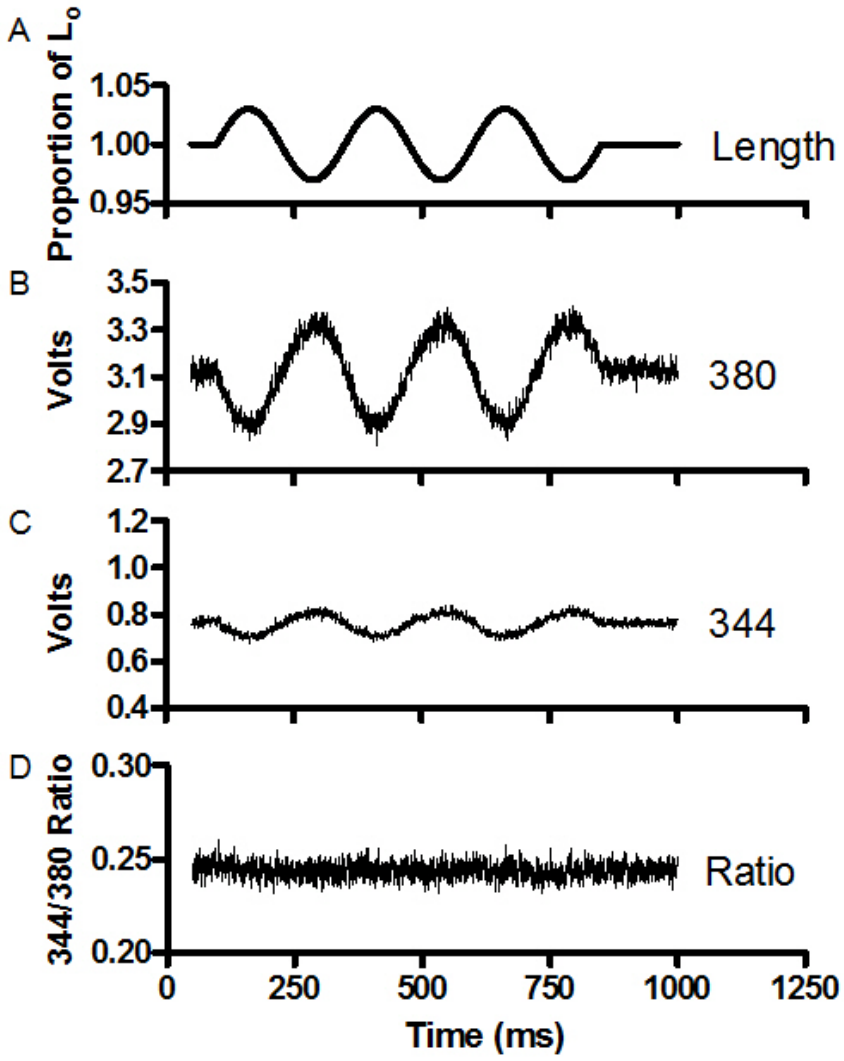

Figure II-4 - Ratiometric cancellation of motion artifact
Motion of a muscle within the field of view, such as that seen during a contraction results in changes in the emitted light signal based on changing amounts of indicator in the field along with changes in the area of focus. These differences are independent of the changes in $[Ca^{2+}]_i$. This figure demonstrates how using a ratiometric indicator circumvents this problem as light is collected at two different wavelengths, and motion affects both wavelengths proportionally. These data result from a single lumbrical muscle loaded with furaptra and subjected to sinusoidal length changes (A) which cause fluctuations in the emitted light from both 380 (B) and 344 (C) nm excitation. The resulting ratio (D) of these fluorescent signals (i.e. 344/380 after correction for autofluorescence) results in the cancellation of the fibre motion, thus any resulting signal during the experimental protocol can be attributed to changes in $[Ca^{2+}]_i$.

Myosin phosphorylation

Two sets of parallel experiments were performed in which no contractile or fluorescence data were collected to obtain RLC phosphate content of lumbrical and EDL muscles in the unpotentiated and potentiated states. This was a collaborative process with Brock University and the University of Texas. Lumbrical (performed by I. Smith, University of Waterloo) and EDL (performed by W. Gittings, Brock University) muscles were quick frozen in liquid nitrogen ~30 s before and 2.5 s after the PS. All samples were stored at -80°C until they were packed on dry ice and shipped to the laboratory of J. Stull (University of Texas, Southwestern Medical Center, Dallas, TX; analysis performed by Dr. Jian Huang) for quantification of RLC phosphorylation. Details regarding these methods and procedures have been presented elsewhere (Ryder *et al.*, 2007;Xeni *et al.*, 2011).

MYPT2 and skMLCK content of mouse muscles

Lumbrical, soleus, and EDL muscles were harvested from the mouse hind limb for determination of skeletal myosin light chain kinase (skMLCK) and myosin phosphatase targeting subunit 2 (MYPT2) content as described in Smith *et al.* (2010). In brief, skMLCK and MYPT2 content was assessed in whole muscle homogenates by Western blot analysis after separation of proteins by electrophoresis using 7.5% polyacrylamide gels and standard SDS/PAGE protocols (Laemmli, 1970). Protein concentrations were determined by the bicinchoninic acid method (Sigma-Aldrich), and Ponceau S (BioShop Canada Inc.) staining was used to control for variation in well loading. Either 8.0 (MYPT2) or 10.0 (skMLCK) μg of total protein was loaded for each muscle sample, with two mice per gel. A linear relationship between band density and protein load for each mouse was established for 2.0–8.0 μg of total

protein in soleus for MYPT2 or 2.5–10.0 μg of total protein in EDL for skMLCK. After transfer of proteins to polyvinyl difluoride membranes, MYPT2 was probed using a polyclonal rabbit antibody, whereas skMLCK was probed using a polyclonal goat antibody (provided by J. Stull). Secondary probing was performed with either goat anti–rabbit (MYPT2; Santa Cruz) or donkey anti–goat (skMLCK; Santa Cruz) antibodies conjugated with horseradish peroxidase (HRP). Quantification was performed using an HRP substrate detection kit (Luminata; EMD Millipore) and subsequent densitometric analysis (GE Healthcare). MYPT2 content in EDL and lumbrical was expressed relative to soleus, whereas skMLCK content in soleus and lumbrical was expressed relative to EDL, as determined by comparing the band densities to those determined by the generated linear scales at equivalent protein loads.

Fibre typing

Myosin heavy chain (MHC) expression was determined in lumbrical, soleus, and EDL cross sections by immunofluorescence analysis as described by Bloemberg and Quadrilatero (2012). In brief, sections were blocked with 10% goat serum, incubated with primary antibodies against MHC I, MHC IIa, and MHC IIb (Developmental Studies Hybridoma Bank), and then washed in PBS. Sections were then incubated with isotype-specific Alexa Fluor 350 anti–mouse, Alexa Fluor 488 anti–mouse, and Alexa Fluor 555 anti–mouse (Molecular Probes) secondary antibodies, washed in PBS, and mounted with an anti-fade reagent (Prolong Gold; Molecular Probes). This staining procedure allowed for the identification of type I (blue), type IIA (green), type IIB (red), type IIX (unstained), and hybrid (types I/IIA, IIAX, and IIXB) fibres. Type I/IIA hybrid fibres were identified as those staining positively for MHC type I and type IIa. Type IIAX fibres were identified as those staining positive for MHC IIa but at a lower

intensity than fibres identified as type IIA. Similarly, fibres were labeled type IIXB if they stained positively for MHC IIb but at a lower intensity than type IIB fibres. Images were captured using a structured illumination fluorescent microscope (Axio Observer Z1) equipped with a camera (AxioCam HRm) and associated software (AxioVision; all from Carl Zeiss).

Statistics

All data are reported as mean ± SEM. Relative changes in mean values for various twitch force and Ca^{2+} parameters were compared by a repeated measures ANOVA followed by Tukey's HSD post-hoc analysis. Differences were considered significant at $P < 0.05$.

Results

Mechanical, immunofluorescence, and immunohistochemical data presented here describe a fast-twitch muscle model that appears to be somewhat unique in that isometric twitch force potentiation occurs in the total absence of myosin RLC phosphorylation. Although fast muscles from skMLCK knockout mice display a small amount of potentiation in the absence of stimulation-induced elevations in RLC phosphorylation, lumbrical muscles from wild-type mice appear to mimic this response. Thus, unlike traditional studies performed on wild-type muscles, this attribute of the lumbrical allows for a direct analysis of the contribution of altered $[Ca^{2+}]_i$ to potentiation.

Isometric twitch contractile responses

Representative isometric twitch force records obtained before and after the PS are depicted in Figure II-5A. These records show how stimulation produced a modest twitch potentiation that dissipated rapidly. Absolute mechanical data characterizing the mouse

lumbrical in vitro muscle model are compiled in Table II-1, with relative changes to twitch force amplitude and kinetics summarized in Figure II-5 (B-D). The PS produced a maximal increase in isometric twitch force of 17 ± 3% when determined 2.5 s after the cessation of stimulation (n = 10; P < 0.01). From this point onwards, potentiation decreased in a monotonic fashion with a halftime of ~10 s; as a result, twitch force returned to prestimulus unpotentiated levels by 30 s. Along with the elevations in twitch force, twitch time course kinetics were faster and maximal rates of force production and relaxation were higher after the PS (Table II-1). Interestingly, these effects were still evident 30 s later, despite the fact that twitch force had returned to pre-PS levels (Table II-1); this effect resolved before the subsequent set of contractions (see Appendix 3). Finally, force returned to baseline in the time period between potentiated twitches (as depicted in the force traces of Figure II-5 and Figure II-7), and there was no latent elevation in baseline tension after the PS (not depicted).

Table II-1 - Twitch parameters before and after a PS in mouse lumbrical at 37^{o}C

Twitch Parameter	Pre-PS	Post-PS		Relative Change (Post-PS/Pre-PS)	
	- 60 s	2.5 s	30 s	2.5 s	30 s
Amplitude (mN)	16.23 ± 1.51	18.87 ± 1.61*	16.61 ± 1.50†	1.17 ± 0.03*	1.03 ± 0.01†
Time to peak (ms)	11.39 ± 0.40	10.0 ± 0.32*	10.70 ± 0.42*†	0.88 ± 0.01*	0.94 ± 0.01*†
½ RT (ms)	12.16 ± 0.69	11.41 ± 0.73*	11.25 ± 0.72*	0.94 ± 0.02*	0.92 ± 0.01*†
+dF/dt (mN/ms)	3.41 ± 0.31	4.57 ± 0.42*	3.60 ± 0.33†	1.34 ± 0.02*	1.05 ± 0.01*†
-dF/dt (mN/ms)	-1.14 ± 0.11	-1.40 ± 0.13*	-1.23 ± 0.11*†	1.23 ± 0.04*	1.08 ± 0.01*†

All data are presented as mean ± SEM (n =10 muscles). Time markers correspond to 60 s before start and 2.5 and 30 s after the potentiating stimulus (PS) (20 Hz for 2.5 s. Peak twitch force occurred at 2.5 s after the PS in every muscle examined; all data collected at optimal length for twitch force (L_o). Data correspond to intracellular Ca^{2+} transient data presented in Table II-2. Amplitude, twitch force from baseline to peak; time to peak, the time for force to rise from baseline to peak; ½ RT, time for force to relax from peak to 50% peak; +dF/dt, maximum rate of force production; -dF/dt, Maximum rate of force relaxation. See also Appendix 3.

* Post - PS value at 2.5 or 30 s is significantly different than Pre-PS value (P < 0.05).

† Post-PS value at 30 s significantly different than Post-PS value at 2.5 s (P < 0.05).

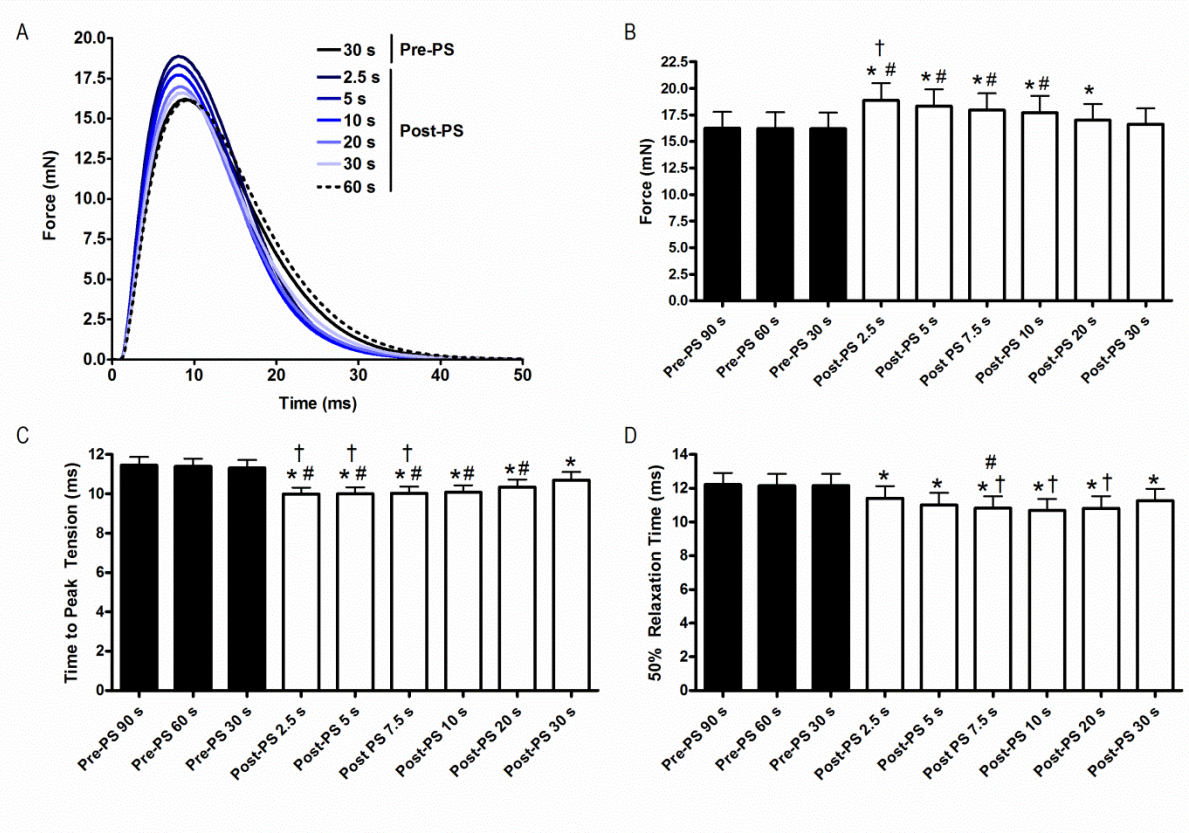

Figure II-5 - Change in isometric twitch parameters in potentiated lumbrical muscle
(A) Representative twitch force records from one muscle before and up to 60 s after a potentiating stimulation (PS) of 20 Hz for 2.5 s. (B) Peak isometric twitch force pre-PS (closed bars) and up to 30 s post-PS (open bars). *, value is greater than all pre-PS values; †, value is greater than post-PS 7.5, 10, 20, and 30 s; #, value is greater than post-PS 20 and 30 s. (C) Absolute time to peak tension of twitches measured pre-PS and up to 30 s post-PS. *, value is less than all pre-PS values; †, value is less than post-PS 20 s; #, value is less than post-PS 30 s. (D) Absolute half-relaxation time of twitches pre-PS and up to 30 s post-PS. *, value is less than all pre-PS values; †, value is less than post-PS 2.5 s; #, value is less than post-PS 30 s. $P < 0.05$ for B–D.

Fluorescence measurements

An important limitation of fluorescence ratio signals from high affinity Ca^{2+} indicators (fura-2 and indo-1) is that they cannot provide quantitatively useful data regarding the amplitude or kinetic characteristics of the ICT. By the same token, fluorescence ratio signals from low affinity Ca^{2+} indicators such as furaptra cannot be expected to provide quantitatively useful data regarding resting $[Ca^{2+}]_i$ (Baylor & Hollingworth, 2000;Baylor & Hollingworth,

2011). Thus, a complementary approach using both dyes was adopted to provide a more comprehensive picture regarding the influence of prior stimulation on ECC that could account for changes in isometric twitch force and kinetics. Ratio data from all fluorescence experiments are compiled in Table II-2. Averaged fura-2 fluorescence ratio records are shown in Figure II-6A, with relative changes summarizing all experiments shown in Figure II-6B.These data clearly show a relatively small but consistent elevation in basal $[Ca^{2+}]_i$ that was highly significant (fura-2: $n = 9$; $P < 0.001$) at all potentiation time points. By 30 s after stimulation, the resting fluorescence ratio was still elevated although potentiation had dissipated. Resting fluorescence did, however, return to prestimulus (unpotentiated) levels after another 30 s (i.e., within 60 s of completion of the PS). Virtually identical experiments ($n = 8$) were performed using the indicator indo-1, which has similar Ca^{2+} affinity as fura-2. In these experiments, there was an 8.1 ± 1.3% increase in the resting fluorescence ratio as determined 2.5 s after the PS ($P < 0.001$ vs. prestimulus). This increase dissipated with a similar time course as did the twitch force potentiation, returning to prestimulus levels by 30 s after the PS (Figure II-6 C and D). Thus, the elevation in resting $[Ca^{2+}]_i$ reported by indo-1 fluorescence was quantitatively similar to that reported by fura-2 fluorescence in terms of both magnitude and duration.

Averaged furaptra-based fluorescence ratio signals from identical experiments are shown in Figure II-7, with relative changes for ICT amplitude and full width at half-maximum shown in Table II-2, respectively. These data clearly show that, even when measured at the potentiation peak 2.5 s after stimulation, neither the amplitude nor the time course of the ICT was altered relative to the unpotentiated state ($n = 10$; $P > 0.20$). Although the fluorescence ratio signals of the high and low-affinity indicators have been analyzed independently of one another, the results indicate that stimulation-induced elevations in resting $[Ca^{2+}]_i$ potentiate

isometric twitch force in the complete absence of change to either the amplitude or time course of the subsequent ICT *per se*.

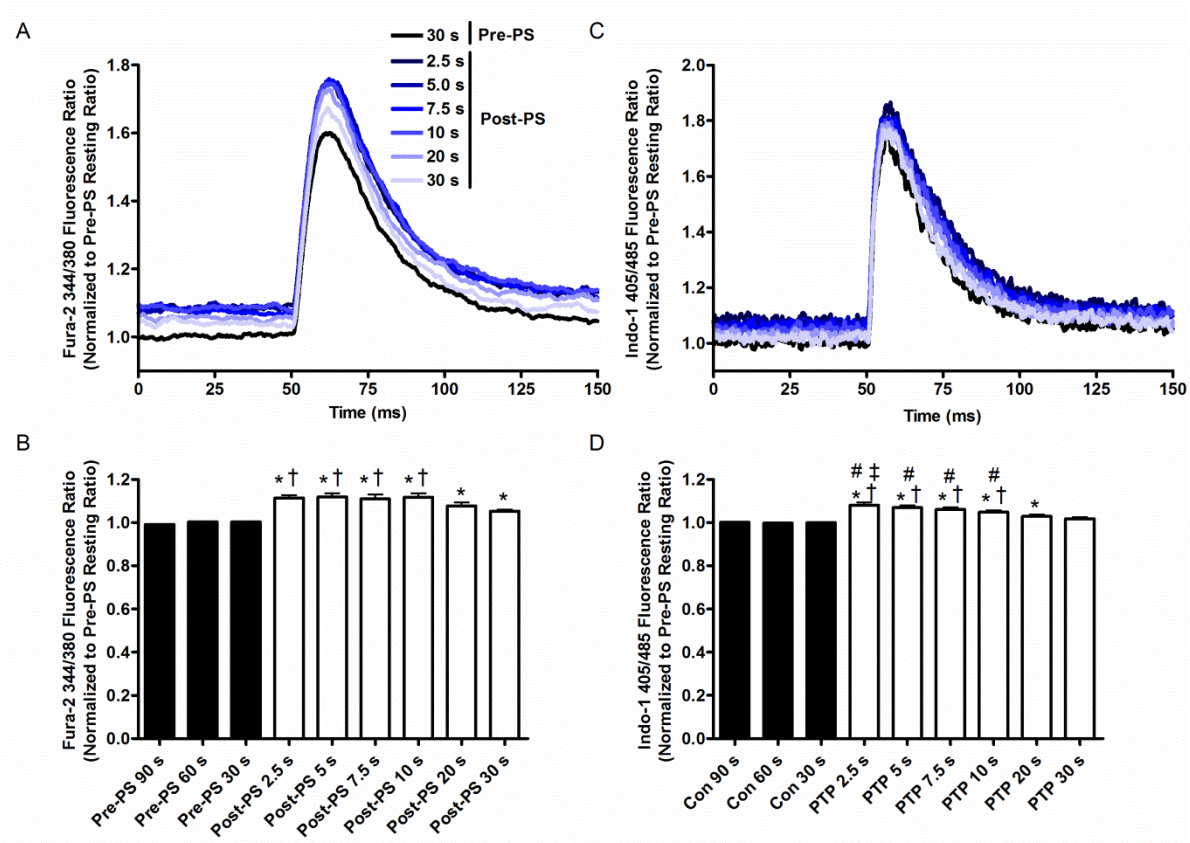

Figure II-6 - Resting Ca^{2+} and representative tracings using high affinity Ca^{2+} indicators
Averaged traces showing unpotentiated (pre-potentiating stimulus (PS)) and potentiated (post-PS) intracellular calcium transients are shown for fura-2 (A) and indo-1 (C) Each trace is the average of nine and eight muscles for fura-2 and indo-1 respectively. Relative changes in the fluorescence ratios measured just before the indicated stimulus after a PS of 20 Hz for 2.5 s are shown in panels B (fura-2) and D (indo-1).
* Value is greater than all pre-PS values ($P < 0.001$)
† Value is greater than post-PS 30 s ($P < 0.001$).
# Value is greater than 20 s Post-PS ($P<0.05$).
‡ Value is greater than 10 s Post-PS ($P<0.05$).

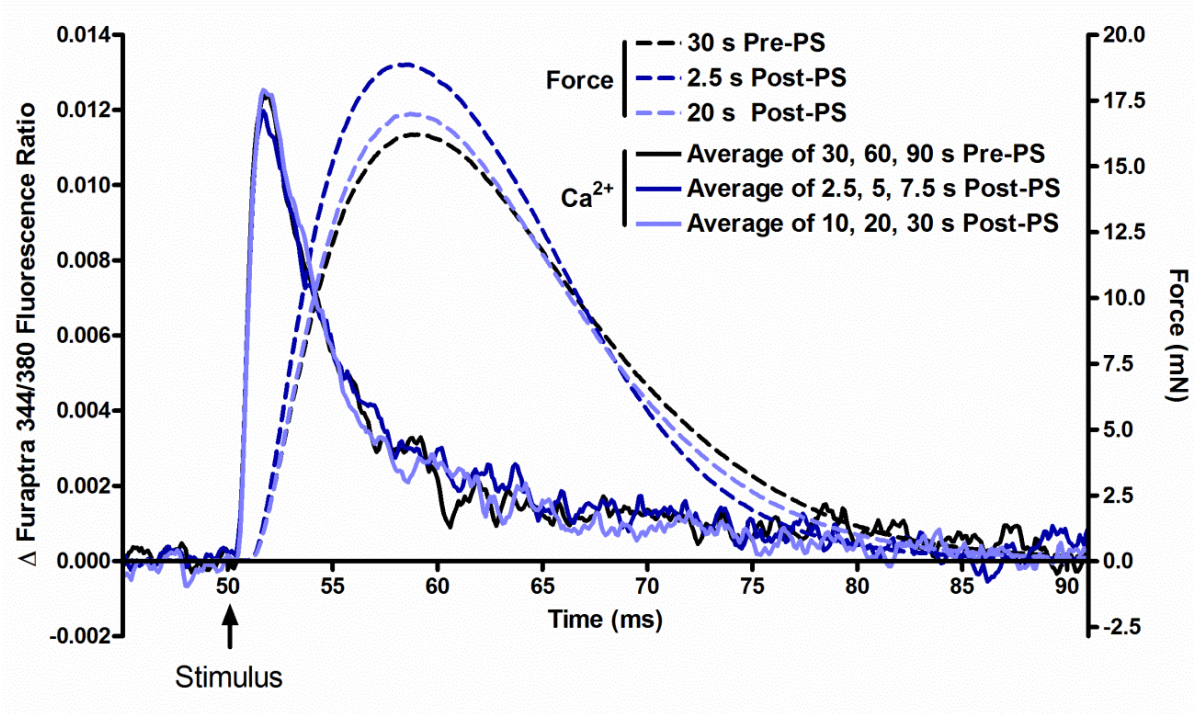

Figure II-7 – Change in furaptra fluorescence in potentiated lumbrical muscle
Averaged traces showing isometric twitch force and intracellular calcium transients before and after the potentiating stimulus (PS) of 20 Hz for 2.5 s. Each trace is the average of 10 muscles.

Table II-2- Intracellular calcium at rest and during stimulation in mouse lumbrical muscles at 37°C

Dye and Parameter	Time Pre-PS	Time Post-PS	
Furaptra	- 60 s	5.0 s	20 s
Amplitude (Ratio Units)	0.0131±0.0007	0.0127±0.0007	0.0132±0.0007
Time to peak (ms)	1.8 ± 0.1	1.8 ± 0.1	1.8 ± 0.1
ICT 50% decay time (ms)	3.1 ± 0.6	2.7 ± 0.4	2.8 ± 0.4
FWHM (ms)	3.6 ± 0.5	3.7 ± 0.4	3.7 ± 0.4
Fura-2	-30 s	2.5 s	30 s
Resting Ca^{2+} (Ratio Units)	0.376 ± 0.017	0.418 ± 0.022 *	0.395 ± 0.019 * †
Indo-1	-30 s	2.5 s	30 s
Resting Ca^{2+} (Ratio Units)	1.076±0.194	1.155 ± 0.209 *	1.091 ± 0.191 †

All data are presented as mean ± SEM (n = 10 furaptra, n = 9 fura-2, n=8 indo-1).Fura-2 and indo-1 data reported for 2.5 and 30 s correspond to peak twitch force potentiation and the first return of peak twitch force to unpotentiated levels after the potentiating stimulus (PS), respectively. Furaptra signals during twitch contractions were averages of those occurring 90, 60, and 30 s before the onset of the PS (denoted as - 60 s), 2.5, 5.0, and 7.5 s after the end of the PS (denoted as 5.0 s) and 10, 20, and 30 s after the end of the PS (denoted as 20 s) for each muscle. PS, potentiating stimulus (20 Hz for 2.5 s at optimum length for twitch tension (L_o)); ICT, intracellular Ca^{2+} transient; FWHM, full width at half-maximum.
* Post-PS value is significantly different than pre-PS value ($P < 0.001$).
† Post-PS value at 30 s is significantly different than post-PS value at 2.5 s ($P < 0.01$).

Myosin RLC phosphorylation, skMLCK, and MYPT2 content

Myosin RLC phosphorylation levels obtained from lumbrical and from EDL muscles are shown in Figure II-8 (A and B). An unexpected result was the complete absence of RLC phosphorylation in lumbrical muscles, as no phosphorylated RLC was detected in samples obtained before or after stimulation. On the other hand, phosphorylated RLC was detected in EDL samples obtained at rest and after stimulation. Consistent with these data was the Western blot analysis showing much lower expression of skMLCK and much higher expression of MYPT2 phosphatase in lumbrical muscle compared with EDL muscle (Figure II-8, C and D). Interesting in this regard was the similarity between soleus and lumbrical levels in both skMLCK and MYPT2 expression.

Fibre-type analysis

Figure II-9 compares the fibre-type composition of lumbrical, EDL, and soleus muscles from adult mice aged 3–5 mo, as determined by immunofluorescence analysis of the myosin isoform (as in Gittings *et al.*, 2011). These data show that the main fibre types contained by adult mouse lumbrical muscle are type IIX and associated hybrids (i.e., type IIAX and type IIXB), comprising ~61% of all fibre types. Notably, only a very small population of type IIB fibres was found. For comparison, the EDL is predominantly type IIB fibres, and soleus is a mainly a mixture of type I and IIA fibres. The total fibre count per lumbrical was 302 ± 17 muscle fibres (i.e., ~40% of that in either soleus or EDL). Both total cross sectional area and cross sectional area per fibre were lower ($P<0.05$) in lumbrical muscle than either EDL or soleus (data not depicted).

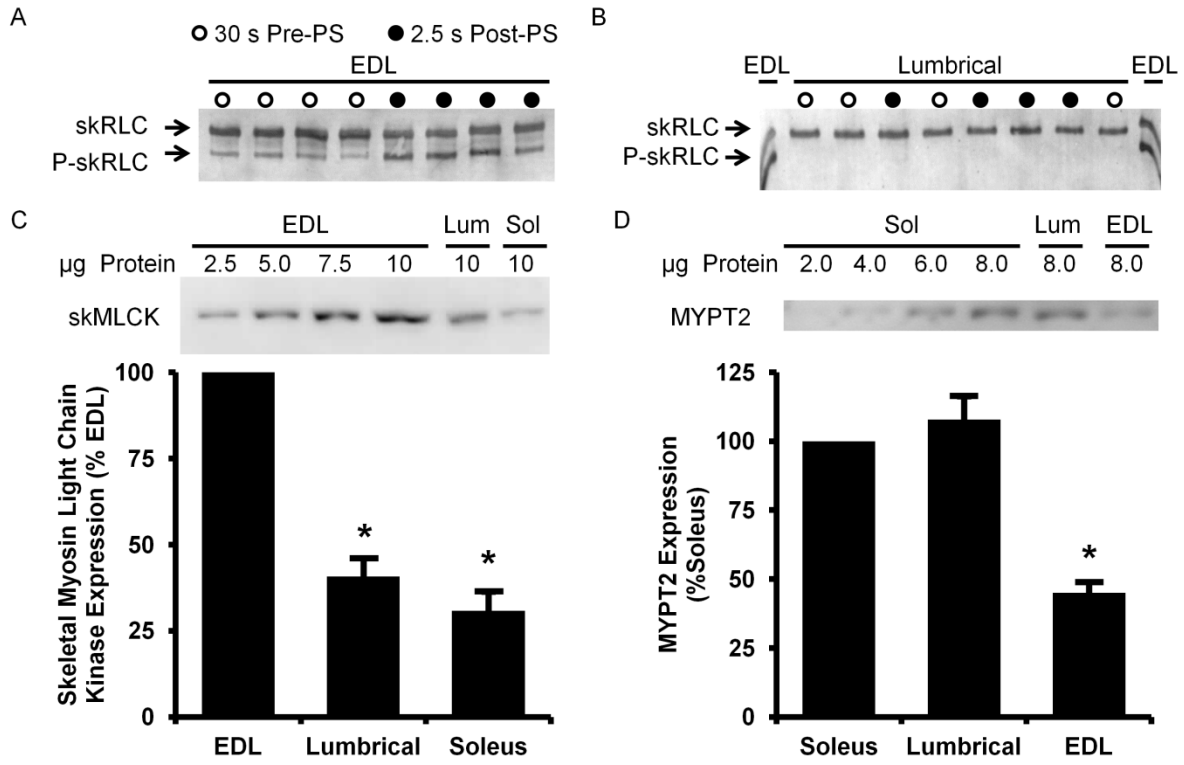

Figure II-8 – Myosin RLC phosphorylation, skMLCK, and MYPT2 in mouse muscles
Example blots showing phosphorylation levels in skeletal isoforms of myosin RLC (skRLC) in mouse EDL (A) and lumbrical (B) muscle 30 s before and immediately after the PS, revealing stimulation-induced elevations in RLC phosphorylation in EDL but not in lumbrical muscle. (C) Example Western blot and summary data showing skMLCK expression in mouse EDL, lumbrical (Lum), and soleus (Sol) muscle expressed relative to that EDL. *, value different than EDL value ($P < 0.01$; $n = 7$). (D) Example Western blot and summary data showing MYPT2 expression in mouse EDL, lumbrical (Lum), and soleus (Sol) muscle expressed relative to the soleus. *, value different than Sol value ($P < 0.01$; $n = 8$). Notes: For the skMLCK blot, each lane is an individual muscle (i.e., no pooling). For the MYPT2 blot, two lumbricals from the same animal (one from each hind foot) are pooled, whereas soleus and EDL are unpooled (because of size differences). For both skMLCK and MYPT2, each blot had the soleus, EDL, and lumbrical muscle from the same mouse lined up together, with two mice per gel.

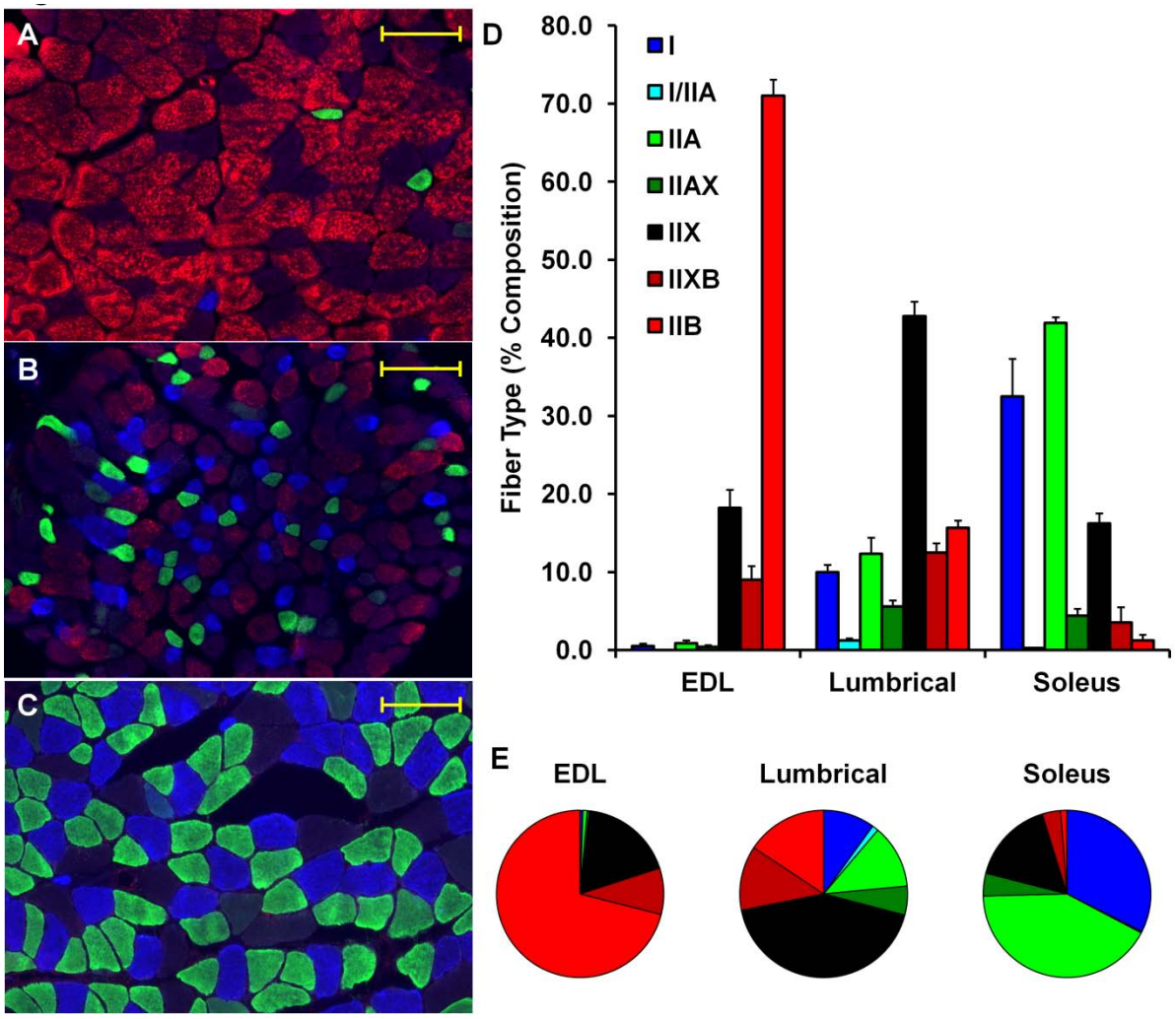

Figure II-9 - Immunofluorescence analysis of MHC isoform expression of mouse muscles Example of immunofluorescence staining performed as explained in the methods showing MHC I (blue), MHC IIa (green), MHC IIx (unstained), and MHC IIb (red) expression patterns in (A) extensor digitorum longus (EDL), (B) lumbrical, and (C) soleus muscle. Bars are scaled to 100 μm. Fibre-type composition was determined for the entire muscle cross section (n = 4 soleus and EDL; n = 8 lumbrical), and the data are presented as percent fibre-type composition by muscle in both bar (D) and pie (E) graph form. Note that the variance in fibre cross-sectional areas apparent in A–C is not a function of scaling but a function of muscle of origin, with fibre CSA being smaller in the lumbrical than the EDL, which is in turn smaller than that of the soleus. See also Bloemberg & Quadrilatero, 2012.

Discussion

The purpose of this study was to establish if the isometric twitch force potentiation observed in mouse lumbrical muscle could be attributed to stimulation-induced changes in myoplasmic free Ca^{2+} concentration, as opposed to putative increases in Ca^{2+} sensitivity as

mediated by RLC phosphorylation. The rationale for this line of inquiry was the presence of potentiation in skMLCK knockout muscles, suggesting at least a minor role for altered ECC in potentiation. By using a fast twitch muscle that has little or no skMLCK expression (Ryder *et al.*, 2007), it was possible to examine potentiation in the absence of the RLC phosphorylation mechanism. The main finding in the present study was the presence of a small and rapidly dissipating potentiation temporally correlated with stimulation-induced elevations in resting $[Ca^{2+}]_i$, independent of change to the ICT itself, thus providing evidence for an alternate mechanism for the activity-dependent increases in twitch force often observed in fast-twitch muscle models. Thus, the data suggest the presence of stimulation- induced alterations to Ca^{2+} handling that acutely increases isometric twitch force, a mechanism that may operate independently of the longer term potentiation offered by skMLCK-catalyzed RLC phosphorylation (see Stull *et al.*, 2011).

The mouse lumbrical at 37°C represents a relatively unique model with which to study force potentiation, making it difficult to make direct comparisons of the present results with the literature. Although comprised of ~89% of type II fibres, no phosphorylated RLC was detected in the samples either at rest or after stimulation. Although the absence of RLC phosphorylation and the minimal potentiation observed here seems incompatible with the typical rodent fast-twitch muscle profile (Schiaffino & Reggiani, 2011), the Western blot analysis, showing low skMLCK and high MYPT2 phosphatase expression in lumbrical relative to EDL muscle, corroborates the absence of detectable RLC phosphorylation in the current experiments. As a general point of comparison, the potentiation of mouse EDL muscle at 35°C reported by Moore *et al.* (1990) was approximately twice as great in magnitude and duration as observed here. The difference in potentiation between the two studies is perhaps accounted for by the

fact that, in their study, stimulation at 5 Hz for 20 s significantly elevated RLC phosphorylation levels. Interesting results from Ryder *et al.* (2007) may also apply to the current experiments. These investigators used transgenic mice over-expressing the skMLCK enzyme in skeletal muscle to show that despite similar levels for RLC phosphorylation (i.e., 50–60% phosphorylated), twitch force potentiation was much greater in EDL than in soleus muscles (Ryder *et al.*, 2007). This apparent uncoupling between RLC phosphorylation and twitch potentiation was hypothesized to be caused by the presence of type I and IIA fibres and the absence of type IIB fibres in soleus relative to EDL muscle; these data thus indicate a strong dependence within species fibre type for the ability of RLC phosphorylation to increase Ca^{2+} sensitivity (Ryder *et al.*, 2007). Indeed, the present work extends these data by showing that, in the wild-type mouse, skMLCK-catalyzed RLC phosphorylation may be restricted to IIB fibres with little RLC phosphorylation occurring in either IIX or IIA fibres. The relatively minor population of type IIB fibres found in the lumbrical helps account for the low overall skMLCK expression in this muscle. Moreover, although a fibre-type dependence for MYPT2 expression could not be identified here, the relatively high expression of MYPT2 suggests a limited ability to phosphorylate the RLC despite the prevalence of fast fibres.

Putative potentiation mechanism

Any adequate explanation for the current results must account for an increased twitch force in the absence of any myosin RLC phosphorylation–mediated increase in Ca^{2+} sensitivity. Although the data do not provide any mechanistic insights, the finding of an unchanged ICT amplitude superimposed upon an elevated basal $[Ca^{2+}]_i$ suggests that the Ca^{2+} activation of the thin filament may have been increased after stimulation. As pointed out by

Baylor and Hollingworth (2011), little is known regarding the aftereffects of tetanic stimulation on basal $[Ca^{2+}]_i$. Because this parameter was elevated for as long as potentiation was observed (i.e., 20–30 s) and was reversed shortly thereafter (i.e., 30–60 s), it was hypothesized that this change was mechanistically related to twitch force enhancement. One way in which an elevated basal $[Ca^{2+}]_i$ could have directly potentiated twitch force is through an increased binding and, thus, occupancy of the intracellular Ca^{2+} buffer protein parvalbumin in resting muscle. In this hypothesis, although basal $[Ca^{2+}]_i$ was not elevated above the threshold level for force development, partial saturation of parvalbumin-buffering capacity may have increased the fraction of free Ca^{2+} released from the sarcoplasmic reticulum that was able to bind to TnC on the thin filament, an effect not reflected by changes to the ICT itself. Indeed, the increased +dF/dt of potentiated twitches is consistent with an enhanced Ca^{2+} occupancy of TnC at the onset of contraction (Lee *et al.*, 2010). An alternate interpretation of the results is that the increase in basal $[Ca^{2+}]_i$ indirectly potentiated twitch force via some influence on thick filament distribution and/or structure. As an example, Brenner *et al.* (1982) used permeabilized rabbit psoas skeletal fibres to show the presence of a population of attached but non-force–generating cross-bridges at low ionic strength in the absence of Ca^{2+}. Further to this, Lehrer (2011) has recently proposed the existence of a regulated cross-bridge state that is sensitive to resting or sub-threshold levels of $[Ca^{2+}]_i$. Collectively, these studies seem to allow for the possibility that elevations in basal $[Ca^{2+}]_i$ may promote the transition of the attached but pre-force–generating cross-bridge state to the attached and force-generating cross-bridge state during the twitch (Lehrer, 2011;Brenner *et al.*, 1982). A final possibility worth considering is that elevations in basal $[Ca^{2+}]_i$ potentiate twitch force by increasing the occupancy of Ca^{2+}/Mg^{2+}-binding sites located on the RLC (Bagshaw & Reed, 1977;Robertson *et al.*, 1981).

Ca^{2+} binding to myosin has been shown to disorganize myosin head position on the thick filament surface of scallop muscle (e.g., Zhao & Craig, 2003;Zhao & Craig, 2008). If this effect of ligand binding to the myosin RLC has the same effect on thin filament–regulated vertebrate skeletal muscle as it does for thick filament–regulated molluscan muscle, it may facilitate the ability of cycling crossbridges to attain force-generating states (Diffee *et al.*, 1995;Diffee *et al.*, 1996). Thus, although the present data cannot rule out alternate mechanisms related to changes in metabolites brought about by stimulation (e.g., Pi) (Barclay, 1992), they may be adequately accounted for by the influence of altered basal Ca^{2+} homeostasis in resting muscle on cross-bridge structure and/or distribution.

Relation to previous studies

Decostre *et al.* (2000) tracked fluorescence signals from the surface of mouse EDL muscles loaded with fura-2 (20°C) during posttetanic potentiation. These investigators observed an ~10% increase in isometric twitch force immediately after stimulation at 125 Hz for 1 s, a potentiation that then decayed slowly and was absent 300 s later. Consistent with the current results, however, elevations in basal and peak $[Ca^{2+}]_i$ were observed, although the absolute change in ICT amplitude was similar in potentiated versus unpotentiated states (Decostre *et al.*, 2000). Interestingly, the application of 1 μM adrenaline to maintain post-stimulus elevations in myosin RLC phosphate content produced a greater and more prolonged potentiation of twitch force (10–15% for >300 s) that was evident after the stimulation-induced alterations in $[Ca^{2+}]_i$ had been reversed. This outcome suggests that, although stimulation-induced elevations in $[Ca^{2+}]_i$ may contribute, they are not a requisite for twitch force potentiation. This helps account for why rat fast-twitch muscle models displaying reduced

RLC phosphorylation also exhibit reduced potentiation (Tubman *et al.*, 1996;Tubman *et al.*, 1997). Based on these and the present results, stimulation-induced elevations in resting $[Ca^{2+}]_i$ and in RLC phosphorylation may provide an acute and persistent twitch force potentiation, reversed by the rapid return of resting Ca^{2+} homeostasis and/or the slow rate of RLC dephosphorylation by PP1 phosphatase activity, respectively (Stull *et al.*, 2011).

Study limitations

The advantages and disadvantages of using high and low Ca^{2+} affinity indicators for determination of $[Ca^{2+}]_i$ in intact skeletal fibres have recently been presented by Baylor and Hollingworth (2011). Although use of AM dyes offers many advantages, an intractable issue is that of a non-cytosol-specific compartment component to the global fluorescent signal (see Morgan *et al.*, 1997). Thus, although it was assumed that the loci for the elevated resting $[Ca^{2+}]_i$ was the myoplasm, this cannot be absolutely confirmed from the present experiments. In addition, although furaptra retains the ability to precisely track the ICT in the range of 28 to 35°C (Hollingworth *et al.*, 1996), it is possible that the high temperature used may have mitigated the ability to detect changes in ICT duration caused by the PS.

Summary

The present results provide a putative mechanism for posttetanic potentiation of isometric twitch force reported in the absence of myosin RLC phosphorylation. Although the skMLCK-catalyzed phosphorylation of the myosin RLC should still be considered the primary mechanism, repetitive or high frequency stimulation that elevates resting $[Ca^{2+}]_i$ may contribute a fast-acting component to isometric twitch force potentiation, reversed by the rapid

return of Ca^{2+} homeostasis after stimulation. The functional implications of this mechanism remain to be determined.

Chapter III - Staircase potentiation is enhanced by slowing of the calcium transient

Outline

While posttetanic potentiation occurs without affecting the intracellular cytosolic Ca^{2+} transients that trigger contraction, animal models which potentiate without increasing myosin regulatory light chain phosphorylation typically exhibit greater staircase potentiation than posttetanic potentiation. Therefore it is possible that alterations in the cytosolic Ca^{2+} may occur and contribute to staircase potentiation. Additionally, staircase potentiation and temperature are proportionally related, but the contribution of the Ca^{2+} transient to this relationship has not been determined. Thus this study aimed to determine if Ca^{2+} transients are altered during staircase potentiation at either 30 (n=6) or 37^{o}C (n=7). Mouse lumbricals were loaded with AM-furaptra, a Ca^{2+}-sensitive fluorescent indicator, and stimulated at 8 Hz for 8 s while force and fluorescence signals were recorded. Unpotentiated twitches were similarly recorded at 30 s intervals prior to the staircase protocol. After 8 s, twitch force was 26.8 ± 3.2 % higher ($P<0.05$) at 37^{o}C and 6.8 ± 1.9 % lower ($P<0.05$) at 30^{o}C relative to unpotentiated values. Peak amplitude of Ca^{2+} transients dropped at both temperatures and remained low throughout the protocol, however this decline was greater at 30^{o}C ($P<0.05$). Beginning ~2 s into the protocol, the duration of the Ca^{2+} transients began to increase, a change mirrored by twitch contraction times. Regression analysis revealed that the raw peak amplitudes of Ca^{2+} transients, which are reflective of the peak intracellular Ca^{2+} concentration, progressively increased at 37^{o}C and progressively decreased at 30^{o}C. In conclusion, progressive increases in the duration of the Ca^{2+} transient contribute to force enhancement during staircase potentiation, while temperature-dependent declines in the amplitude of the Ca^{2+} transient contribute to the reduced or absent potentiation seen at lower temperatures.

Introduction

Excitation-contraction coupling is the process by which electrical impulses are converted into mechanical forces in muscle. The force a muscle produces is largely regulated by changes in intracellular Ca^{2+} which are increased following an applied voltage or action potential. Ca^{2+} is released from the sarcoplasmic reticulum through the ryanodine receptor where it can bind to troponin C, freeing myosin binding sites on actin, allowing crossbridge formation and force production. Cytosolic Ca^{2+} levels are returned to resting levels by the sarco-endoplasmic reticulum Ca^{2+}-ATPase (SERCA), an ATP dependent pump which translocates Ca^{2+} across the SR membrane. The force a muscle produces in response to a single action potential or electrical impulse is known as a twitch contraction.

The force of a twitch contraction is dependent on the contractile history of the muscle. Repetitive stimulation of fast twitch skeletal muscle at low stimulation frequencies (<10 Hz) produces a stepwise increase in twitch force known as staircase potentiation (Isaacson, 1969). The primary mechanism causing potentiation in general is an increase in the phosphate content of the myosin regulatory light chain (RLC) (Sweeney *et al.*, 1993;Grange *et al.*, 1993). This causes the myosin heads to project outwards from the thick filament, reducing the distance between the myosin heads and the myosin binding sites on the thin filament (Levine *et al.*, 1996;Yang *et al.*, 1998). This increases the Ca^{2+} sensitivity of crossbridge formation resulting in an increased number of strongly bound cross bridges for any given submaximal concentration of Ca^{2+} in the vicinity of the contractile proteins, thereby enhancing submaximal forces such as those seen during a twitch contraction (Sweeney & Stull, 1990).

A small but growing body of evidence indicates that there are multiple complementary mechanisms localized within the muscle which can cause potentiation. Extensor digitorum

longus of mice devoid of the kinase responsible for phosphorylating the RLC (Zhi *et al.*, 2005;Gittings *et al.*, 2011) and denervated rat gastrocnemius (Rassier *et al.*, 1999;MacIntosh *et al.*, 2008) exhibit staircase potentiation without associated increases in RLC phosphate incorporation. While an alternative mechanism has not definitively been identified, it has been recently investigated. A recent investigation (Chapter II;Smith *et al.*, 2013b) examined intracellular Ca^{2+} transients during posttetanic potentiation in mouse lumbrical muscle which exhibits short-lasting posttetanic potentiation without RLC phosphorylation. It was concluded that while changes to the intracellular Ca^{2+} transient do not contribute to post-tetanic potentiation, the potentiation appeared to be caused by elevations in basal Ca^{2+}. It remains to be determined if changes in the intracellular Ca^{2+} transient can contribute to staircase potentiation. This scenario seems quite likely given that staircase potentiation is maintained, though reduced, in models with no myosin regulatory light chain phosphorylation and no post-tetanic potentiation (Zhi *et al.*, 2005;Rassier *et al.*, 1999;MacIntosh *et al.*, 2008). Therefore the primary purpose of this study was to determine if changes in the Ca^{2+} transients contribute to the force responses during staircase potentiation.

Also of interest, both staircase and post-tetanic potentiation are reduced as a muscle cools (Krarup, 1981;Moore *et al.*, 1990;Close & Hoh, 1968;Hanson, 1974;Walker, 1951;Vandenboom *et al.*, 2013). As characteristics of the action potential are similar during bouts of repetitive stimulation at 22 and 37^{o}C (Hanson, 1974), particularly over short durations, the mechanism must be a change in a downstream signal. Thus far the temperature-dependency of potentiation has been attributed to reduced myofilament activation during twitches at higher temperatures (Moore *et al.*, 1990;Close & Hoh, 1968) caused by a greater relative increase in the rate of Ca^{2+} uptake compared to that of myosin ATPase activity

(Bennett, 1985). However, this argument is not wholly satisfactory as it is inconsistent with the inverse relationship between temperature and myosin RLC phosphate incorporation during a constant potentiation-inducing stimulation (Moore *et al.*, 1990). Therefore, this study also aimed to determine if the experimental temperature can affect the Ca^{2+} transient during staircase potentiation. As a part of this investigation, the expression of the proteins important for initiating relaxation following contraction were characterized, namely the sarco-endoplasmic reticulum Ca^{2+} ATPase isoforms SERCA1a and SERCA2a, along with parvalbumin in EDL, soleus and lumbrical muscles.

In this study, temperature-dependent declines in the amplitude and the Ca^{2+}-time integral of the Ca^{2+} transient, along with increases in the duration of the Ca^{2+} transient which coincide with increases in the duration of the twitch contraction late in a staircase inducing stimulation protocol are reported.

Methods

All methods used in this study were approved by the University of Waterloo Committee for Animal Care, and all experiments were performed in the laboratory of Dr. Russ Tupling at the University of Waterloo. Detailed descriptions of the methods used in this study are described in Chapter II and as recently reported (Smith *et al.*, 2013b) . Briefly, lumbrical muscles from the hind feet of male C57BL/6 mice aged 3-6 months were excised in Tyrode's dissecting solution (mM: 136.5 NaCl, 5.0 KCl, 11.9 $NaHCO_3$, 1.8 $CaCl_2$, 0.40 NaH_2PO_4, 0.10 ethylenediaminetetraacetic acid (EDTA), and 0.50 $MgCl_2$, pH 7.5; on ice). Muscles were then suspended at optimum length for twitch force production (L_o) between a high speed length controller (model 322C; Aurora Scientific Inc.) and a force transducer (model 400A; Aurora Scientific Inc.) in a bath containing circulating oxygenated (95% O_2, 5% CO_2) Tyrode's

experimental solution (mM: 121.0 NaCl, 5.0 KCl, 24.0 $NaHCO_3$, 1.8 $CaCl_2$, 0.40 NaH_2PO_4, 5.50 glucose, 0.10 EDTA, and 0.50 $MgCl_2$, pH 7.3) at either 30 (n=6) or 37^oC (n=7). The free concentrations of Ca^{2+} and Mg^{2+} were estimated to be 1.7 and 0.5 mM respectively, in both Tyrode's solutions. Stimulation was applied through flanking platinum plate field stimulus electrodes using a model 701C stimulator (Aurora Scientific Inc.) at supramaximal voltage. Lumbrical muscles were loaded with the low affinity ratiometric Ca^{2+} indicator AM-furaptra (Molecular Probes) to detect transient changes in the intracellular Ca^{2+} concentration. Monochromator (Photon Technology International) controlled light at either 380 or 344 nm provided the excitation signal to the muscle-bound furaptra, and the resulting 510 nm fluorescence emission signals were collected through an inverted microscope photometer system (D-104; Photon Technology International) affixed with a photomultiplier tube (PMT; model 814; Photon Technology International). Analog force and fluorescence signals were digitized and collected at 10,000 Hz and stored for later analysis.

Experimental Protocol

A schematic illustration of the stimulation protocol used in this study is shown in Figure III-1. AM-furaptra loaded lumbricals were stimulated once per 30 s to produce a steady isometric twitch force response. Fluorescence emission signals from the last five twitches were used to determine the characteristics of the unpotentiated Ca^{2+} transient. This pacing procedure was then halted and an 8.0 Hz staircase protocol lasting for 8.0 s was initiated with continuous fluorescence emission monitoring. This protocol was used as it allowed force to return to resting values between consecutive twitches at both 30 and 37^oC. The muscle was then subjected to the pacing protocol for 4 min to monitor dissipation of the potentiation response.

The excitation wavelength was adjusted and the stimulation protocol was repeated 10 times per muscle, alternating between 380 and 344 nm excitation to produce 5 fluorescence ratio signals which were averaged together during data analysis. Data were further condensed by averaging the five unpotentiated twitches into a single record, and staircase was condensed into four windows where all twitches within 2.0 s blocks were averaged together i.e. 16 twitches per window. The different number of twitches per window in the unpotentiated and potentiated states did not affect the final results as demonstrated in Chapter IV. Statistical analysis was performed using 2 way split-plot ANOVA using temperature (between groups) and time (repeated measures).

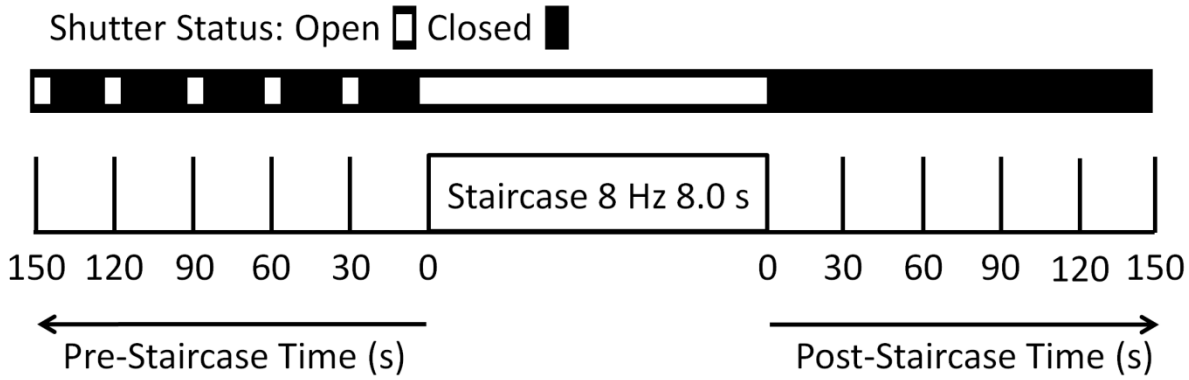

Figure III-1 – 8.0 s staircase potentiation experimental time line
Lumbricals were stimulated at 30 s intervals to elicit control twitch contractions. Next staircase potentiation was induced by an 8.0 s 8 Hz contraction followed by twitches at 30 s intervals to monitor the dissipation of potentiation. This procedure was repeated 10 times for each muscle with 30 - 60 s gaps between consecutive trials. The shutter controlling exposure to light was open for 1.0 s windows during individual twitch contractions and for 9.0 s windows during staircase contractions. The wavelength of light used to excite furaptra was alternated between 344 and 380 nm between consecutive trials, producing five ratio signals (380/344 nm) per twitch per muscle.

Western Blotting

Western blotting techniques were used to determine relative expression levels of muscle relaxation enzymes (SERCA1a, SERCA2a, parvalbumin) in whole muscle

homogenates of the lumbrical, soleus and EDL of the mouse (n=8). Separation of proteins was performed by electrophoresis using either 7.5% polyacrylamide glycine gels (SERCA1a, SERCA2a) or 13% polyacrylamide tricine gels (parvalbumin) and standard SDS/PAGE protocols (Laemmli, 1970). Protein concentrations of homogenates were determined by the bicinchoninic acid method (Sigma). A linear relationship between band density and protein load was established for each mouse using either EDL (SERCA1a, parvalbumin) or soleus (SERCA2a) to form a scale against which the other muscles were compared. Following semi-dry transfer of proteins to polyvinyl difluoride membranes, primary and secondary probing was performed as described in Table III-1. Detection was performed using a Luminata HRP substrate detection kit (Millipore, MA, USA) and subsequent quantification was based on densitometric analysis obtained using GeneSnap and GeneTools software (GE Healthcare).

Table III-1 - Antibodies used in Western blotting analysis

Protein	Primary Antibody (Source)	Secondary Antibody (source)
SERCA1a	Monoclonal anti-SERCA1a A52 (Gift from Dr. David MacLennan)	Goat anti-mouse (Santa Cruz)
SERCA2a	Anti-SERCA2a 2A7-A1 (Affinity Bioreagents)	Goat anti-mouse (Santa Cruz)
Parvalbumin	PVG 214 Goat Anti-Parvalbumin (Swant)	Donkey anti-goat (Santa Cruz)

Statistics

All data are reported as mean ± SEM. Relative changes in mean values for various twitch force and Ca^{2+} parameters were compared by a repeated measures ANOVA followed by Tukey's HSD post-hoc analysis using Statistica 7 software. Linear regression analyses were performed using GraphPad Prism 4.0 software. Differences were considered significant at $P < 0.05$.

Results

Mechanical Recordings 37^{o}C

The force and kinetic recordings during the 8.0 s staircase potentiation protocol point to the existence of two distinct phases which are characterized by the changes in twitch time course (Figure III-2). The first phase (~0 – 2 s) is associated with enhanced twitch time course with decreased times to peak tension (TPT) and 50% relaxation times (1/2RT). During this time, there are only small increases in peak twitch force and the peak rate of force production (+df/dt) is slow to rise whilst the rise in the peak rate of relaxation (-df/dt) is approximately linear. The second phase is characterized by relative increases in the TPT and 1/2RT from the minima achieved in the first 2.0 s. During this second phase, +df/dt and peak twitch force increase and approach a plateau by the 8.0 s time point, whereas the peak rate of relaxation increases up to ~ 6.0 s until slowing into the final 2.0 s of the protocol. Thus a maximally potentiated lumbrical using this protocol is characterized as a twitch with 26.8 ± 3.2% higher force, 4.4 ± 1.9 % lower TPT, 11.4 ± 2.5% higher 1/2RT, 43.6 ± 1.6% faster +df/dt and 11.1 ± 2.5% faster –df/dt than an unpotentiated twitch (all $P<0.05$; See also representative tracings in Figure III-2A and raw force values in Table III-2).

Mechanical Recordings 30^{o}C

Like the 37^{o}C data, the force recordings at 30^{o}C can be separated into two phases based on the changes in the twitch time course (Figure III-2). Also much like the 37^{o}C data, the first phase (~0-2 s) is marked by steep declines in both the TPT and 1/2RT with a slow rise in the +df/dt and a relatively linear increase in the –df/dt. However, the peak twitch force declines over the first phase rather than increasing as it does at 37^{o}C. Additionally, the relative increases

in +df/dt and -df/dt are lower and the relative declines in TPT and 1/2RT are larger at 30°C than 37°C. The second phase of staircase at 30°C is characterized by a relatively slow decline in the TPT and progressive increases in the 1/2RT. Force remains relatively constant at the depressed levels achieved in the first phase while +df/dt increases to a plateau at 6.0 and –df/dt reaches plateau at ~4.0 s before slowing to near unpotentiated levels by the end of the protocol. Thus the 8.0 s Hz protocol results in changes in the characteristics of the final twitch with 6.8 ± 2.0% lower force ($P<0.05$), 19.0 ± 3.7 % lower TPT ($P<0.05$), 8.8 ± 3.9% lower 1/2RT ($P<0.05$), 18.3 ± 3.6% faster +df/dt ($P<0.05$) and 1.6 ± 3.2% slower –df/dt (not significant) than an unpotentiated twitch. Interestingly, 30 s following the staircase protocol, the differences in the kinetic characteristics of the twitches at 30 and 37°C became quite similar. Twitches at both temperatures exhibited force potentiation (3.4±1.1% and 7.4±2.4% relative to unpotentiated levels at 30 and 37°C respectively), while –df/dt was faster and 1/2RT was reduced relative to unpotentiated twitches (all $P<0.05$; not depicted).

Table III-2 - Raw force values and potentiation during 8.0 s of 8 Hz stimulation

Condition		**Force (mN)**		**Potentiation (%)**
Twitch Number	**90 s Pre**	**1**	**64**	**64**
30°C	22.7 ± 1.8	22.5 ± 1.7	21.0 ± 1.6 *	-6.8 ± 1.9
37°C	17.4 ± 1.7 †	17.3 ± 1.7 †	21.7 ± 1.8 *	26.8 ± 3.2 †

Mouse lumbrical muscles were stimulated at 8 Hz for 8.0 s at either 30 or 37°C. Peak twitch force is reported for the first (Twitch 1) and last twitches (Twitch 64) of this protocol, along with an unpotentiated twitch occurring 90 s prior to the initiation of the stimulation protocol (90 s Pre). % Potentiation refers to the relative change in peak force seen between the first and last twitches within each condition. See Figure III-2 for more detailed tracings. All values are presented as mean ± SEM. * Different from twitch 1 and 90 s Pre ($P<0.05$). † Different than 30°C ($P<0.05$).

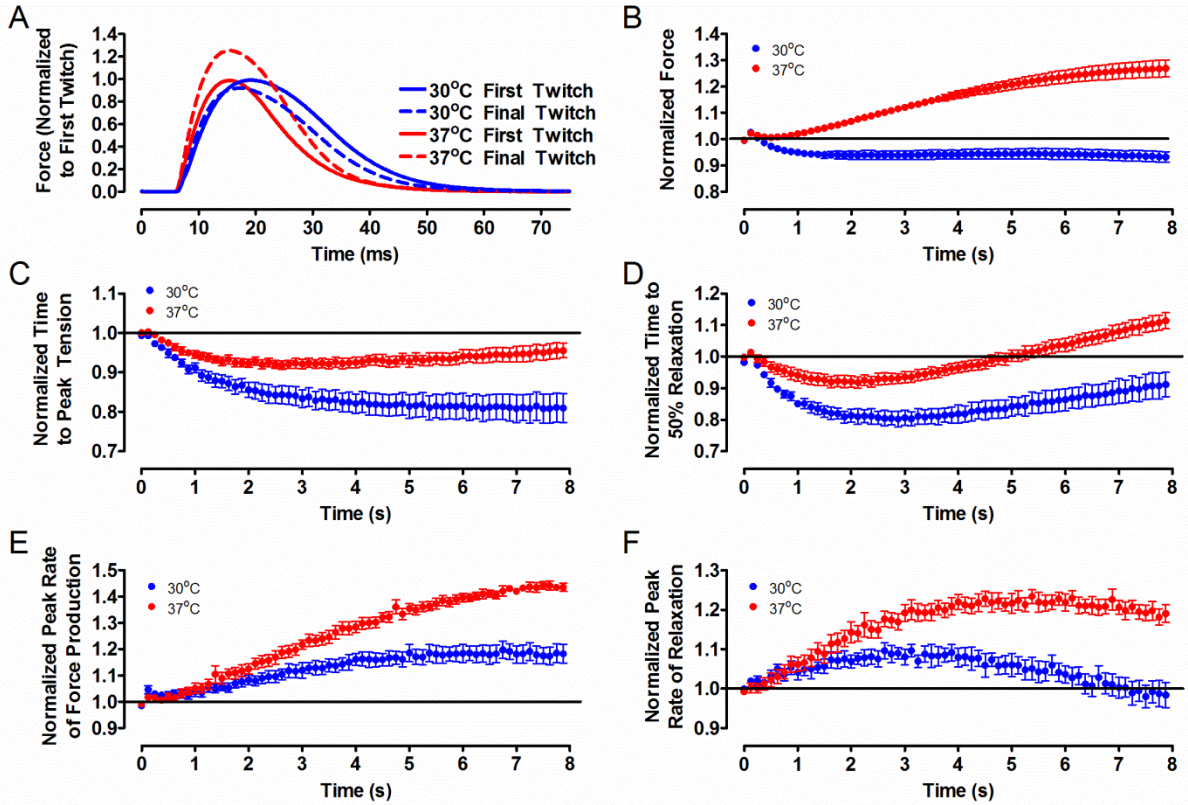

Figure III-2 - Twitch characteristics during 8.0 s of 8 Hz stimulation at 30 and 37°C
Mouse lumbrical muscles were subjected to 10 cycles of 8 Hz stimulation for 8.0 s separated by 5 minute resolution periods during which the muscles were stimulated once every 30 s. Experiments were performed at either 30 (n=6; blue) or 37°C (n=7; red). Sample tracings of the first and final twitch of the 8 Hz protocol are illustrated in panel A. Peak force (B), time to peak tension (C), time to 50% relaxation (D), peak rate of force production (E) and peak rate of relaxation (F) were all normalized to the average of the 3 twitches immediately preceding the onset of the 8 Hz stimulation protocol for each temperature. Data were averaged across the 10 trials for each muscle, and the mean ± SEM of these values are plotted above.

Fluorescence Recordings

Ratio signals from lumbricals loaded with AM-furaptra and subjected to 8 Hz stimulation for 8.0 s are shown in Figure III-3A and C. Linear regression analysis of raw ratio signals during the staircase protocol revealed an inability of the muscles to maintain peak amplitude of the Ca^{2+} transients at 30°C while at 37°C the peak amplitude increased (Figure III-3B, D). While caution should be taken when interpreting changes in furaptra signals at low

calcium concentrations due to the low affinity of the indicator to Ca^{2+}, there were noticeable increases in the basal ratios during the first 4 twitches at both temperatures. However, regression analysis across the full 8 s staircase procedure indicated the basal ratios were increased at 37^{o}C ($P<0.05$), but not at 30^{o}C (Figure III-3B, D).

Furaptra records were adjusted for basal ratios and averaged together in 2.0 s windows during staircase and for 5 unpotentiated twitches occurring at 30 s intervals before the staircase protocol. The resulting transient records are plotted in Figure III-4A and B. Analysis of these transients revealed that regardless of temperature, peak amplitude was lower during the staircase protocol relative to the unpotentiated transients (Figure III-4C). The decline in peak amplitude was reflected by a decline in the Ca^{2+}-time integral during the first 2.0 s of staircase, however, the Ca^{2+}-time integral returned to initial unpotentiated values by the 6-8 s window (Figure III-4D). This time-dependent increase corresponded to an increase in the decay time of the Ca^{2+} transient as indicated by the progressive elevations in 50% relaxation time and full width at half maximum as the stimulation protocol progressed (Figure III-4F). While these were all temperature-independent effects, the magnitudes of the initial decreases in the peak ratios ($3.13x10^{-3} \pm 0.44x10^{-3}$ vs. $1.68x10^{-3} \pm 0.44x10^{-3}$ ratio units; $P<0.05$) and Ca^{2+}-time integrals ($1.74x10^{-2} \pm 0.45x10^{-2}$ vs. $0.87x10^{-2} \pm 0.42x10^{-2}$ ratio units•ms; $P=0.09$) were higher at 30^{o}C than 37^{o}C. Collectively, these results indicate that the changes in force and force kinetics seen late in the protocol correspond well to changes seen in the Ca^{2+} transient.

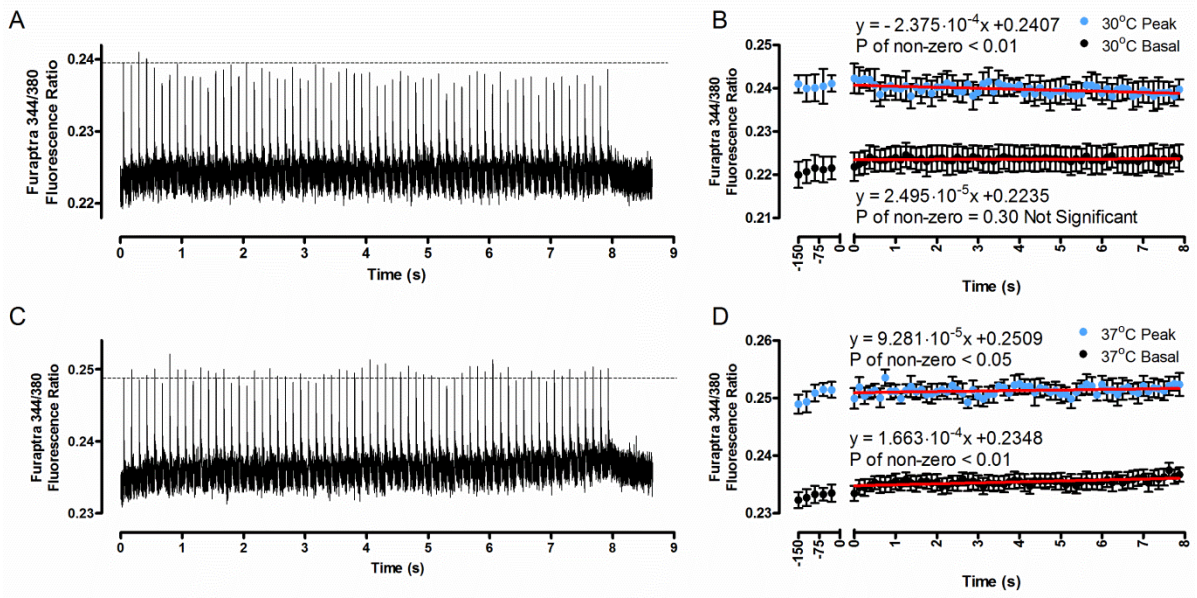

Figure III-3 - Raw furaptra ratios during 8.0 s staircase potentiation

Mouse lumbrical muscles loaded with AM-furaptra were subjected to a staircase potentiation inducing protocol of 8 Hz for 8.0 s. Fluorescence emission by furaptra was measured at 505 nm following excitation at alternating wavelengths of 380 and 344 nm, alternating between consecutive staircase trials. The resulting 344/380 nm emission ratios were averaged across all trials and muscles at 30 (n=6) and 37^{o}C (n=7) as illustrated in panels A and C respectively. The dashed line serves as a reference to the peak amplitude of the Ca^{2+} transient of the first twitch in the protocol. Also note also the increases in the basal fluorescence ratio in the first 1.0 s of the protocol and the reductions in basal fluorescence after the end of the stimulation protocol at 8.0 s. The peak amplitude of each Ca^{2+} transient and the average fluorescence ratio during the 10 ms immediately preceding each Ca^{2+} transient (basal) were plotted for each muscle (mean ±SEM; panels B and D) and analyzed using linear regression. Equations of the regression lines and the probabilities (P) of the slopes being different from zero are shown, demonstrating declining peak amplitudes at 30^{o}C, and rising basal Ca^{2+} and peak amplitudes at 37^{o}C. Time points less than zero correspond to measures taken during unpotentiated twitches.

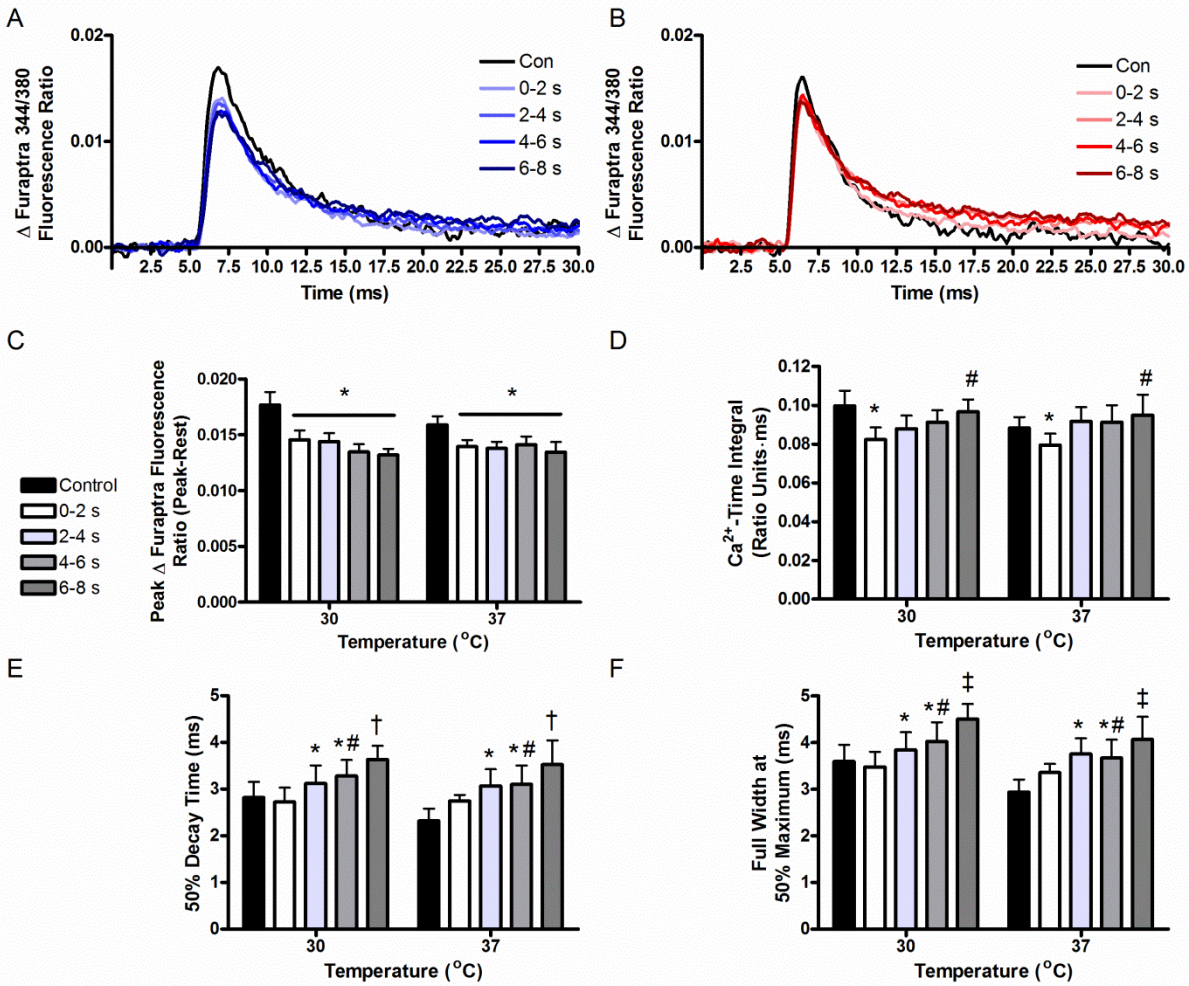

Figure III-4 - Ca^{2+} transients and kinetic characteristics during staircase potentiation (8.0 s)

Intracellular Ca^{2+}-transients from mouse lumbricals loaded with AM-furaptra during individual twitch contractions applied at 8 Hz for 8 s at either 30 (n=6; A) or 37°C (n=7; B) were averaged over 2.0 s intervals. Control twitches (6 per record) were measured at 30 s intervals prior to the onset of the staircase protocol. Values are expressed relative to the average ratio over the 10 ms immediately preceding each contraction (i.e. basal). The peak Δ furaptra ratio (C) represents the difference between the maximum ratio during the Ca^{2+} transient and the basal amplitude. Ca^{2+}-time integrals represent the area confined by the basal ratio and the transient ratio, lasting 20 ms after the stimulation (D). 50% decay time (E) refers to Ca^{2+}-removal phase of the transient and is defined as the time it takes the signal to decline from the peak Δ furaptra ratio to 50% of this value. Similarly, the full width at 50% maximum is the duration of the transient at 50% of the peak Δ furaptra ratio (F). All values are mean ± SEM. All symbols shown correspond to main effects; no interactions were found. * - Different from Control. # - Different from 0-2 s. † - Different from Control, 0-2 and 2-4 s. ‡ - Different from Control, 0-2, 2-4 and 4-6 s. All $P<0.05$.

Western Blotting Results

Relative expression levels of muscle relaxation proteins were established for EDL, soleus and lumbrical muscles as illustrated in Figure III-5. In general, the expression profile of Ca^{2+}-sequestering proteins (i.e. the proteins responsible for muscle relaxation) of lumbrical lies between the extremes set by the slow-relaxing soleus and fast-relaxing EDL. More specifically, comparing EDL to lumbrical, EDL has ~62% more SERCA1a ($P<0.05$), and ~5 fold higher expression of parvalbumin ($P<0.05$) than the lumbrical. No significant difference was detected in SERCA2a levels between the EDL and lumbrical. Comparing EDL to soleus, EDL has ~3.3 fold higher expression of SERCA1a ($P<0.05$), ~60% less SERCA2a ($P<0.05$) and ~19x more parvalbumin ($P<0.05$) than soleus muscle. The lumbrical was found to have 2x more SERCA1a ($P<0.05$), 47% less SERCA2a ($P<0.05$) and 3.7x more parvalbumin ($P<0.05$) than soleus.

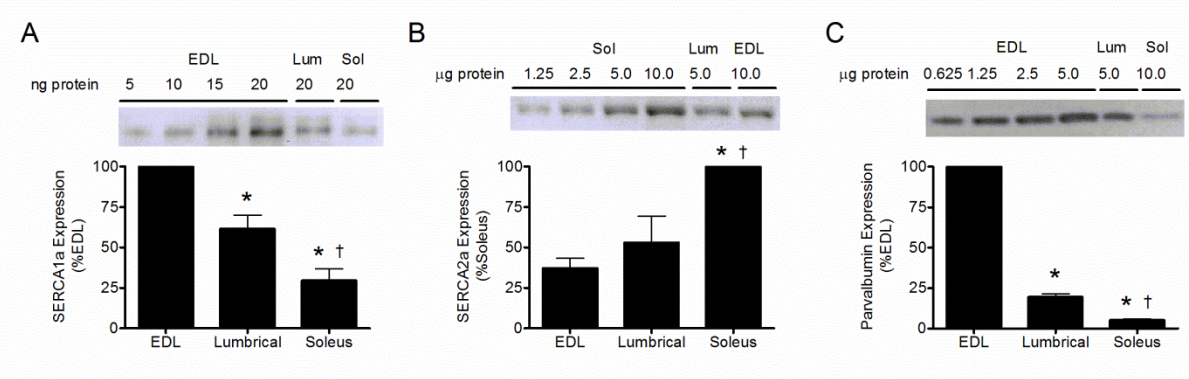

Figure III-5 – Protein expression of Ca^{2+}-sequestering proteins
This figure depicts sample Western blots and summarized densitometric analysis data for SERCA1a (A), SERCA2a (B) and parvalbumin (C). All values are expressed relative to a linear protein gradient established with either extensor digitorum longus (EDL) (SERCA1a and parvalbumin) or soleus (sol) (SERCA2a). N=8 for all muscles and proteins. * Significantly different than EDL. †Significantly different than lumbrical (lum). Significance was taken at $P<0.05$. Notes: Two lumbricals from the same animal (one from each hind foot) are pooled, whereas soleus and EDL are not pooled due to size differences. For both SERCA isoforms, each blot had the soleus, EDL, and lumbrical muscle from the same mouse lined up together, with two mice per gel, while the parvalbumin blots were run with only one mouse required an entire gel due to the larger number of data points on the protein gradient scale required due to the larger differences between EDL and soleus. See Appendix 2 for simpler versions of these blots.

Discussion

The primary purpose of this study was to determine if changes in the characteristics of the Ca^{2+} transient during staircase potentiation could contribute to the elevations in force seen during staircase potentiation. This question is of particular interest given fast twitch muscles that do not phosphorylate their myosin RLC, ~50% of staircase potentiation is maintained while posttetanic potentiation is largely absent (Zhi *et al.*, 2005;Rassier *et al.*, 1999;MacIntosh *et al.*, 2008).To this end, Ca^{2+} transients were measured during 8.0 s of 8 Hz contraction in mouse lumbrical muscle, a model which was recently shown to exhibit post-tetanic potentiation without RLC phosphorylation (Smith *et al.*, 2013b). A part of this investigation aimed to determine if changes in the Ca^{2+} transient may contribute to the declines in

potentiation as temperature decreases (Krarup, 1981;Moore *et al.*, 1990;Close & Hoh, 1968;Hanson, 1974;Walker, 1951). This study, along with the accompanying follow up study (Chapter IV) which examines the changes in the Ca^{2+} transient within the first 2 seconds of staircase potentiation, are the first studies to measure Ca^{2+} transients during staircase potentiation.

Potentiation by the Ca^{2+} Transient

The current results indicate a temporal match between prolongations of the durations of the intracellular Ca^{2+} transient and the twitch contraction during the latter half of staircase potentiation. This occurred independent from the temperature effects. This prolongation of the Ca^{2+} transient appears causative to the changes in twitch duration in the latter half of the protocol as increased exposure to Ca^{2+} allows greater opportunity for crossbridge production. It is unclear if the slowing of the Ca^{2+} transient was due to slower Ca^{2+} sequestering by SERCA or due to diminishing Ca^{2+} buffering due to parvalbumin saturation. It is likely a combination of these two factors as increased basal levels of Ca^{2+} were noted in Figure III-3, which suggests an increase in parvalbumin saturation (Hollingworth & Baylor, 2013), and a variety of metabolic byproducts such as ADP and Pi are known to slow the Ca^{2+} pumping activities of SERCA (Stienen *et al.*, 1993;MacDonald & Stephenson, 2001), and these would be expected to increase during the protocol. While the slowing of the Ca^{2+} transient and twitch contraction occurred at both 37 and 30^{o}C, there was a progressive increase in twitch force at 37^{o}C while the force at 30^{o}C was essentially constant in the last half of the protocol. This appeared to be an effect of the changes in the peak amplitude of the Ca^{2+} transients as the peak furaptra ratio for each twitch, a measure of peak cytosolic Ca^{2+} concentrations, increased during the staircase

protocol at 37°C, it declined at 30°C (Figure III-3). However, changes in metabolite concentrations may also play a role (see below).

The first 1-2 s of potentiation is characterized by declining force and faster twitch times. Coinciding with this, at both 30 and 37°C, is a decline in the amplitude of the Ca^{2+} transient and the Ca^{2+}-time integral (Figure III-4) relative to the unpotentiated twitches, with larger declines at 30°C. As the duration of the Ca^{2+} transient was not affected, it is believed that this is the result of impairments in Ca^{2+} release and not enhanced Ca^{2+}-uptake. As such, the declines in force during the first seconds of staircase could be caused by reduced exposure to the levels of intracellular Ca^{2+} necessary to maintain consistent twitch force.

Potentiation by Resting Ca^{2+}

The increase in force from twitch 1 to twitch 2, the enhanced rates of force production above unpotentiated levels from twitch 2 onwards (particularly at 30°C due to lower force than the first twitch of staircase), and the maintenance of force above unpotentiated levels throughout the protocol at 37°C (Figure III-2) despite lower Ca^{2+} transient amplitude (Figure III-4) point to the existence of a potentiating mechanism that operates independently from myosin RLC phosphorylation and the prolongation of the Ca^{2+}-transient. This is most likely an effect of the elevated resting Ca^{2+} concentrations, as suggested by the increases in the furaptra fluorescence ratio seen during the staircase protocol (Figure III-3). Elevated resting Ca^{2+} may lead to enhanced force production in the protocol by increasing the Ca^{2+} occupancy of cytosolic Ca^{2+} buffers, such as parvalbumin, thereby reducing competition for Ca^{2+} binding to troponin C resulting in enhanced thin filament activation and thereby enhancing force production. Consistent with this, enhancing the Ca^{2+} occupancy of troponin C can enhance the

rate of force production (Lee *et al.*, 2010). Alternate mechanisms including enhanced crossbridge binding at rest and Ca^{2+} binding directly to myosin and its light chains have been previously discussed (Smith *et al.*, 2013b) Chapter II and references within). The current investigation offers no additional insights into a putative mechanism.

Comparison to other studies

Though this is the first investigation of staircase using mouse lumbrical, the findings in the contractile measurements are not unique per se. The present investigation has reproduced many of the features of Krarup's comprehensive examination of rat EDL contractility during staircase at 20-37.5^{o}C (Krarup, 1981). These include greater reductions in contraction time at lower temperatures, greater potentiation at higher temperatures, and both early decreases and late increases in force and contraction times. Similar results have been reported in mouse EDL using comparable methods (Zhi *et al.*, 2005;Ryder *et al.*, 2007). Though the lumbrical is a relatively unique model in which to study potentiation, the current findings fit well with the established body of literature regarding the mechanical patterns of staircase potentiation and are generally applicable to findings using EDL muscle.

Consistent with models exhibiting potentiation without RLC phosphorylation (Zhi *et al.*, 2005;Rassier *et al.*, 1999;MacIntosh *et al.*, 2008), the mouse lumbrical appears to exhibit greater staircase potentiation (26.8 ±3.2%) than posttetanic potentiation (17±3% from Smith *et al.*, 2013b). However, quantification of RLC phosphorylation was not specifically performed in this study. Since the lumbrical contains the skeletal muscle isoform of myosin light chain kinase (skMLCK), it has the ability to phosphorylate the RLC, the potentiation seen in this study cannot be definitively attributed to changes in intracellular Ca^{2+}, particularly since this

protocol (8 Hz for 8.0 s) is of longer duration than the conditioning stimulus used to induce posttetanic potentiation in the previous study (20 Hz for 2.5 s). However, the finding of depressed force at 30^{o}C during the staircase protocol counters this argument, as a similar procedure (5 Hz 20 s at 30^{o}C) in mouse EDL, with intact RLC phosphorylation pathways, resulted in approximately a 19% increase in twitch force (Moore *et al.*, 1990). Moreover, while skMLCK overexpression enhances RLC phosphorylation in both EDL and soleus muscle, which are predominantly type IIB and a mix between type I and type IIA fibre types respectively, this only enhanced potentiation in the EDL muscle (Ryder *et al.*, 2007). Thus not all fast fibre types are capable of an RLC phosphorylation mediated increase in twitch tension. When considering the predominance of type IIX fibres in lumbrical and their lack of RLC phosphorylation they exhibited in a previous investigation (Smith *et al.*, 2013b), RLC phosphorylation-dependent potentiation may be limited to type IIB fibres. In addition, the lumbrical has low levels of skMLCK, and high levels of RLC phosphatase (Smith *et al.*, 2013b). Therefore it is reasonable to attribute potentiation seen in this study to the changes in the intracellular Ca^{2+} reported. Regardless of the contribution of different mechanisms to the potentiation reported here, it is hard to refute that there is a contribution of the Ca^{2+} transient to the potentiation response given the parallel increases in twitch and Ca^{2+} transient duration.

Mechanisms of force and Ca^{2+} alteration

Based on the short duration and low energetic demands of the current protocol, it can be assumed that the phosphocreatine (PCr) and glycolytic energy systems will be of primary importance. Using this assumption, it is possible to make inferences regarding the specific metabolites that may result in the changes in force and Ca^{2+} handling properties noted in the current protocol. It is known that ATP levels do not significantly change during exercise, and

lactate and creatine have little effect on contractile and Ca^{2+} handling properties (reviewed in Allen *et al.*, 2008). Additionally, the pH is not expected to change appreciably during this protocol as the H^+ produced during glycolysis will be opposed and perhaps even surpassed by the H^+ consumed by PCr breakdown (Westerblad & Allen, 1992a;Metzger & Fitts, 1987). AMP is not expected to accumulate as adenylate kinase reactions only become important after PCr depletion (Allen *et al.*, 2008). Similarly, production of reactive oxygen species is dependent on mitochondrial O_2 consumption which should be a minor component of the current protocol. Therefore discussion of the influence of metabolic products will be limited to Mg^{2+}, Pi and ADP.

Early decline in the amplitude and area of the Ca^{2+}-transient

Declines in Ca^{2+} release with closely spaced action potentials have been reported previously. For example, when pairs of action potentials are spaced 10 ms apart, the amount of SR Ca^{2+} released during the second action potential is 60-75% lower than that of the first (20-28^{o}C) (Posterino & Lamb, 2003;Hollingworth *et al.*, 1996;Caputo *et al.*, 2004). When action potentials are spaced further apart, these reductions are reduced to 15% declines at 100 ms, 10% declines at 1000 ms intervals and recovery is not fully complete at 10000 ms intervals (Caputo *et al.*, 2004). The magnitude of these reductions in Ca^{2+} release appear to be temperature dependent, with 74, 63, and 54% reductions in the rate of SR Ca^{2+} release at 16, 28 and 35^{o}C and with 15, 10, and 8 ms temporal spacing respectively (Hollingworth *et al.*, 1996). A more recent investigation by Barclay (2012) using heat production as a measure of ATP utilization by the SR Ca^{2+} pumps to re-sequester Ca^{2+} has confirmed that the resolution of this inactivation of Ca^{2+} release is indeed temperature dependent, and that the resolution time depends on muscle type, with longer durations and less temperature-sensitivity in soleus than

EDL. Using the time constant and temperature coefficient (Q_{10}) values published in Barclay's study, thus the 99% resolution time is calculated to be ~60 and 375 ms at 30^{o}C and ~25 and 170 ms at 37^{o}C in the in EDL and soleus respectively. Since this recovery time is based upon removal of Ca^{2+} from the vicinity around the calcium release channel, the Ca^{2+}-binding activities of SERCA function, and parvalbumin are expected to play a role (Barclay, 2012;Posterino & Lamb, 2003;Lamb *et al.*, 1995), thus the lumbrical could be expected to exhibit recovery times falling between those of the EDL and soleus based on the expression patterns observed in Figure III-5. Consistent with short recovery time of reductions in Ca^{2+}-release, it was noted that twitch force 30 s post-staircase was actually potentiated by 2.8±1.1% ($P<0.05$; not depicted) rather than depressed by 6.8±2.0% ($P<0.05$) as it was at the end of, and essentially throughout, the 8 Hz stimulation protocol. Also of interest was the additive nature of multiple stimuli on the declines in Ca^{2+} release, where the magnitude of the response to each successive stimulus represented a relatively constant proportion of the preceding stimulus (Barclay, 2012). Thus perhaps the increases in Ca^{2+} transient duration noted for the present study may have prevented further declines in the amplitude of the Ca^{2+} transient following the initial response. The declines in Ca^{2+} release following stimulation appears to be caused by cytosolic Ca^{2+}-feedback mechanisms, as it is unaffected by SR Ca^{2+} load (Posterino & Lamb, 2003). The reductions in peak Ca^{2+} (17.4 ± 1.7 vs 11.9 ± 2.4 % at 30 and 37^{o}C respectively) and Ca^{2+}-time integral (17.0 ± 3.4 vs 9.7 ± 4.3 % at 30 and 37^{o}C respectively) seen in the present study (with 125 ms spacing), including the greater reductions seen at 30 than 37^{o}C, fit well with these data. Interestingly, these reductions in Ca^{2+} amplitude should therefore also exist in posttetanic potentiation, though their expected small amplitude at ~5000 ms post-PS

may have precluded the ability to detect them in Chapter II where non-significant declines in Ca^{2+} transient amplitude of 3% were reported (Smith *et al.*, 2013b).

Complementary to the above explanation, metabolite accumulation may contribute to the early reductions in Ca^{2+} transient amplitude as Mg^{2+}, Pi and ADP each have inhibitory effects on SR Ca^{2+} release. For example, cytosolic ATP is a strong agonist of SR Ca^{2+} release through a cytosolic binding site on the ryanodine receptor and while ADP is also a RyR agonist, its influence is weaker than that of ATP (Laver *et al.*, 2001;Meissner *et al.*, 1986). Elevations in ADP cause competition for the nucleotide binding site on the RyR, thereby reducing Ca^{2+} release through less effective activation. Additionally, Mg^{2+} is a potent inhibitor of the RyR, even at basal concentrations, and elevations in Mg^{2+} can decrease the open probability of the channel and lower the amount of Ca^{2+} released in response to an applied stimulation (reviewed in Allen *et al.*, 2008). Though Mg^{2+} is present at high concentrations (~1 mM) at rest, and only doubles to 2 mM during fatigue (Allen *et al.*, 2008) its effects may be potent enough, or its accumulation so localized that even a small increase has a functional consequence. It is possible that this may occur as a result of Mg^{2+} offload from parvalbumin as it becomes increasingly saturated by Ca^{2+} (Haiech *et al.*, 1979). Finally, elevated concentrations of Pi may inhibit SR Ca^{2+} release, though the effects are inconsistent and highly situation dependent. For example, elevated Pi is thought to cause Ca^{2+}-Pi precipitation in the SR. This would reduce the amount of luminal Ca^{2+} available for release while simultaneously reducing back inhibition on SERCA, thereby enhancing the rate of Ca^{2+} uptake (Westerblad & Allen, 1996;Allen *et al.*, 2008;Allen & Trajanovska, 2012;Fryer *et al.*, 1995;Tupling, 2004). However, this is likely only of importance in highly fatigued muscles, and there is no direct evidence of Ca^{2+}-Pi formation in the SR (reviewed in Tupling, 2004). Mechanically skinned fibres in the presence

of high concentrations of ADP and Pi exhibit enhanced SR Ca^{2+} leak through SERCA thereby providing an alternate mechanism to achieve reduced Ca^{2+} release without Ca^{2+}-Pi precipitation (Duke & Steele, 2001a). This would lead to the elevations in cytosolic Ca^{2+} and slowed Ca^{2+} uptake commonly observed during fatigue (reviewed in Tupling, 2004). Further complicating this story, isolated ryanodine receptors exhibit enhanced open probability in the presence of Pi (Fruen *et al.*, 1994;Balog *et al.*, 2000) which should enhance Ca^{2+} release, but may also reduce SR Ca^{2+} load. Finally, at concentrations lower than those thought to cause Ca^{2+}-Pi precipitation, Pi has been demonstrated to reduce SR Ca^{2+} release in a pathway that is enhanced with increasing concentrations of Mg^{2+}, though the precise mechanism of this pathway has not yet been determined (Duke & Steele, 2001b;Westerblad & Allen, 1992b;Steele & Duke, 2003). Thus the possibility exists that elevations in Pi can contribute to the declines in Ca^{2+} release observed in this study though the veracity of this claim is uncertain.

The relationship between temperature and metabolite influence on SR Ca^{2+}-release is not well established in the literature. As such, potential mechanisms causing the greater drop in the amplitude at 30^{o}C compared to 37^{o}C via a metabolic pathway are purely speculative. It is possible that Ca^{2+}-Pi precipitation is of greater importance at lower temperatures, as the solubility product would decrease proportionally with temperature. Another possibility worth considering is that due to the high temperature sensitivity of SERCA activity (Masuda & De Meis, 1977;Puglisi *et al.*, 1996), luminal SR Ca^{2+} loads may be lower at 30^{o}C than 37^{o}C or slower to refill following contraction, leading to greater inhibition of the RyR Ca^{2+} channel via the internal SR signaling cascade through calsequestrin, triadin and junctin (Beard *et al.*, 2008), though data from Posterino and Lamb (2003) suggest this is not the case.

Regardless of the mechanism, a decline in cytosolic Ca^{2+}-transient amplitude and Ca^{2+}-time integral will likely contribute to the declines in force seen early in the protocol. This is investigated further in Chapter IV.

Slowing of the Ca^{2+} transient

There are two mechanisms by which Ca^{2+} transients could be slowed in the latter half of the staircase protocol. The first mechanism is a decline in the rate of Ca^{2+} uptake by SERCA. This may occur via changes in metabolite concentration. It is plausible that phosphocreatine became depleted as the protocol extended, leading to ADP accumulation in the latter half of the protocol. As SERCA is an ATP dependent enzyme, it is highly sensitive to the products of ATP hydrolysis. Accordingly, high concentrations of Pi and ADP and low concentrations of ATP inhibit Ca^{2+} uptake and SERCA function (Stienen *et al.*, 1993;MacDonald & Stephenson, 2001). The second mechanism by which Ca^{2+} transients may be slowed is through saturation of Ca^{2+} binding sites on the cytosolic Ca^{2+} buffering protein, parvalbumin. Relaxation of fast twitch rodent and frog muscle is dominated by the Ca^{2+}-binding properties of parvalbumin, accounting for 50-73% of the rate of Ca^{2+} transient decay (Carroll *et al.*, 1997;Hollingworth *et al.*, 1996;Hou *et al.*, 1993). As parvalbumin retains Ca^{2+} sequestered in the cytosol for several seconds after the end of stimulation (Hollingworth & Baylor, 2013), the increases in resting Ca^{2+} noted in Figure III-3 and in Chapter IV suggest that parvalbumin saturation could progressively increase, thereby decreasing its relative contribution to the decay of the Ca^{2+} transient, leading to the prolonged time course of the Ca^{2+} transient as seen in Figure III-4. Consistent with this possibility there was a significant amount of parvalbumin in lumbrical (Figure III-5). Therefore the increases in resting Ca^{2+} could be responsible for the slowing of the Ca^{2+} transient. However, as no measurements of metabolite concentrations were made in

this study, no comments can be made on the relative contribution of metabolic fatigue versus Ca^{2+} buffer saturation to the slowing of the Ca^{2+} transient. In addition, due to the confounding factor of parvalbumin saturation diminishing its ability to buffer Ca^{2+} during the potentiated contractions, the possibility that the rate of SERCA pumping is being actively regulated via some Ca^{2+}-mediated mechanism cannot be ruled out. However, it is clear that any contribution of enhanced SERCA activation is minor relative to the influence of the factors that slow the Ca^{2+} transient.

Ca^{2+}-sequestering proteins

Based on the previous characterization of the fibre type profiles for EDL, lumbrical and soleus (Smith *et al.*, 2013b), the pattern of parvalbumin expression where EDL>lumbrical>soleus (Figure III-5) is consistent with previous results showing that parvalbumin expression in different fibre types follows the pattern: IIB>IIX>IIA>I. (Füchtbauer *et al.*, 1991).

Previously published ratios of SERCA1a to SERCA2a pumps in soleus and EDL of ~14:1 and 91:1 respectively (Smith *et al.*, 2013a) were used to approximate the ratio of total SERCA pumps between the different muscles used in the current study, based on the results in Figure III-5. Regardless of whether the 14:1 value for EDL or the 91:1 value for soleus was used as the basis for normalization of the present data, the relative number of SERCA pumps•unit mass^{-1} for soleus:lumbrical:EDL in the current study was ~1:1.95:3.1 (~1:1.6 for lumbrical:EDL). These results are consistent with previous findings that SERCA density is ~3-8 fold higher in EDL than soleus (Wu & Lytton, 1993;Murphy *et al.*, 2009;Vangheluwe *et al.*, 2005;Smith *et al.*, 2013a). As the current value for the soleus:EDL SERCA expression ratio of

1:3.1 differs from the previous finding of 1:4.9 (Smith *et al.*, 2013a), two different values were produced for the ratio of SERCA1a:SERCA2a in lumbrical, 39:1 using the EDL values and 54:1 using the soleus values, both of which lie between the ratios for EDL and soleus stated above. When the ratio of total SERCA expression is compared to the ratio of parvalbumin expression (SERCA expression 1:1.95:3.1 versus parvalbumin expression 1:3.7:19; in soleus: lumbrical: EDL), it becomes apparent that the ratio of parvalbumin:SERCA follows the pattern: EDL>lumbrical>soleus. Interesting in this regard are findings from Hollingworth and Baylor (2013) who report that the return of the Ca^{2+} transient to basal levels is actually faster in slow twitch muscles than in fast twitch muscle with time constants of ~2 and ~12 s respectively. They attribute this to the presence of parvalbumin which abbreviates the Ca^{2+} transient by binding Ca^{2+}. This keeps cytosolic Ca^{2+} low, reducing SERCA activity, and Ca^{2+} is effectively maintained in the cytosol for extended periods of time. When this information is taken with the calculated differences in the ratio of parvalbumin to SERCA, it seems possible that the parvalbumin to SERCA ratio could play a role in determining the duration of the delay in returning cytosolic Ca^{2+} to basal levels, and the increases in resting Ca^{2+} following a contraction may be of longer duration in predominantly type IIB muscles, such as the EDL than those of predominantly type IIX muscles such as the lumbrical. Also of interest, as the Q_{10} of SERCA is higher than that of parvalbumin (Hou *et al.*, 1992;Stein *et al.*, 1982;Masuda & De Meis, 1977;Puglisi *et al.*, 1996), the duration of the elevations in resting Ca^{2+} following contraction may be prolonged at lower temperatures beyond that simply expected based only on the effects of temperature on SERCA activity. These lines of investigation warrant further research.

Limitations and Future Directions

The scope of this paper was focused on the changes in force seen later in staircase potentiation. As such discussion of the mechanisms abbreviating the twitch duration and causing the early potentiation of force are limited. These topics are discussed in detail in the companion paper (Chapter IV).

Although the low affinity Ca^{2+}-sensitive indicator, furaptra, used in this study is limited in its ability to track low level changes in Ca^{2+} such as those seen at rest, it is hardly unexpected that Ca^{2+} would be increased following a contraction, particularly given the previous results with posttetanic potentiation (Smith *et al.*, 2013b), and the prolongation of the Ca^{2+} tails following contraction of fast-twitch skeletal muscle noted by Hollingworth & Baylor (2013). Moreover, the elevations in basal Ca^{2+} were confirmed using the high affinity indicator fura-2 in Chapter IV. Along similar lines, both Mg^{2+} and Ca^{2+} increase the fluorescence ratio of furaptra, therefore these results most likely contain contamination from the Mg^{2+} signal at rest, and may contain a progressively increasing Mg^{2+} artifact during the repetitive stimulation protocol (see Hollingworth *et al.*, 1996;Konishi *et al.*, 1991). However, due to the low intensity of this protocol, the progressive component of this Mg^{2+} contamination is unlikely to be of significant magnitude to be of consequence to the overall conclusions made in this study.

While it was assumed that the locus of the furaptra was the cytosol, AM dyes are known to compartmentalize forming localized non-cytosolic contributions to the universal fluorescence which may have a confounding effect on the results (see Morgan *et al.*, 1997). Additionally, while the ability of furaptra to precisely track cytosolic Ca^{2+} transients is established for temperatures between 28 and 35^{o}C, it has not been definitively demonstrated for 37^{o}C (Hollingworth *et al.*, 1996). Therefore, the ability to detect changes in intracellular

Ca^{2+} transient time course may have been diminished; however, the parallel responses at 30 and 37^{o}C lends ostensible validity to the 37^{o}C data.

Conclusions

In conclusion, the force responses of a typical fast-twitch muscle to the repetitive low frequency stimulations utilized to induce staircase potentiation are the result of the balance between mechanisms of force enhancement and force diminishment. While the force enhancing effects of myosin regulatory light chain phosphorylation and its effects on the Ca^{2+}-sensitivity of crossbridge formation are well documented (Stull *et al.*, 2011), this study has highlighted the importance of slowed Ca^{2+} sequestering to the enhanced force seen in staircase potentiation, which can explain the robust presence of staircase and absence of post-tetanic potentiation commonly reported in the absence of RLC-phosphorylation. Further, this study in conjunction with the previous (Smith *et al.*, 2013b) and following (Chapter IV) studies provide evidence that elevations in resting Ca^{2+} also enhances twitch force following contractile activity, though the mechanism is still uncertain. Also, reductions in the amplitude of cytosolic Ca^{2+}-transients were found to occur early in potentiation. This may contribute to reductions in force seen early in staircase protocols, particularly those at low temperatures, though the importance of the declining Ca^{2+}-transient amplitude on crossbridge function relative to that of metabolite accumulation remains to be seen.

Chapter IV - Early force declines during staircase potentiation are caused by changes in calcium and crossbridge function

Outline

Stimulation of a muscle at 5-10 Hz results in a progressive increase in twitch force known as staircase potentiation. However, the first 1-2 seconds of staircase potentiation typically differs from the rest of the response in that force commonly declines, as does twitch relaxation time. The cause of these changes is not well understood. Thus the purpose of this study was to characterize the role of cytosolic Ca^{2+} in the force response of the first 2 s of staircase potentiation. To this end, isolated mouse lumbrical muscles were loaded with Ca^{2+}-sensitive indicators, either AM-fura-2 or AM-furaptra to track resting and peak Ca^{2+} during stimulation respectively, during 8 Hz stimulation at either 30 or 37^{o}C for 2.0 s. This resulted in a 5.3±0.8 % increase ($P<0.05$) in twitch force at 37^{o}C and a 7.2±0.9% decrease ($P<0.05$) in twitch force at 30^{o}C whereas the 50% relaxation time was decreased by 21.2± 1.3% and 15.4±1.0% at 30 and 37^{o}C respectively. Fura-2 signals indicated that the increases in resting Ca^{2+} during the protocol followed the same time course at 30 and 37^{o}C, with the greatest elevations occurring between twitches 1 and 2 and corresponding to increases in twitch force of 3.1±0.4% and 2.4±0.1% at 30 and 37^{o}C respectively ($P<0.05$). Both the peak amplitude of the Ca^{2+} transient and the Ca^{2+}-time integral declined over the course of the protocol at 30^{o}C, but not 37^{o}C. Additional groups of AM-furaptra loaded lumbricals were treated with 0.5 mM caffeine to prevent the declines in Ca^{2+} transient amplitude. Caffeine enhanced the potentiation at 37^{o}C ($P<0.05$), attenuated the force loss at 30^{o}C ($P<0.05$) and prevented the declines in both Ca^{2+} transient amplitude and Ca^{2+}-time integral at 30^{o}C. However, caffeine administration did not reverse the declines in 50% relaxation times, but further enhanced the speed of relaxation regardless of temperature (30^{o}C: 21.2 ± 1.3 vs 25.6 ± 1.0%, 37^{o}C: 15.4 ± 1.0 vs 17.0 ± 2.3 % faster than twitch 1 without and with caffeine respectively; $P<0.05$). It is concluded that 1) elevations in resting Ca^{2+} can cause force potentiation, though the mechanism is still unclear 2)

the declines in force during staircase potentiation are caused by both declines in Ca^{2+} transient amplitude and a relaxation-enhancing factor operating independently of Ca^{2+}, which may be inorganic phosphate 3) the temperature-dependency of staircase potentiation is influenced by inactivation of Ca^{2+} release and this relaxation-enhancing factor.

Introduction

Muscle activity can cause biochemical changes which can enhance the rate of force development in fast-twitch muscle fibres. This results in elevations in submaximal contraction force, and is caused by an increase in the rate of crossbridge attachment following contraction (Sweeney *et al.*, 1993;Grange *et al.*, 1993). This phenomenon, known as force potentiation, is particularly beneficial during rapid concentric contractions (Caterini *et al.*, 2011;Gittings *et al.*, 2012;Abbate *et al.*, 2000), and may also help mask the effects of fatigue (Gittings *et al.*, 2011;Gordon *et al.*, 1990;Stull *et al.*, 2011;Vandenboom *et al.*, 2013). In experimental settings, potentiation is typically investigated under isometric conditions using one of two methods: posttetanic potentiation and staircase potentiation. Posttetanic potentiation is evoked using a tetanic contraction flanked by twitches with the twitches post-contraction having higher force than those pre-contraction. Staircase potentiation is the elevation in twitch force seen when a muscle is subjected to low frequency stimulation (<10 Hz).

While both staircase and posttetanic potentiation are primarily caused by the same mechanism, a kinase-mediated phosphorylation of myosin regulatory light chain resulting in an increase in the Ca^{2+} sensitivity of crossbridge formation (Sweeney *et al.*, 1993;Grange *et al.*, 1993;Stull *et al.*, 2011;Vandenboom *et al.*, 2013), there is strong evidence that there are multiple mechanisms at work. Muscles devoid of the skeletal muscle isoform of myosin light chain kinase are incapable of phosphorylating their myosin RLC during exercise, and as such

exhibit little to no posttetanic potentiation (Gittings *et al.*, 2011;Zhi *et al.*, 2005). However, these same muscles exhibit staircase potentiation, though to a lesser extent than their wildtype counterparts (Zhi *et al.*, 2005). Similar results have been found using models of muscle atrophy and denervation (MacIntosh *et al.*, 2008;Rassier *et al.*, 1999;Tubman *et al.*, 1996;Tubman *et al.*, 1997). Recent characterization describes the mouse lumbrical as a type IIX muscle which does not phosphorylate its regulatory light chain but still exhibits both posttetanic potentiation (Smith *et al.*, 2013b) and staircase potentiation (Chapter III). Using this model, it was demonstrated the contribution of elevations in resting cytosolic Ca^{2+} (Smith *et al.*, 2013b) and longer duration of Ca^{2+} transients (Chapter III) to the enhancements in twitch force seen in potentiated twitches.

Coinciding with potentiation is enhancement of twitch relaxation. This is observed in both posttetanic potentiation and staircase potentiation (the first 1-2 seconds of staircase in particular) presenting as faster peak rates of relaxation and reductions in relaxation time (Krarup, 1981;Smith *et al.*, 2013b). This phenomenon has been widely demonstrated (reviewed in Vandenboom *et al.*, 2013), but lacks a clear mechanistic explanation as each of RLC phosphorylation (Gittings *et al.*, 2011;Brown & Loeb, 1999;Patel *et al.*, 1998), elevated intracellular Ca^{2+}(Smith *et al.*, 2013b) and prolongation of Ca^{2+} transients (Chapter III) should result in longer durations of twitch contractions. It was recently reported that there are declines in the Ca^{2+}-time integral and peak amplitude of the intracellular Ca^{2+} transients which trigger potentiated contractions during the first 2 s of staircase, particularly at lower temperatures (Chapter III). Similarly, the force of the contraction also declines during this period (Chapter III;Krarup, 1981;Zhi *et al.*, 2005;Ryder *et al.*, 2007). While the most likely explanation for the declines in Ca^{2+} transient amplitude during staircase potentiation is a Ca^{2+}-induced inactivation

of Ca^{2+} release in the terminal cisternae (Chapter III;Posterino *et al.*, 2003;Barclay, 2012), the extent to which this affects the force and force kinetics during the early stages of staircase potentiation are unknown. Thus the primary purpose of the current investigation was to determine whether the declines in Ca^{2+} transient amplitude and area are causative to the declines in force and faster relaxation kinetics seen during the first seconds of staircase potentiation. To this end, mouse lumbrical muscles loaded with AM-furaptra (a Ca^{2+}-sensitive fluorescence indicator) were exposed to either normal Tyrode's solution or 0.5 mM caffeine (a potent agonist of sarcoplasmic reticulum Ca^{2+} release (Kovacs & Szucs, 1983) in Tyrode's solution, and subjected to 8 Hz stimulation protocols lasting 2.0 s during continuous monitoring of force and light signals. While the caffeine treatment was intended to prevent the stimulation-induced declines in Ca^{2+}-transient amplitude and area, to date there has been no specific investigation on the effects of caffeine on Ca^{2+} release during closely spaced twitch contractions. However, the postulated mechanism behind the declines in Ca^{2+}-release during twitch contractions in close succession is related to elevations in cytosolic Ca^{2+}, particularly in the vicinity of the terminal cisternae (Posterino & Lamb, 2003;Schneider & Simon, 1988;Caputo *et al.*, 2004;Barclay, 2012). Given the potency of caffeine as an agonist of sarcoplasmic reticulum Ca^{2+} release in the comparable condition of fatigue (eg. Rosser *et al.*, 2009), it was hypothesized that caffeine can maintain Ca^{2+} release during successive twitch contractions as well.

A component of this investigation was to characterize the changes in resting and peak cytosolic Ca^{2+} during the first 2 s of staircase using more sensitive methodology than that which was used in Chapter III. To accomplish this both high and low affinity Ca^{2+}-sensitive indicators were used and smaller groupings of twitches were used for fluorescence analysis.

This investigation reports that 0.5 mM caffeine attenuates the reductions in Ca^{2+}-transient amplitude seen with repeated contractions, an effect which was associated with not only enhanced force potentiation, but also reductions in relaxation times and faster peak rates of relaxation. Thus this study provides evidence that there is a Ca^{2+} component to the declines in force seen early in staircase potentiation, the enhancements in relaxation are not caused by changes in the Ca^{2+} transient, and the relaxation enhancing mechanism may actually be sensitized by the caffeine treatment. The case is made for inorganic phosphate (Pi) as the moiety responsible for this effect. Finally, the small potentiation seen in the second twitch of staircase protocols is most likely caused by an elevation in the resting cytosolic Ca^{2+} concentration following the first twitch contraction.

Methods

The methodology and experiments used in this study were approved by the University of Waterloo Committee for Animal Care. The methods used in this study were reported in detail in Chapters II and III as well as in a recent report (Smith *et al.*, 2013b). Briefly, intact lumbrical muscles were dissected on ice from the hind feet taken from male C57BL/6 mice. Dissection was performed on ice in Tyrode's dissecting solution (containing in mM: 136.5 NaCl, 5.0 KCl, 11.9 $NaHCO_3$, 1.8 $CaCl_2$, 0.40 NaH_2PO_4, 0.10 ethylenediaminetetraacetic acid (EDTA), and 0.50 $MgCl_2$, pH 7.5). Muscles were suspended between a model 322C high speed length controller (Aurora Scientific Inc) and a model 400A force transducer (Aurora Scientific Inc) mounted in a chamber containing circulating oxygenated (95% O_2, 5% CO_2) Tyrode's experimental solution (containing in mM: 121.0 NaCl, 5.0 KCl, 24.0 $NaHCO_3$, 1.8 $CaCl_2$, 0.40 NaH_2PO_4, 5.50 glucose, 0.10 EDTA, and 0.50 $MgCl_2$, pH 7.3) at either 30 or 37^{o}C. Free Ca^{2+} and Mg^{2+} concentrations were estimated at 1.7 and 0.5 mM respectively in both Tyrode's

dissecting solution and Tyrode's experimental solution. A computer controlled model 701C stimulator (Aurora Scientific Inc.) provided supramaximal stimulation voltages via flanking platinum plate field stimulus electrodes. Lumbrical muscles were stretched to optimum length for twitch force production (L_o) and then loaded (32^{o}C for 2x30 min) with either AM-furaptra or AM-fura-2 (Molecular Probes) to detect changes in intracellular Ca^{2+}-transients and resting Ca^{2+} respectively. Excitation light was applied to the muscles at 380 and 344 nm via a monochromator (Photon Technology International) and fluorescence emission was collected at 510 nm through an inverted microscope photometer system (D-104; Photon Technology International) affixed with a photomultiplier tube (PMT; model 814; Photon Technology International). The resulting analog force and fluorescence signals were digitized and stored at 10,000Hz for later analysis.

Experimental Protocol

Following AM indicator loading, muscles were brought to experimental temperature of either 30 or 37^{o}C and allowed to incubate for 5 minutes. Muscles were then subjected to a pacing protocol in which a single twitch contraction was induced every 30 s to achieve a steady twitch force. Next muscles were stimulated for 2.0 s at 8 Hz (16 twitches) to induce staircase potentiation, during which fluorescence emission was continuously monitored. The muscles were returned to the pacing protocol for 4 minutes to monitor the dissipation of potentiation. This protocol was then repeated allowing for 5 unpotentiated twitches before onset of the next staircase protocol. This was repeated 10 times per muscle alternating between 344 and 380 nm excitation wavelengths in order to produce 5 fluorescence ratios which were then averaged together. Muscles loaded with furaptra were subject to further data averaging by combining twitches 1-6, 6-11, and 11-16. Force and kinetic data were compiled for each of the 10

repetitions performed for each muscle and averaged together to form a single set of values for that animal (i.e. an n of 1 is the averaged result of 10 repeated trials), resulting in the low variability seen in the force and kinetic data.

To prevent the declines in Ca^{2+} release which were previously found using this protocol (Chapter III), separate groups of AM-furaptra-loaded muscles were exposed to 0.5 mM caffeine in the circulating Tyrode's experimental solution at 30 and 37^{o}C for the duration of the experiment.

Statistical analysis was performed by 3-way split plot ANOVA using temperature (between groups), caffeine (between groups) and time (repeated measures). A schematic illustration of the stimulation protocol used in this study is shown in Figure IV-1.

Additional data are presented using the muscles from Chapter III where staircase lasted for 8.0 s and fluorescence was measured during unpotentiated twitches. These data have been re-analyzed using only the first 2.0 s of staircase using the same twitch groupings for signal averaging as those described above (i.e. twitches 1-6, 6-11 and 11-16 versus the 0-2, 2-4, 4-6, and 6-8 s blocks used in Chapter III). These data have been included to allow comparison to unpotentiated twitches as fluorescence signals were not collected for these contractions during the present study.

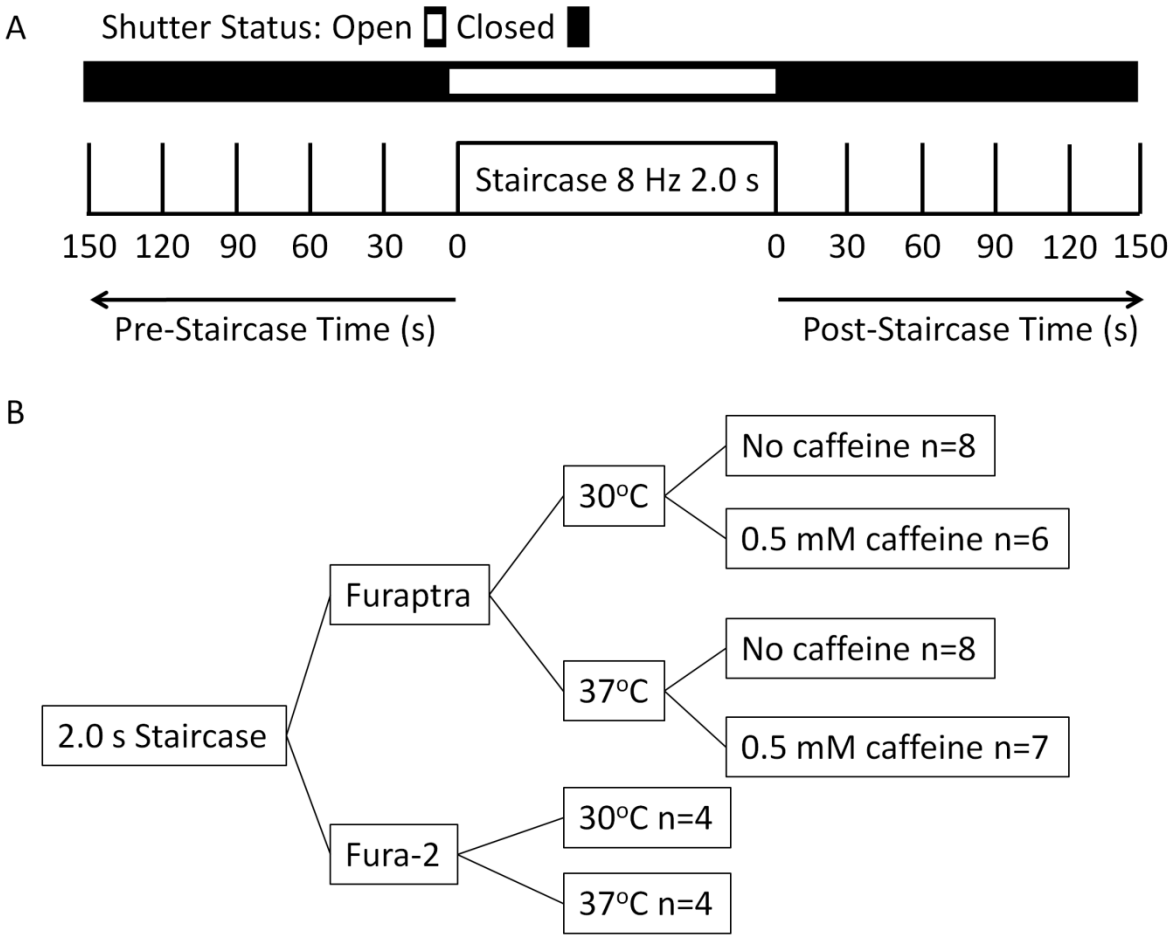

Figure IV-1 - Experimental timeline and schematic for 2.0 s staircase protocol
Isolated mouse lumbricals loaded with either AM-furaptra or AM-fura-2 were stimulated at 30 s intervals prior to a 2.0 s 8 Hz volley to elicit staircase potentiation, after which twitch contractions were resumed at 30 s intervals to monitor the dissipation of the potentiation response. Fluorescence signals were collected throughout the staircase protocol. This procedure was repeated 10 times, alternating 344 and 380 nm excitation light between consecutive trials, resulting in 5 344/380 fluorescence ratio signals which were averaged together. These experiments were performed at either 30 or 37°C for both fura-2 and furaptra. Separate groups of muscles were exposed to caffeine to mitigate the declines in Ca^{2+} transient amplitude described in Chapter III.

Results

Force Response

Sample tracings of twitch contractions are shown in Figure IV-2A demonstrating the force and kinetic responses of the 8 Hz stimulation protocol at 30 and 37°C, while the degree of

potentiation for each twitch is shown in Figure IV-2B. Stimulation at 8.0 Hz for 2.0 s resulted in force potentiation at 37^{o}C and force depression at 30^{o}C. However, regardless of temperature, twitch force was 2-3% higher during the second twitch of the protocol relative to the first twitch, a change which was associated with faster peak rates of force production (+df/dt) and relaxation (-df/dt) at both 30 and 37^{o}C, and slower half relaxation time (1/2RT) at 30^{o}C (Table IV-1). This initial slowing of relaxation stood in contrast to the overall pattern of twitches getting faster as the protocol progressed. Beyond the 2nd twitch, peak twitch force dropped for all remaining twitches at 30^{o}C, while at 37^{o}C, peak force of twitches 3-5 progressively declined before changing course and progressively increasing during twitches 6-16. Peak rates of force production (+df/dt) and relaxation (-df/dt) were faster at the end of the protocol for both temperatures ($P<0.05$), though the relative increases were higher at 37^{o}C (Table IV-1). Similarly, the times to peak tension (TPT) and 50% relaxation times (1/2RT) were lower at the end of the protocol ($P<0.05$), though with relatively larger decreases at 30^{o}C than 37^{o}C (Table IV-1).

Force response with caffeine

Addition of 0.5 mM caffeine to the circulation buffer increased the peak force of a single twitch by ~7% regardless of temperature ($P<0.05$) but had no effects on resting tension. The overall patterns of change in the force (Figure IV-2B) and kinetic responses (Table IV-1) with caffeine treatment were very similar to those of the non-treated groups at both 30 and 37^{o}C. The most striking differences were the increased degree of potentiation at 37^{o}C and the attenuation of force loss seen at 30^{o}C. Additionally, caffeine treatment enhanced the relative increases in the rate of relaxation and decreases in 1/2RT seen at the end of the stimulation

protocol relative to the untreated groups (P<0.05). However, repeated stimulation with caffeine had proportionally similar effects on TPT and +df/dt as the untreated groups (Table IV-1).

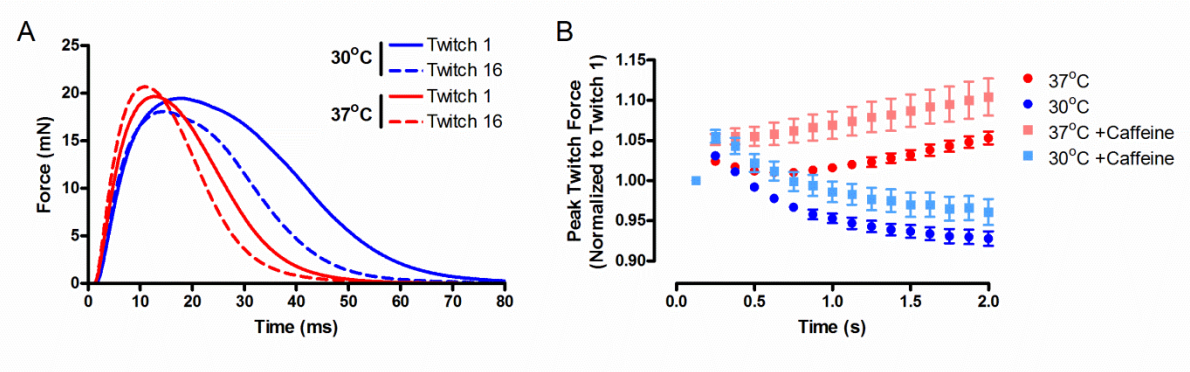

Figure IV-2 - Twitch force characteristics
Isolated mouse lumbrical muscles were subjected to 10 cycles of 8 Hz stimulation protocol for 2.0 s at either 30 or 37°C to induce staircase potentiation once every 7 min. Sample force records of mouse lumbrical muscles at both 30 and 37°C are shown for the first and 16th (i.e. last) twitch of the protocol (A). The relative changes in peak twitch force (B) during the protocol reveal the stimulation protocol caused potentiation at 37°C and depression at 30°C. Muscles treated with caffeine exhibited ~5% and ~3% more potentiation/less force depression at 37°C, and at 30°C respectively than untreated muscles (Main effect, P<0.05). Notably, largest increase in potentiation occurred in the second twitch regardless of caffeine treatment., and at no time was potentiation depressed relative to the preceding twitch at 37°C in the caffeine treated group, whereas it fell between twitches 1 and 6 in the 37°C untreated group and at all time points beyond twitch 2 in both 30°C groups. All values are reported as mean ±SEM.

Table IV-1 – Twitch force and kinetics during 2.0 s of 8 Hz stimulation

Condition	Twitch Number	30°C (n=8)	37°C (n=8)	30°C +0.5 mM Caffeine (n=7)	37°C + 0.5 mM Caffeine (n=6)
Force (mN)	1	19.5 ± 0.8	19.7 ± 1.5	21.8 ± 1.1	20.9 ± 1.6
	2	20.1 ± 0.9*	20.1 ± 1.5*	23.1 ± 1.1*	21.9 ± 1.7*
	16 (# †)	18.1 ± 0.9*	20.7 ± 1.5*	20.9 ± 1.0*	23.1 ± 1.8*
ΔForce (%)	2 †	3.1 ± 0.4*	2.4 ± 0.1*	5.5 ± 0.8*	5.1 ± 0.7*
	16 # †	-7.2 ± 0.9*	5.3 ± 0.8*	-3.9 ± 1.6*	10.4 ± 2.3*
TPT (ms)	1 # †	16.6 ± 0.6	13.0 ± 0.3	17.3 ± 0.5	14.1 ± 0.6
	2 # †	16.6 ± 0.6	12.9 ± 0.3	17.4 ± 0.5	14.1 ± 0.7
	16 # †	14.1 ± 0.5*	11.4 ± 0.2*	14.8 ± 0.4*	12.4 ± 0.5*
ΔTPT (%)	2 †	-0.1 ± 0.3	-0.6 ± 0.4	0.5 ±0.4	0.4 ±0.3
	16 #	-15.4 ± 0.5*	-11.8 ± 0.7*	-14.2 ± 0.5*	-11.6 ± 0.9*
1/2RT (ms)	1 #	20.8 ± 1.5	14.9 ± 0.7	19.4 ± 0.8	14.7 ± 1.3
	2 #	21.1 ± 1.5*	14.9 ± 0.7	19.6 ± 0.7 (*)	14.7 ± 1.3
	16 #	16.2 ± 1.0*	12.6 ± 0.6*	14.3 ± 0.4*	12.1 ± 0.8*
Δ1/2RT (%)	2	1.8 ± 0.3*	-0.1 ± 0.2	1.1 ± 0.7	1.0 ± 1.0
	16 # †	-21.2 ± 1.3*	-15.4 ± 1.0*	-25.6 ± 1.0*	-17.0 ±2.3*
+df/dt (mN/ms)	1 #	3.14 ± 0.14	3.75 ± 0.23	3.38 ± 0.21	4.09 ± 0.38
	2 #	3.31 ± 0.16*	3.88 ± 0.25*	3.56 ± 0.19*	4.28 ± 0.40*
	16 #	3.36 ± 0.16*	4.37 ± 0.27*	3.54 ± 0.17*	4.90 ± 0.44*
Δ+df/dt (%)	2 #	5.6 ± 0.6*	3.4 ± 0.8*	5.7 ± 1.7*	4.7 ± 0.8*
	16 #	7.3 ± 0.7*	16.6 ± 1.8*	5.5 ± 2.7*	19.9 ± 2.4*
-df/dt (mN/ms)	1 # †	-0.98 ± 0.04	-1.17 ± 0.08	-1.14 ± 0.02	-1.31 ± 0.14
	2 # †	-1.02 ± 0.05*	-1.19 ± 0.09*	-1.23 ± 0.03*	-1.37 ± 0.14*
	16 # †	-1.08 ± 0.04*	-1.42 ± 0.10*	-1.35 ± 0.02*	-1.63 ± 0.15*
Δ-df/dt (%)	2 # †	3.3 ± 0.3*	1.4 ± 0.6*	7.9 ± 1.3*	5.0 ± 1.4*
	16 # †	9.6 ± 1.7*	20.7 ± 0.9*	18.8 ± 1.8*	25.4 ± 2.3*

Isolated mouse lumbrical muscles were stimulated at 8 Hz for 2.0 s at either 30 or 37°C, with or without 0.5 mM caffeine in the circulating buffer. Changes in the twitch properties (denoted by Δ) compare the 2nd or 16th twitch to the 1st twitch in the 8 Hz protocol. All values are presented as mean ± SEM. * Different from twitch 1 of the same condition ($P<0.05$). # Main effect of temperature ($P<0.05$). † Main effect of caffeine ($P<0.05$). A negative value for the change in time to peak tension (TPT) or half relaxation time (1/2RT) indicates a shorter duration of the parameter, while a positive value for changes in peak rate of force production (+df/dt) or peak rate of relaxation (-df/dt) indicates that the rate has increased. Symbols in parentheses indicate $P<0.10$.

Fura-2 Ratios

Lumbricals loaded with the high affinity Ca^{2+}-sensitive indicator AM-fura-2 demonstrated the increase in basal $[Ca^{2+}]_i$ during the staircase protocol as summarized in Figure IV-3. Importantly, since temperature can affect the fura-2 fluorescence ratio independent of changes in Ca^{2+} (Oliver *et al.*, 2000) and no calibration attempt was made in this study, attempts to directly compare resting $[Ca^{2+}]_i$ between temperatures are inappropriate. However, relative changes over time are perfectly valid. To facilitate this comparison, the change in fluorescence ratio for each temperature was normalized on a scale of 0-1 with the fura-2 ratios at twitch 1 serving as zero (i.e. control levels of Ca^{2+}) and twitch 16 serving as 1.0 (i.e. the peak increase in resting $[Ca^{2+}]_i$). The resulting data demonstrate that the largest increases in resting cytosolic Ca^{2+} occurred following the first contraction in the protocol, and reached a plateau by 2.0 s. The time course of the increases in resting Ca^{2+} was not influenced by the differences in bath temperature. Fura-2 fluorescence was not measured in the presence of caffeine.

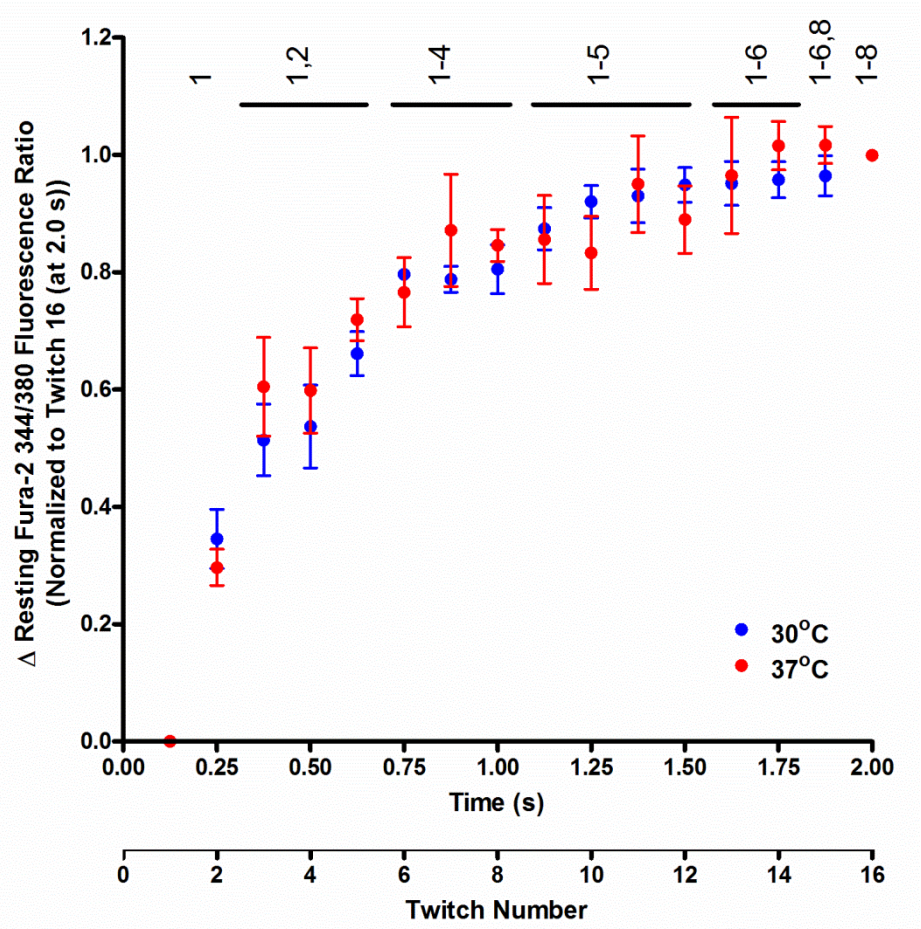

Figure IV-3 – Time course of relative changes in resting fura-2 ratio during staircase potentiation
Mouse lumbrical muscles were loaded with the AM form of the high-affinity Ca^{2+}-sensitive indicator fura-2 and subjected to an 8 Hz stimulation protocol as described in the methods. Fura-2 ratios were collected as the average ratio over the 20 ms immediately preceding each twitch of the protocol. All values are mean ± SEM. N=4 per temperature. There were no statistical differences in the relative rise in fura-2 ratio between temperatures, but there was a main effect of time/twitch number. These differences are marked numerically above the data points with the numbers corresponding to the twitches which exhibited significantly lower values. All $P<0.05$.

Furaptra ratios

Furaptra fluorescence ratios corresponding to cytosolic Ca^{2+}-transients were condensed into 3 groups corresponding to twitches 1-6, 6-11, and 11-16, inclusively. Raw tracings of furaptra ratio signals and summary data are shown in Figure IV-4. The time course of the

intracellular Ca^{2+}-transient was affected by temperature, with longer time to peak Ca^{2+}, 50% decay time and full width at half maximum at 30°C (All $P<0.05$). These measures were not affected by repeated stimulation. However, at 30°C, both the peak amplitude of the Ca^{2+} transient and the Ca^{2+}-time integral were reduced in the 6-11 group and 11-16 group relative to the 1-6 group ($P<0.05$). These effects did not occur at 37°C. To allow comparison to a control condition of isolated twitches (30 s apart), the twitch grouping parameters of this study were applied to the muscles used in Chapter III (Figure IV-5). This approach revealed that the Ca^{2+}-time integral is reduced throughout the 8 Hz stimulation protocol while peak amplitude of the Ca^{2+}-transient is well maintained during twitches 1-6 at 30°C and through twitches 1-11 at 37°C. Moreover, the changes in the Ca^{2+}-time integral and peak amplitude during 8 Hz contraction are virtually identical between these independent data sets, illustrating the repeatability of these findings.

The presence of 0.5 mM caffeine to the circulating buffer did not affect the 50% decay time, time to peak Ca^{2+} or full width at half maximum at either 30 or 37°C. However, the Ca^{2+}-time integral was higher with caffeine treatment (main effect $P<0.05$; ~17% higher at 30°C and ~30% higher at 37°C). This effect appeared to be a result of a small increase in the furaptra ratio throughout the Ca^{2+} transient. Most notably, in the presence of caffeine, the reductions in the peak amplitude of the Ca^{2+} transient and the Ca^{2+}-time integral associated with repeated contractions at 30°C were at least attenuated if not prevented outright (Figure IV-4D-E). As a caveat, the caffeine treatment cannot be confirmed as 100% successful at abolishing the reductions in the Ca^{2+} transient amplitude, particularly at 30°C, as there was no unpotentiated group against which to compare and the changes in the peak amplitude of the Ca^{2+} transients were all 2-way interactions in the 3-way ANOVA.

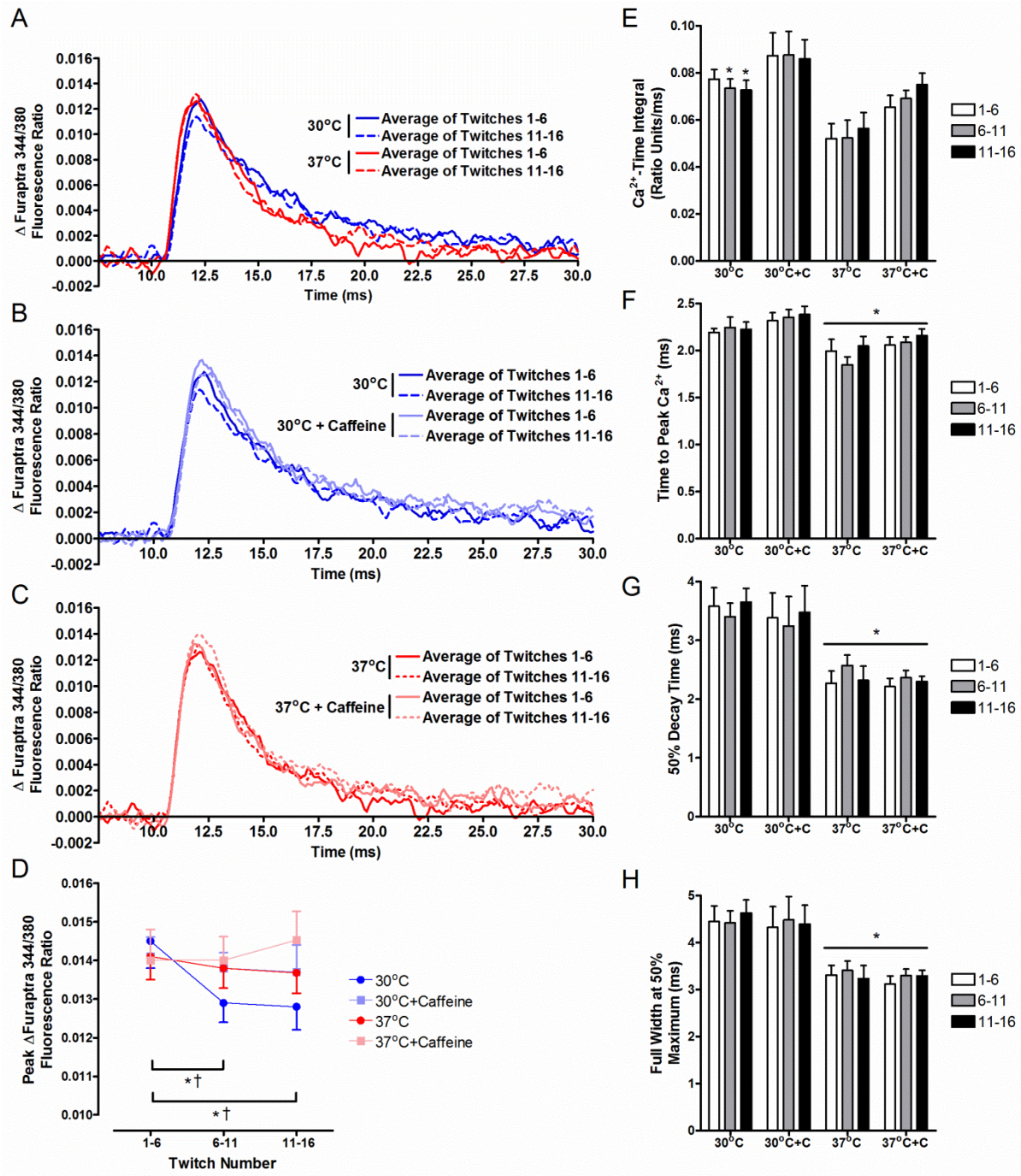

Figure IV-4 - Ca^{2+} transients and kinetic characteristics during staircase potentiation (2.0 s)

Intracellular Ca^{2+} transients derived from AM-furaptra signals in mouse lumbrical muscles at 30 and 37°C (A) during 8 Hz stimulation for 2.0 s were averaged over 5 cycles of this protocol. Signals were further averaged into 3 blocks of 6 twitches corresponding to the beginning (twitches 1-6), middle (twitches 6-11) and end (twitches 11-16) of the stimulation protocol. Raw tracings are the average of all muscles (n=8 per temperature). Additional muscles were treated with 0.5 mM caffeine in the bathing solution and subjected to the same stimulation protocol as above and the resulting furaptra records are superimposed over duplicates of the

records shown in panel A (B: n=6 30°C; C: n=7 37°C). Peak changes in the amplitude of the fluorescence ratio are shown in D. * - Interaction effect of temperature and time (1-6 > 6-11, 11-16 at 30°C; P<0.05). † - Interaction effect of caffeine and time (1-6 > 6-11, 11-16 without caffeine; P<0.05). Mixed-design ANOVA analysis revealed main effects of caffeine (caffeine > no caffeine; P<0.05) and temperature (30°C>37°C) on the Ca^{2+}-time integral (E). However, repeated measures ANOVAs ran separately for each group revealed declines in the Ca^{2+} time integral at 30°C that were not seen in any other condition. *- Value < Value of twitches 1-6; P<0.05. Time to peak Ca^{2+} (F), full width at 50% maximum (G) and time to 50% decay (H) were faster at 37°C than 30°C. * - Main effect of temperature; P<0.05. +C designates the inclusion of 0.5 mM caffeine in the circulation buffer.

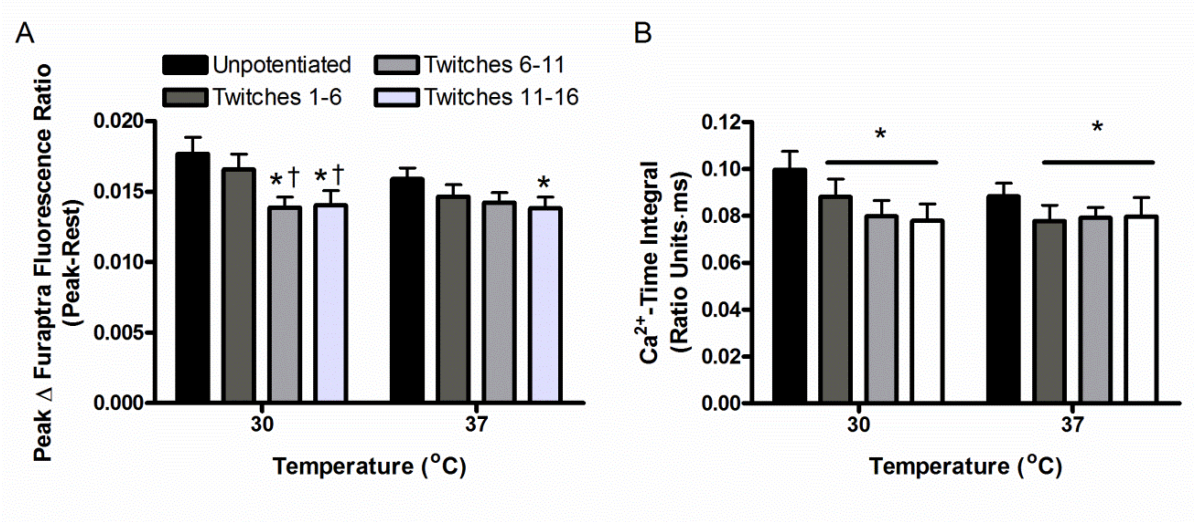

Figure IV-5 - Peak furaptra ratios and Ca^{2+}-time integrals before and during 8 Hz stimulation

Lumbricals loaded with AM-furaptra were stimulated at 30 s intervals for 2.5 minute while fluorescence emission was monitored in 1.0 s windows during each twitch to determine the peak changes in the furaptra fluorescence ratio and the Ca^{2+}-time integral during unpotentiated twitches at either 30 (n=6) or 37°C (n=7). These unpotentiated data are reproduced from Chapter III. Following the unpotentiated twitches, muscles were stimulated at 8.0 Hz for 8.0 s while furaptra fluorescence was continuously monitored. The resulting Ca^{2+} records from the first 2.0 s of this protocol were condensed to 3 groupings: Twitches 1-6, 6-11 and 11-16. These data are a deconstruction of the corresponding 0-2 s time points in Chapter III, and is presented here to facilitate comparisons to unpotentiated twitches and demonstrate the repeatability of the results presented in Figure IV-4. * Value is lower than unpotentiated (P<0.05). † Value is lower than twitches 1-6 (P<0.05).

Discussion

The goal of this investigation was to determine whether the declines in Ca^{2+}-transient amplitude and Ca^{2+}-time integral demonstrated in Chapter III could contribute to the declines

in force and enhancements of relaxation noted during the first seconds of staircase potentiation while simultaneously testing the ability of caffeine to attenuate the inactivation of Ca^{2+} release caused by the protocol. To this end, the low-affinity Ca^{2+}-sensitive fluorescence indicator, AM-furaptra was used to image the Ca^{2+} transients in wild type mouse lumbrical during 2.0 s of 8 Hz contraction revealing successful attenuation of the declines in Ca^{2+} release by administration of 0.5 mM caffeine in the circulation buffer (Figure IV-4). Mechanical data revealed that caffeine treatment resulted in immediate and persistent enhancement of twitch force both prior to and during the 8 Hz stimulation protocol, with increases in potentiation at 37^{o}C and attenuated force losses at 30^{o}C (Table IV-1, Figure IV-2). Thus the reductions in Ca^{2+} transient amplitude and area can be confirmed to have a depressive effect on force potentiation. Despite the increased Ca^{2+} availability and increased force, caffeine treatment was associated with greater reductions in 1/2RT and increases in the rate of relaxation with repeated stimulation than the caffeine free conditions (Table IV-1). These changes occurred in the absence of any change in the duration or decay time of the cytosolic Ca^{2+} transient (Figure IV-4), highlighting the existence of a myofilament-based mechanism which enhances the rate of force relaxation that that has yet to be identified.

A secondary goal of this investigation was to better characterize the changes in resting Ca^{2+} during the onset of staircase potentiation. To this end, lumbrical muscles loaded with AM-fura-2 were subject to the 2.0 s 8 Hz protocol at either 30 or 37^{o}C. This line of investigation revealed a large increase in resting Ca^{2+} immediately following the first twitch in the protocol, with progressively smaller increases following subsequent stimuli, as indicated by the 344/380 fura-2 fluorescence ratio, reaching a steady state near the 2.0 s mark (Figure IV-3). Coinciding with the large increase in resting Ca^{2+} prior to twitch 2 was a large increase in

potentiation (Figure IV-2, Table IV-1). The increase in resting Ca^{2+} was interpreted to be causative to the force enhancement, much like the elevations in twitch force and resting Ca^{2+} seen during posttetanic potentiation in Chapter II (Smith *et al.*, 2013b), though the mechanism is still unclear.

The effects of caffeine on excitation-contraction coupling

The enhancement of submaximal forces by caffeine is multifaceted. While caffeine does not affect membrane depolarization itself, caffeine desensitizes SR Ca^{2+} release to the t tubule membrane potential that normally keeps SR Ca^{2+} release under tight control, slowing the rate of channel closing following t-tubule repolarization, and increasing the open probability of the channel (Simon *et al.*, 1989;Kovacs & Szucs, 1983;Shirokova & Ríos, 1996). This increases the amount of Ca^{2+} available to activate the thin filament via Ca^{2+} interactions with troponin C, thereby allowing more crossbridge production. Second, caffeine can impair SR Ca^{2+} pumping, as high doses of caffeine (2-5 mM) can impair SR Ca^{2+} uptake by as much as 40% (Allen & Westerblad, 1995;Weber, 1968;Poledna & Morad, 1983). However, sub-millimolar doses appear to have no effect on SR Ca^{2+} uptake, as demonstrated in frog lumbrical by Poledna and Morad (1983). Third, caffeine increases the Ca^{2+} sensitivity of force production (Wendt & Stephenson, 1983;Gulati & Babu, 1985;Allen & Westerblad, 1995). However, this effect is small as high doses of caffeine (5-20 mM) left-shift the force-pCa relationship by only 0.09-0.13 log units, without affecting either the Hill slope (Allen & Westerblad, 1995;Palmer & Kentish, 1994) or the Ca^{2+} binding affinity of troponin C (Palmer & Kentish, 1994). Finally, caffeine is known to enhance staircase potentiation, though this effect is only apparent at long sarcomere lengths (Rassier *et al.*, 1998). Experiments performed

at L_o report no differences in the degree of potentiation with caffeine treatment (MacIntosh & Gardiner, 1987;Rassier *et al.*, 1998;Rassier & MacIntosh, 1999).

Based on this information, it is possible to interpret the effects of caffeine on the present results. The main finding that the declines in Ca^{2+} transient amplitude and Ca^{2+}-time integral with repeated contractions are prevented with caffeine treatment are consistent with the recovery of depolarization-induced Ca^{2+} release following administration of caffeine to fatigued muscle (Rosser *et al.*, 2009). Based on this interpretation, the result of enhanced potentiation and reduced force losses seen with repetitive contraction can be attributed to a relative consistency in the amplitude of the Ca^{2+} transient following caffeine administration. However, this interpretation is complicated by the disproportionately large increase in the Ca^{2+}-time integral following caffeine treatment relative to the increases in Ca^{2+}-transient amplitude, along with the absence of an increase in the duration of the Ca^{2+} transient to compensate (Figure IV-4D-H). This can be explained by increased fluorescence ratio signals in the tail region of the Ca^{2+} transients of caffeine-treated muscles, which can be seen in Figure IV-4B-C. This suggests that 0.5 mM caffeine may have caused some impairment in SERCA function in the preparation, which stands in contrast to the results of Poledna and Morad (1983) who found no effects using this same caffeine dosage in frog lumbrical. This implies that the resting cytosolic Ca^{2+} concentration would be higher in the caffeine treated condition in every twitch following the first contraction and could therefore contribute to the enhanced potentiation in the 2^{nd} twitches, and to the enhanced potentiation at 37^oC, and the attenuated force losses at 30^oC seen for the remainder of the protocol. Therefore the enhanced potentiation cannot definitively be credited to either the enhanced resting Ca^{2+} or the attenuation of the loss in Ca^{2+} release. It seems likely that both contribute.

The finding of greater potentiation with caffeine treatment is inconsistent with the findings of MacIntosh's group (MacIntosh & Gardiner, 1987;Rassier *et al.*, 1998;Rassier & MacIntosh, 1999). The reason that most likely explains this discrepancy involves the atypically short duration of the current protocol. For example, it is possible that caffeine may decrease the time required to reach peak potentiation, as has been demonstrated in fatigued muscles (MacIntosh & Gardiner, 1987). Alternatively, it is possible that the caffeine treatment is only effective at enhancing potentiation early in the protocol contraction, with a disproportionally large influence of fatigue influencing later contractions. Consistent with this, caffeine treatment is known to accelerate muscle fatigue (MacIntosh & Kupsh, 1987), an effect which may be due to the greater energy demands of higher force and Ca^{2+} cycling. This may also help explain the enhanced rates of relaxation seen with caffeine treatment.

Early declines in force

Despite attenuation of the loss in Ca^{2+} transient amplitude with caffeine treatment, the lumbrical muscles still exhibited force loss beyond twitch 2 at 30^{o}C. While it is possible that this is due to incomplete restoration of Ca^{2+} release, a more likely scenario involves the accumulation of metabolic byproducts, inorganic phosphate (Pi) in particular. High levels of Pi reduce maximum Ca^{2+}-activated force in skinned muscle fibres (Allen *et al.*, 2008;Allen & Trajanovska, 2012;Debold *et al.*, 2004;Debold *et al.*, 2006;Debold, 2012;Millar & Homsher, 1990;Debold, 2012). This effect may be caused by a reversal or inhibition of the transition of the actomyosin-ADP-Pi crossbridge state to a strongly bound, force producing state that is dependent on Pi dissociation, resulting in a lower fractional number of crossbridges in force producing states (Dantzig *et al.*, 1992;Debold *et al.*, 2006;Takagi *et al.*, 2004;Hibberd *et al.*, 1985b;Hibberd *et al.*, 1985a). Alternatively, following Pi release and the transition of the

crossbridge to a force-producing state, Pi may interact with this cross-bridge state forming an entirely new actomyosin-ADP-Pi transition state. This new strongly bound transition state may (Kerrick & Xu, 2004) or may not (Palmer & Kentish, 1994) be force producing. This transition state facilitates the release of ADP, shifting the equilibrium towards a greater number of non-force producing crossbridges (Kerrick & Xu, 2004;Palmer & Kentish, 1994). Regardless of the mechanism, elevations in Pi also reduce the maximum force achievable via Ca^{2+}-activation (Debold *et al.*, 2006;Millar & Homsher, 1990). Interestingly, the depressive effect of Pi on peak force is greater at lower temperatures (Debold *et al.*, 2004;Coupland *et al.*, 2001). This effect has been attributed to the greater temperature dependence of the forward reaction of the force generation step than the Pi-mediated reverse reaction, leading to an equilibrium point that favors greater forces at high temperatures than low temperatures when Pi concentrations are elevated (Zhao & Kawai, 1994). Similarly, Pi accumulation decreases the Ca^{2+} sensitivity of force production. While the mechanism is unclear, it may involve antagonistic relationship of Ca^{2+} and Pi on force production where elevated Pi favors a strongly bound but not force producing crossbridge state which is less sensitive to Ca^{2+} (Palmer & Kentish, 1994). Consistent with this, muscle stiffness, a measure of strong crossbridge binding, has lower sensitivity to Pi than does force production (Martyn & Gordon, 1992). However, unlike the effects of Pi on peak Ca^{2+} activated force (Debold *et al.*, 2004) the Pi-mediated reductions in Ca^{2+} sensitivity are enhanced at higher temperatures (Debold *et al.*, 2006). Why Pi should reduce Ca^{2+}-sensitivity with greater efficacy than force at high temperatures is currently unknown.

In addition to the Pi effects, Mg^{2+}, which may increase via either ATP breakdown (reviewed in Allen *et al.*, 2008) or by parvalbumin offload (Haiech *et al.*, 1979), can also

decrease the Ca^{2+} sensitivity of the contractile proteins (Blazev & Lamb, 1999b) with no effect on peak force (Dutka & Lamb, 2004) and as such may have contributed to the declines in twitch force seen after the second twitch of the staircase protocol. This effect is not temperature sensitive (Godt & Lindley, 1982). Conversely, increased concentrations of ADP increase the Ca^{2+} sensitivity of force production by slowing the rate of crossbridge detachment (Westerblad *et al.*, 1998;Cooke & Pate, 1985).

A potentially confounding factor in this analysis is the lack of data at 37^{o}C. Studies have only examined the force-Pi relationship at near-physiological temperatures of 30^{o}C and below, thus the nature of the relationship is not established at physiological temperatures. Nonetheless, the data are most consistent with an increase in Pi which contributes to the reductions in force seen after the 2nd twitch at both temperatures. However, it is unclear if the effects of Pi on crossbridge function can contribute to the greater declines in force seen at 30^{o}C.

As stated earlier, the Hill slope of the force-pCa relationship may be higher in the presence of Pi (Debold *et al.*, 2006;Millar & Homsher, 1990). This suggests that Pi could increase the cooperativity of crossbridge binding and thereby contribute to the enhanced rate of force production seen in potentiated twitches in this study (i.e. increase f_{app}). Should this occur, it could only serve as a complementary factor to the force enhancing effects caused by elevations in resting Ca^{2+}, as the Pi-induced reductions in Ca^{2+}-sensitivity of crossbridge binding and force production in general (reviewed in Debold, 2012;Allen *et al.*, 2008;Allen & Trajanovska, 2012) would delay the onset of force production and reduce twitch force.

Abbreviated Twitch Duration

The coexistence of faster relaxation times and increased force in potentiated twitches is a long-standing conundrum in the study of muscle contractility, and one to which few explanations have been offered. Here the argument is made that it is most likely mediated by Pi.

In the two state model of force production described by Huxley (1957), the proportion of crossbridges in the strongly bound state (αFs) is equal to the rate of crossbridge transition from the non-force producing state to the force-producing state (f_{app}) divided by the sum of f_{app} and its reverse step g_{app} (the rate of crossbridge transition from the force producing to non-force producing state). Force potentiation by myosin RLC phosphorylation increases f_{app} but has no effect on g_{app}, thereby increasing αFs and force (Sweeney *et al.*, 1993), and has been demonstrated to cause increased relaxation times (Patel *et al.*, 1998). However many studies examining potentiation report reduced twitch durations and faster relaxation times (reviewed in Vandenboom *et al.*, 2013), an effect which occurs regardless of whether or not the RLC has been phosphorylated.

The effect of enhanced relaxation is not unique to the study of isolated twitch contractions, nor is it only present in ex-vivo conditions. For example, the difference in force between the peaks and valleys of unfused, electrically induced tetanic contractions increases following cycling exercise (Fowles & Green, 2003) and intermittent isometric knee extension exercise (Ratkevicius *et al.*, 1995;Vøllestad *et al.*, 1997) in human subjects. These differences in amplitude, termed force ripple (Ratkevicius *et al.*, 1995) or ΔF (Vøllestad *et al.*, 1997), are inversely related to the relaxation time of the muscle (Vøllestad *et al.*, 1997) and noticeably

increase over the course of a single contraction. Note that this final point has never been quantified to the best of the author's knowledge, but has been personally observed many times during experimentation (See Figure 5 in Fowles & Green, 2003 as an example).

Despite the prevalence of these findings, few explanations have been brought forth and tested. Postulated theories for the enhanced rates of relaxation have included faster rates of Ca^{2+}-uptake (Vøllestad *et al.*, 1997;Tupling, 2009), increases in muscle temperature (Vøllestad *et al.*, 1997), and increased rates of myosin ATPase activity (Vøllestad *et al.*, 1997), and changes in the fibre activation pattern of muscles (Vøllestad *et al.*, 1997). Of these, increases in muscle temperature and changes in the fibre type activation pattern have already been discounted (Vøllestad *et al.*, 1997). The current data support these conclusions. Specifically, care was taken to use a supramaximal stimulation voltage, thus ensuring complete and synchronized excitation of all fibres. The small size of the lumbrical, low degree of activation, short protocol duration, and continuous buffer circulation argue against heat accumulation, as based upon a temperature coefficient (Q_{10}) of contractile speed of ~2 (Stein *et al.*, 1982), temperature would have to increase by 2-3^{o}C in less than 2.0 s to account for the 20-30% reductions in contraction time seen in this study. This leaves only elevations in the rate of Ca^{2+} uptake and increased myosin ATPase activity as possible explanations.

Previous assessment of the possibility that there are changes in the duration of the Ca^{2+} transients during potentiated contractions concluded that the Ca^{2+} transients are unchanged during PTP (Chapter II;Smith *et al.*, 2013b) and that the Ca^{2+} transient duration is actually longer during the typical (i.e. long duration) staircase potentiation protocol, though declines in Ca^{2+}-transient amplitude were noted (Chapter III). However, this previous staircase study may have lacked the sensitivity to detect these changes based upon the protocol of averaging 2.0 s

blocks of twitches (16 twitches) together, though the coexistence of slower Ca^{2+} transients, higher force, lower 1/2RT and higher –df/dt seen between 2 and 4 s in the 8 Hz for 8 s at 37^{o}C contraction protocol make this rather unlikely. The current study enhances the sensitivity by using blocks of 6 twitches (0.67 s), thereby allowing more meaningful interpretations of the data. Current results show that although the peak declines in twitch duration during staircase potentiation occur simultaneously with the lowest peak and area values of the cytosolic Ca^{2+} transients, treatment of muscles with 0.5 mM caffeine attenuates these impairments to the Ca^{2+} transient and actually leads to greater reductions in twitch duration and relaxation time (Figure IV-4, Table IV-1). The rapidity of the enhancement of relaxation (<2 s to achieve maximum effect) argues against a complex molecular pathway that is dependent upon enhancing the activity or concentration of low-concentration moieties such as reactive oxygen species, phospholamban or sarcolipin causing post-translational modification of SERCA (see also Appendix 4). Therefore, barring a complex interaction between caffeine and calcium and/or byproducts of metabolism which progressively enhances SERCA activity in concert with caffeine's agonistic effect on Ca^{2+} release, the current results clearly indicate that the enhancements in relaxation are not due to enhanced Ca^{2+} sequestering, thus another theory must be brought forth.

This leaves only enhancements in myosin ATPase activity as a possible explanation for enhanced relaxation following contractile activity. More specifically, there must be either an increase in the rate of crossbridge detachment or transition to non-force producing states. Interesting in this regard are the findings of Kerrick & Xu (2004) who report that elevating the concentration of Pi increases g_{app}, and that the effects are greater at low pCa values. Their findings are consistent with the greater effectiveness of Pi at reducing contractile force at low

pCa than high pCa values (Debold *et al.*, 2006), along with the Pi-dependent increases in the steepness of the force-pCa curve of skinned rabbit psoas (Millar & Homsher, 1990) soleus fibres (Debold *et al.*, 2006). However, Palmer and Kentish (1994)found no such elevations in Hill slope in rabbit psoas, and Debold *et al.* (2006) report decreased Hill slopes with Pi treatment in rabbit gastrocnemius fibres. Importantly, each of these mechanisms can only affect force after the formation of strongly bound crossbridges, thereby creating a model which is suitable for the enhanced rates of force production caused by either myosin RLC phosphorylation or elevations in resting Ca^{2+}. Thus Pi-induced increases in g_{app} at low pCa values (Kerrick & Xu, 2004) similar to those seen during a twitch contraction, provides a plausible mechanism by which relaxation kinetics can be enhanced following muscle activity. Moreover, given the short duration and low intensity of the contractile protocol, and the fast fibre-type profile of the lumbrical muscle (Chapter II;Smith *et al.*, 2013b), it is probable that almost all energy during this protocol was derived from the high energy phosphocreatine system, and therefore only Pi and creatine would exhibit noticeable increases. Cumulatively, this makes the Pi theory of enhanced relaxation during potentiation very attractive. This theory should be tested in a fast-twitch muscle of a creatine kinase- skMLCK double knockout muscle, as these animals should not accumulate Pi (Steeghs *et al.*, 1997) or exhibit any increases in twitch duration caused by RLC phosphorylation (Patel *et al.*, 1998;Zhi *et al.*, 2005) which could mask the desired effects.

As a minor point, examination of –df/dt and 1/2 RT following both posttetanic and staircase potentiation (see Appendix 5) reveals a complex biphasic response where relaxation is initially faster following the potentiating stimulus, regardless of whether it was faster or slower during the staircase potentiation protocol itself. The relaxation then slows to a point

exceeding that of the pre-PS contractions, before finally normalizing to pre-potentiated levels. Thus there are factors simultaneously enhancing and diminishing the rate of relaxation, and the factor(s) which speed relaxation are dominant during brief contractile activity, but their influence is shorter lived than the factors which slow relaxation. More work is warranted in this area.

Conceptual model of potentiation

Based on the available information, a conceptual diagram is presented depicting the various factors which appear to have influence on the magnitude of force potentiation (Figure IV-6). The potentiating factors include: an increase in the rate of crossbridge attachment, which is known to be caused by myosin RLC phosphorylation (Sweeney *et al.*, 1993;Grange *et al.*, 1993), increased duration of the Ca^{2+} transient (Chapter III), which enhances Ca^{2+} availability and duration of troponin C occupation, and increases in resting Ca^{2+} (Chapters II-IV;Smith *et al.*, 2013b), which is still debatable in its precise role. The factors opposing potentiation include reductions in Ca^{2+} transient amplitude, which is likely caused by Ca^{2+}-deactivation of Ca^{2+} release (Barclay, 2012), metabolite accumulation (see Chapter III for discussion), and an increase in the rate of crossbridge detachment which includes enhancement of relaxation kinetics. This effect is believed to be caused by increased Pi (see above). The sum of all these factors will determine the net degree of potentiation experienced by the muscle.

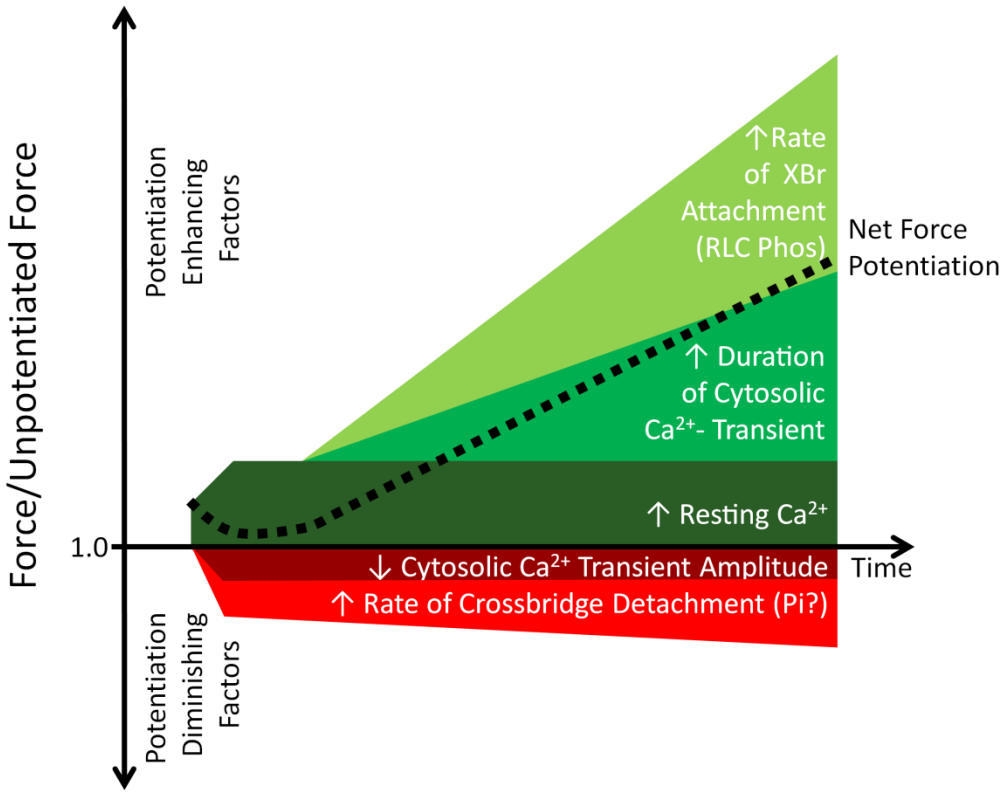

Figure IV-6 – Conceptual diagram of the factors determining the magnitude of staircase potentiation
This figure depicts the relative contribution and time course of the different factors influencing the force occurring during a typical staircase potentiation protocol. Each of the colored regions depicts a net response, with the relative contributions changing according to the specific conditions of the contraction and affecting the force accordingly. Note that this model can also be applied to posttetanic potentiation (PTP) such that the degree of PTP reflects the resolution of these effects over time. Pi – inorganic phosphate. XBr – crossbridge.

Limitations and future directions

While much is known about the reductions in SR Ca^{2+} release per stimulation during repetitive contraction in unfatigued muscle, (i.e. the inactivation of Ca^{2+} release) (Barclay, 2012;Posterino & Lamb, 2003), to the author's knowledge, the influence of caffeine on this effect has not been previously established. The fluorescence detection method used here requires several consecutive Ca^{2+}-transients to be averaged together in order to achieve an acceptable signal to noise ratio. While this requirement prohibits detection of changes in Ca^{2+}

release during successive stimuli, this does not detract from the finding that inactivation of Ca^{2+} release is attenuated with caffeine treatment, but rather illustrates the need for a more focused investigation using a more sensitive method.

The limitations and benefits of Ca^{2+}-sensitive indicators to track cytosolic Ca^{2+} transients have recently been discussed by Baylor and Hollingworth (2011). Most notable are the contributions of a non-cytosolic component to AM-fluorescence signals. Thus it is not absolutely certain that the results are truly representative of changes in the cytosol. Additionally, the use of any cell-bound fluorescence indicator in the cytosol does not offer insights into any single locality in the cell, but rather provides a global average. However, this is a limitation of all Ca^{2+} indicators, and given that this limitation was true in each of Chapters II, III, and IV where data are consistent, any error induced by this fact is repeatable. Additionally, the contribution of Mg^{2+} to the furaptra signal is also unavoidable. However, given the brief nature of this stimulation protocol, the Mg^{2+} component is unlikely to cause changes which would affect the results or interpretations thereof. However, temperature-dependent changes in the fura-2 fluorophore without associated changes in Ca^{2+} limited the ability to detect quantitative differences in amplitudes at different temperatures (Oliver *et al.*, 2000), thus the fura-2 data were presented in a form free from this influence.

Conclusions

In this investigation it was shown that caffeine administration enhances force potentiation at 37^{o}C and attenuates force losses at 30^{o}C during 8 Hz contraction. This effect appears to be caused both by attenuation of the reductions in Ca^{2+} release that occurs with repeated stimulation, and by increasing the resting cytosolic Ca^{2+} concentration. It was also

definitively demonstrated that the enhancement of relaxation rate associated with repeated contraction are not caused by changes in Ca^{2+} handling, and are thus associated with changes to the contractile proteins. The case for Pi as the effective molecule is presented as it can cause both force and relaxation times to decrease in the early stages of staircase, along with having greater effects at lower temperatures. Finally, the fura-2 fluorescence recordings suggest that elevations in resting cytosolic Ca^{2+} are responsible for the potentiation of the second twitch commonly seen in staircase potentiation.

Chapter V - Characterization of resting muscle stiffness during potentiation: contraction force is not affected by changes in resting stiffness

Outline

Elevated twitch force, or potentiation, is seen in fast twitch skeletal muscle following contraction. Mouse lumbrical muscle, which does not exhibit phosphorylation of the myosin regulatory light chain, exhibits potentiation which appears to be caused by elevations in resting cytosolic Ca^{2+} concentration, though it is unclear how this potentiation effect is achieved. This study assessed the hypothesis that elevated resting Ca^{2+} increases the number of bound crossbridges in resting potentiated muscle leading to enhanced thin filament activation via cooperative crossbridge binding. As crossbridge binding can be detected as an elevation in resting stiffness, this study characterizes resting stiffness in potentiated and unpotentiated muscle using 200 Hz sinusoidal length oscillations, ~ 0.5 nm•half sarcomere^{-1} in amplitude applied before and after a potentiating stimulus (PS) of 20 Hz for 2.5 s. Resting stiffness was reduced following the PS with an effect duration similar to that of potentiation. However, the reductions in stiffness were not associated with any change in contractile performance as a single twitch, a stretch protocol and a slack/re-lengthening protocol each caused similar reductions in resting stiffness without affecting contractile characteristics. The declines in stiffness were attributed to ablation of the short range elastic component (SREC) (Hill, 1968). As there were no changes in resting stiffness following SREC ablation between potentiated and unpotentiated muscle, it was concluded that elevations in resting Ca^{2+} do not enhance potentiation by enhancing the number of crossbridges bound at rest.

Introduction

Potentiation refers to the enhancement of submaximal forces seen following muscle activation. While this process is classically attributed entirely to the phosphorylation of myosin regulatory light chain (RLC) (Sweeney *et al.*, 1993;Grange *et al.*, 1993), other complementary

mechanisms have been demonstrated to cause potentiation in the absence of RLC phosphorylation including elevations in resting cytosolic calcium concentration and a protocol-dependent prolongation of the cytosolic Ca^{2+} transient and Ca^{2+}-time integral (Smith *et al.*, 2013b;Chapters II-IV). Prolongation of the Ca^{2+} transient and elevation of the Ca^{2+}-time integral are easily reconciled with higher twitch force via a greater degree of thin filament activation, thereby allowing greater opportunity for crossbridge formation. However, it is less certain how elevations in resting Ca^{2+} contribute to force potentiation, to which three separate hypotheses were put forward in Chapter II (Smith *et al.*, 2013b). The first states that that elevated resting Ca^{2+} could enhance potentiation by either enhancing the Ca^{2+}-occupancy of divalent cation binding sites located on myosin (Bremel & Weber, 1975;Holroyde *et al.*, 1979;Bagshaw & Reed, 1977;Robertson *et al.*, 1981). The second hypothesis was that cytosolic Ca^{2+} buffer saturation increases thereby reducing competition for Ca^{2+} binding to troponin C (TnC). The third hypothesis postulated that elevated resting cytosolic Ca^{2+} could enhance the number of crossbridges in low-force or non-force producing states (Lehrer, 2011;Brenner *et al.*, 1982). It is this third hypothesis that is tested in the current study.

The three-state model of thin filament activation (reviewed in Gordon *et al.*, 2000) describes the thin filament as "blocked" in the absence of Ca^{2+}, with only weak myosin binding sites exposed. In the presence of Ca^{2+}, the troponin-tropomyosin complex moves into the "closed" state where a small proportion of strong myosin binding sites become available. This allows a small number of crossbridges to strongly bind and undergo the powerstroke. The motions involved in the powerstroke physically push the troponin-tropomyosin complex away from the strong myosin binding sites on the nearest neighbor actin molecules, leading to the "open" state of the thin filament with free access to strong myosin binding sites. It has been

hypothesized that there is a small but significant proportion of crossbridges formed in resting muscle (Brenner *et al.*, 1982;Brenner, 1990;Schoenberg, 1988;Campbell & Lakie, 1998;Yagi, 2011;Chalovich *et al.*, 1981;Lednev & Malinchik, 1981), though this hypothesis remains controversial (Bagni *et al.*, 1995;Bagni *et al.*, 1992;Bagni *et al.*, 1999). Upon Ca^{2+}-binding to TnC these weakly bound crossbridges could be quickly converted to strongly bound crossbridges, thereby quickly shifting the tropomyosin off the myosin binding sites, leading to the "open" state of the thin filament and enhancing cooperative crossbridge binding. An elevated resting cytosolic Ca^{2+} concentration could result in increased Ca^{2+} occupancy of TnC, thereby enhancing the number of crossbridges in resting muscle which could facilitate a faster conversion to the "open" state upon subsequent stimulation, thereby explaining the faster rate of force production and greater force production noted during potentiation. Also consistent with this hypothesis, Lehrer (2011) has recently proposed the existence of a regulated cross-bridge state that is sensitive to levels of cytosolic Ca^{2+} sub-threshold for active force production, and strongly bound but non-force producing crossbridges have been reported at low ionic strength (Brenner *et al.*, 1982) and in the presence of inorganic phosphate (Kerrick & Xu, 2004;Palmer & Kentish, 1994).

Increased crossbridge formation can be detected as an increase in muscle stiffness, i.e. an increase in resistance in response to a change in length (Mason, 1977). However, crossbridges are not the only contributor to muscle stiffness, as titin is an important determinant of stiffness in both resting and actively stretched muscle (Maruyama, 1997;Wang *et al.*, 1991;Herzog *et al.*, 2012), and cellular structures such as the sarcolemma can contribute to stiffness at long sarcomere lengths (Rapoport, 1972;Podolsky, 1964;Fields, 1970). As such, this study first sought to characterize the changes in resting stiffness that occur during a

posttetanic potentiation protocol. This characterization quickly revealed decreases in stiffness that were readily inducible by either stretch or contraction. Following this characterization, muscles were subjected to a series of protocols designed to determine if the decreases in stiffness could contribute to the potentiation response, or if the declines in stiffness could have masked a smaller-magnitude increase in stiffness that could be attributed to a population of non-force producing crossbridges at rest. No evidence was found in support of there being an elevated number of strongly bound crossbridges at rest during potentiation.

Methods

The methodology used in these experiments was approved by the University of Waterloo Committee for Animal Care, and all experiments were performed in the laboratory of Dr. Russ Tupling at the University of Waterloo. Lumbrical muscles from the hind feet of male C57BL/6 mice aged 4-6 months were isolated in Tyrode's dissecting solution (mM: 136.5 NaCl, 5.0 KCl, 11.9 $NaHCO_3$, 1.8 $CaCl_2$, 0.40 NaH_2PO_4, 0.10 ethylenediaminetetraacetic acid (EDTA), and 0.50 $MgCl_2$, pH 7.5; on ice). Muscles were then suspended horizontally at optimum length for twitch force production (L_o) between a model 322C high speed length controller (Aurora Scientific Inc.) and a model 400A force transducer (Aurora Scientific Inc.) in a bath containing circulating oxygenated (95% O_2, 5% CO_2) Tyrode's experimental solution (mM: 121.0 NaCl, 5.0 KCl, 24.0 $NaHCO_3$, 1.8 $CaCl_2$, 0.40 NaH_2PO_4, 5.50 glucose, 0.10 EDTA, and 0.50 $MgCl_2$, pH 7.3) at 37^{o}C. Supramaximal stimulation voltages were applied via flanking platinum plate field stimulus electrodes connected to a model 701C stimulator (Aurora Scientific Inc.). Analog force and length signals were digitized and collected at 10,000 Hz and stored for later analysis.

Stiffness measurements

Resting muscle stiffness was assessed using sinusoidal length oscillations of 1.4 μm amplitude (~ 5 Angstroms per half sarcomere based on average muscle length of 3.5 mm), at frequencies ranging from 10 to 200 Hz. The peak velocity of shortening/lengthening thus varied between 0.088 and 1.76 mm/s. The equations of the length and force sine waves (in the form of Equation 1) were assessed over either 5 (for cycles applied at10 Hz) or 10 (for cycles applied at frequencies greater than 10 Hz) complete sinusoidal cycles of the wave using the curve fitting software in GraphPad Prism 4. The elastic and viscous components of the sinusoidal viscoelastic force response to the length oscillations were separated using Equations 2 and 3 respectively (Tidball, 1986).

Equation 1: $$Y = \text{Baseline} + \text{Amplitude} \bullet \sin(\text{Frequency} \bullet X + \text{Phase shift})$$

Equation 2: $$\text{Elastic Stiffness} = \frac{\text{Amplitude}_{\text{Force}}}{\text{Amplitude}_{\text{Length}}} \bullet \sin(\text{Phase shift}_{\text{Force}} - \text{Phase shift}_{\text{Length}})$$

Equation 3: $$\text{Viscous Stiffness} = \frac{\text{Amplitude}_{\text{Force}}}{\text{Amplitude}_{\text{Length}}} \bullet \cos(\text{Phase shift}_{\text{Force}} - \text{Phase shift}_{\text{Length}})$$

Characterization of resting stiffness during potentiation

To investigate whether there may be an increase in strongly bound crossbridges in the rested, potentiated state, muscles were subject to a series of protocols. First, to assess potentiation, muscles were given a single (unpotentiated) twitch contraction 30 s prior to a potentiating stimulus (PS) of 20 Hz for 2.5 s which was previously demonstrated to cause potentiation in mouse lumbrical (Smith *et al.*, 2013b). At select time points (2.5 - 60 s) after

the cessation of the potentiating stimulus, muscles were given twitch contractions to determine potentiation. The muscles were then allowed to rest for 5 minutes, after which the protocol was repeated with 1.4 μm amplitude sinusoidal length oscillations lasting 600 ms replacing the twitch contractions. This was repeated for 10, 20, 50, 100, and 200 Hz. At frequencies above 200 Hz, the signals became too inconsistent for analysis, reflecting the limitations of the sampling frequency used in this study. Sample input and output signals are shown in Figure V-1. Additional muscles were given contractions during the 200 Hz length oscillations flanking the potentiating stimulus, the resting stiffness was assessed 100 ms before and 100 ms after the twitch contractions to determine the effects of a single twitch on resting stiffness.

The effects of passive stretch on force potentiation

To determine if the reduced resting stiffness seen during potentiation could affect subsequent contractions, mouse lumbricals were subjected to a passive lengthening protocol consisting of sinusoidal length oscillations at 33% L_o amplitude, at 20 Hz for 2.5 s to mimic the forces seen during the PS procedure without the biochemical changes associated with contraction. Resting stiffness was assessed 30 s before and 2.5 s after the lengthening protocol using sinusoidal length oscillations at 200 Hz, 1.4 μm amplitude. The effects of the stretch protocol on twitch and tetanic contractions were tested separately with randomized order. Control experiments were performed to determine whether the passive stretch protocol ending with a stretch or a release prior to returning to L_o affected the results. Sample length and force tracings are shown in Figure V-2B.

To determine the contribution of the stimulation protocol to potentiation in the absence of high-force mechanical stresses, lumbricals were shortened to 50% of L_o over 1.0 s followed

by either 20 Hz stimulation for 2.5 s, or no stimulation. Muscle length was then returned to L_o over 1.0 s and a second twitch was applied 1.0 s after the return to L_o which equates to 2.5 s after the end of the 20 Hz stimulation period. Sample force and length tracings are shown in Figure V-2C. Both the passive lengthening and slack/re-lengthening protocols additionally served as a means of comparing resting stiffness in the absence of the easily induced reductions in resting stiffness found in the initial characterization.

Statistical analysis

Statistical testing on contractile data were performed using Student's t-test for paired samples (pre vs post). Analysis of the time course of potentiation and changes in stiffness were analyzed using a one-way repeated measures ANOVA, while comparisons made between trials were made using a two-way repeated measures ANOVA, and comparisons made between different trials and different muscles were performed using a two-way split plot ANOVA. Post-hoc testing was performed using Tukey's HSD where appropriate. Results were considered statistically significant at $P<0.05$. All values are reported as mean ±SEM.

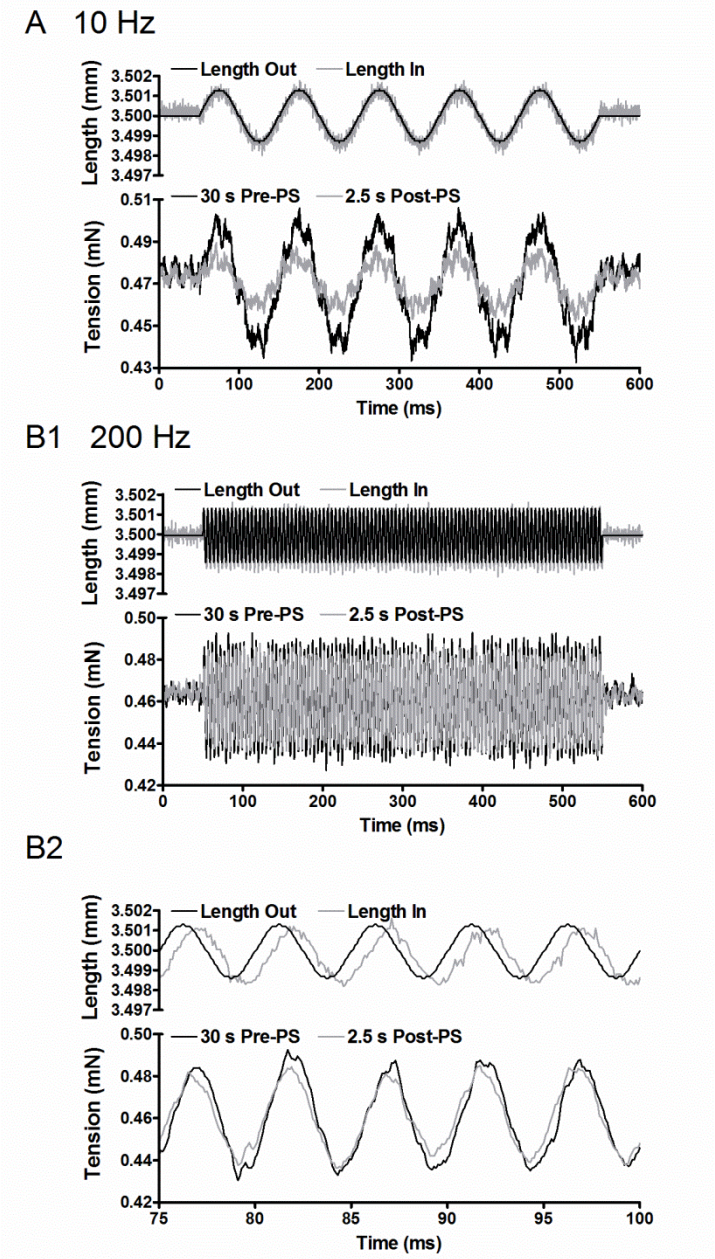

Figure V-1 - Raw force and length tracings during 10 and 200 Hz sinusoidal length oscillations

Isolated mouse lumbrical muscles were subjected to sinusoidal length oscillations at either 10 Hz (A) or 200 Hz (B) 30 s prior to and 2.5 s after the cessation of a potentiating stimulation (PS) of 2.5 s 20 Hz contraction. The amplitude of the resultant force response was diminished following the PS at both frequencies as shown in the sample recordings in the bottom region of each graph. Length signals sent to (Length Out) and position recordings (Length In) are plotted in the top portion of each graph. There was a ~0.7 ms delay in between sending the signal to the computer and receipt of the position recording, as can be seen in panel B2. B1 and B2 are the same force record, only differing in the scaling of the x-axis.

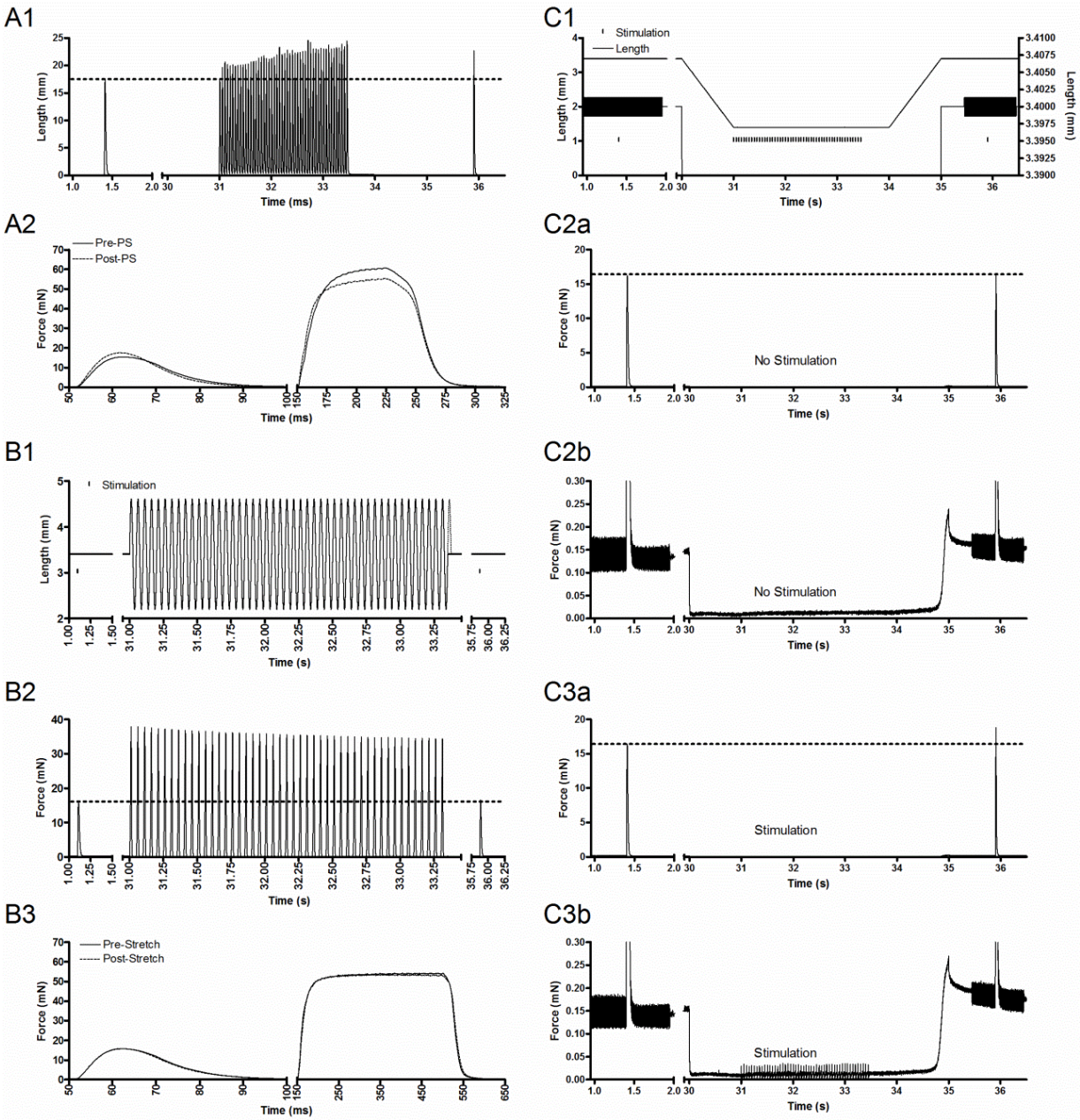

Figure V-2 - The effects of mechanical perturbations and electrical stimulation on twitch force

A1: Force recordings from mouse lumbricals subjected to twitch contractions 30 s before and 2.5 s after a potentiating stimulus (PS) of 20 Hz for 2.5 s. In a variation of this protocol, muscles were given flanking 100 Hz tetanic contractions rather than twitch contractions. The resultant twitch and tetanic force records are compared in panel A2, illustrating higher twitch force, lower tetanic force and faster kinetic rates in both twitch and tetanus following the PS. Panel B1 demonstrates the lengthening protocol applied to lumbricals to mimic the forces seen during the PS without the stimulation. Here muscles were given sinusoidal length oscillations at 20 Hz for 2.5 s with amplitude of 33% L_o. This protocol was performed with four different endings: either a stretch (solid line) or a shortening (dotted line) as the final direction of length change, and either with or without a twitch immediately following the return to L_o. As in A,

this was performed with either flanking twitches or tetanic contractions. A sample force record is shown in B2. Comparative twitch and 100 Hz tetanic contractions are shown in B3. None of the four scenarios caused changes in either twitch or tetanic force. C1 depicts the length signal used during the slack/re-lengthening protocol used to determine the effects of contraction on force and stiffness in the absence of high forces. In this panel, the upper length trace demonstrates the change in length from L_o to 50% L_o and subsequent return. The lower trace demonstrates the sinusoidal length oscillations applied to test stiffness (an identical approach to measuring stiffness was used in the protocols depicted in A and B). C2a and C2b were performed without the PS while the muscle was at 50% L_o, while C3a and C3b were performed with the PS. Twitch force was only elevated in the presence of the PS, while the declines in stiffness are readily visible in C2b and C3b following the twitch contractions. Horizontal dashed lines in A1, B2, C2a and C3a correspond to peak twitch force prior to the perturbing protocol.

Results

Effects of the PS on twitch and tetanic force

Comparing the peak amplitude of twitch force 30 s before and 2.5 s after the PS of 20 Hz stimulation for 2.5 s reveals a 15.7 ± 2.5% ($P<0.01$; n=4) increase in twitch force caused by the PS. Twitch force remained elevated above pre-PS values for 20 s ($P<0.05$; Figure V-3). Conversely, tetanic force was reduced by 7.5 ± 0.7% ($P<0.01$; n=4) 2.5 s after the potentiating stimulus. Both the peak rates of force production and peak rates of relaxation were faster following the PS in both twitch and tetanic contractions ($P<0.05$; not shown). Sample traces are shown in Figure V-2A.

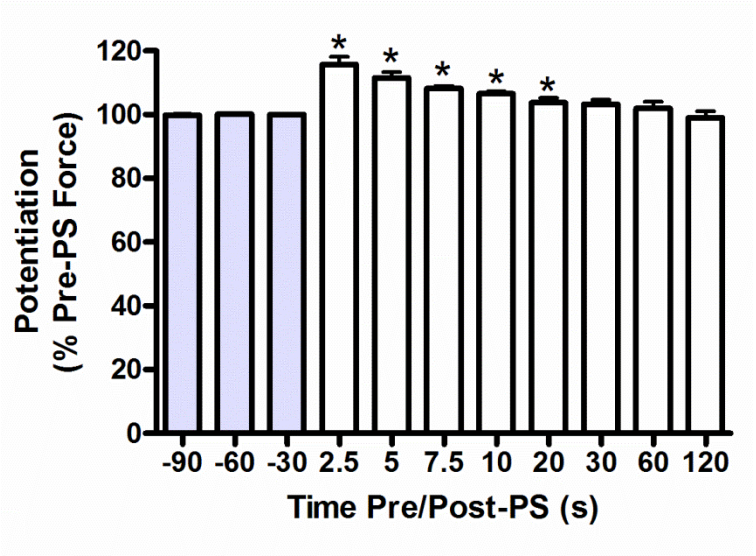

Figure V-3 - Post tetanic potentiation time course
Twitch contractions in mouse lumbrical muscle applied before (designated as a negative value) or after (positive value) a potentiating stimulus (PS) of 20 Hz for 2.5 s. * Significantly different than Pre-PS measurements ($P<0.05$; n=26)

Effects of the PS on elastic and viscous stiffness at rest

The 1.4 μm sinusoidal length oscillations applied before and after the PS revealed a decline in resting stiffness caused by the PS as can be seen by the lower amplitude of the force responses in the post-CS records in Figure V-1. Separation of the elastic element from the force signal using Equations 2 revealed declines in elastic stiffness at all frequencies tested, which remained significantly lower ($P<0.05$) than pre-PS values for 15-20 s (Figure V-4A). The magnitude of the decline in stiffness was relatively constant at all frequencies, ranging from 7.3 to 8.1mN/mm (Figure V-4C). However, the viscous element, calculated using Equation 3, revealed an increase in viscous stiffness following the PS that lasted less than 5 s and was only apparent at high frequencies (Figure V-4B). The lack of an increase in viscous stiffness following the potentiating stimulus at lower frequencies led this investigation to question if there was a temporal mismatch in the signals received from the force transducer and

the position sensing component of the servomotor. Since the length signal sent to the servomotor required ~0.75 ms (see Figure V-1 B2) to be completed by the system – fully 15% of the duration of a 200 Hz wave versus 0.75% of a 10 Hz wave, it was hypothesized that the increases in viscous stiffness at high frequencies could merely be an artifact caused by the reductions in elastic stiffness seen after the potentiating stimulus. To assess this possibility, the 200 Hz sinusoidal force signals were shifted by 0.1 ms intervals up to 0.8 ms both forwards and backwards in time. This resulted in no alleviation in the elevations in viscous stiffness post-PS, thus this hypothesis was rejected. Next all sinusoidal data at both 10 and 200 Hz were averaged across 500 ms intervals and between 7 muscles (35 cycles at 10 Hz; 700 cycles at 200 Hz) and plotted in Figure V-4D. The greater area confined within the loops post-PS clearly demonstrates that the viscosity does in fact increase following the PS during both high and low frequency length oscillations. Moreover, this approach revealed a large region of seemingly negative viscosity at the peak length excursion at 10 Hz Pre-PS that was not present Post-PS. Thus it seems that the inherent noisiness of the 10 Hz signals (see Figure V-1A) masked the post-PS elevations in viscosity which do in fact occur at all frequencies tested.

A comparison of the changes in resting viscous and elastic stiffness induced by a single twitch versus that induced by the PS (Figure V-5) revealed that the changes in stiffness that occur after a single twitch contraction are not different than those following the more intense contraction of the PS.

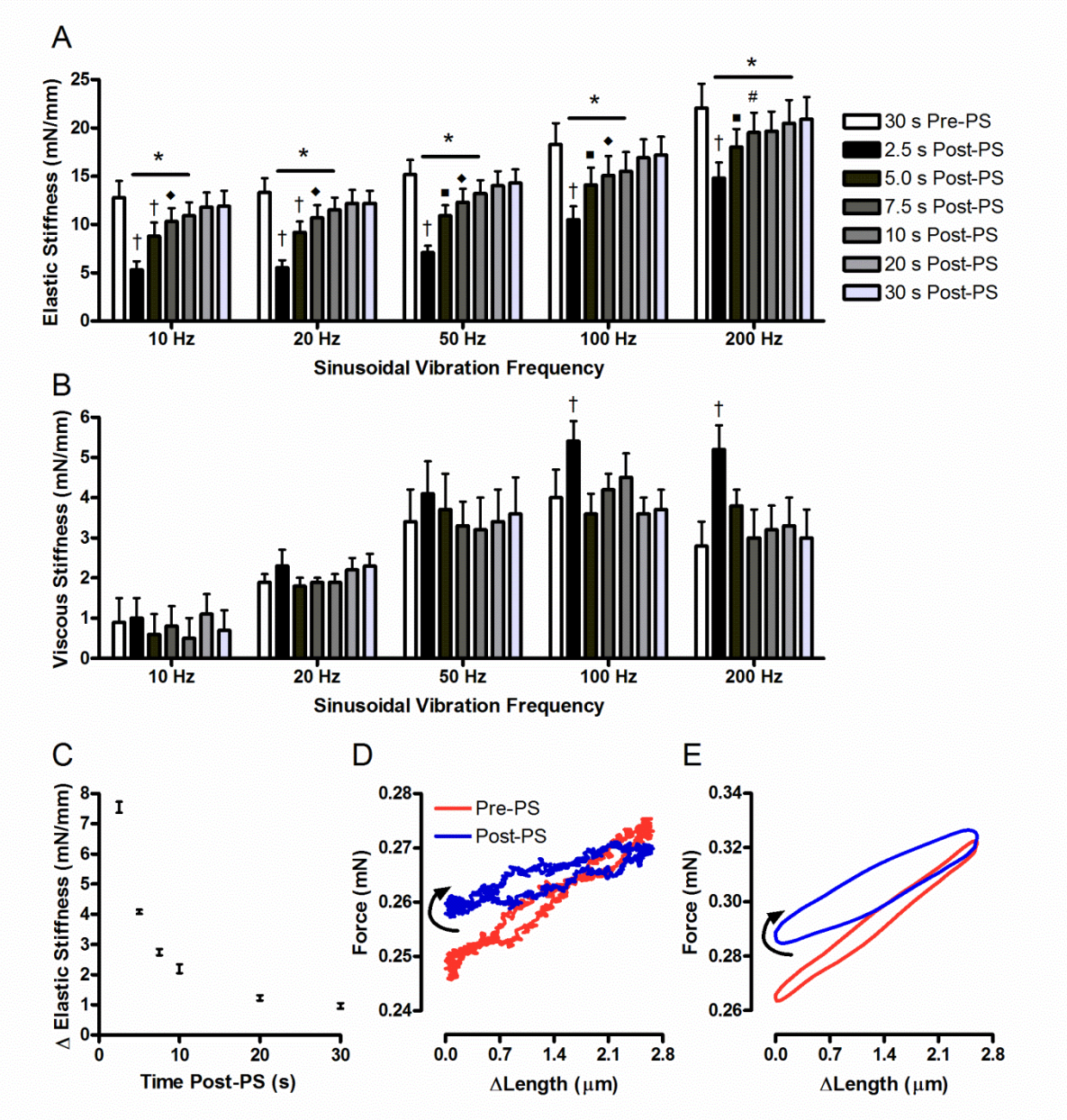

Figure V-4 – Frequency dependence of changes in resting stiffness caused by a potentiating stimulus

Resting mouse lumbrical muscles at L_o were given 1.4 μm amplitude sinusoidal length oscillations at varying frequencies from 10-200 Hz applied before and after a potentiating stimulus (PS) of 20 Hz for 2.5 s.. The elastic (A) and viscous (B) components of the force response were assessed and calculated as described in the methods. *Different than 30 s Pre-PS. †Different than all other values at the same frequency. ■ Different than 10, 20 and 30 s Post-PS. ♦ Different than 20 and 30 s Post-PS. # Different than 30 s Post-PS. All $P<0.05$; all values are mean ± SEM; n=7. The frequency of sinusoidal length oscillation did not affect the magnitude of decline in elastic stiffness as demonstrated by the tight SEM error bars in panel C, where the change in elastic stiffness from Pre-PS values are averaged across all frequencies.

Lack of a return to baseline indicates that the recovery was still incomplete at 30 s Post-PS. Increases in viscous stiffness were only visible at high oscillation frequencies. Averaging force and length data across the 7 muscles for 10 Hz (5 sinusoidal cycles/muscle) and 200 Hz (100 sinusoidal cycles/muscle) trials resulted in the hysteresis loop shown in panels D (10 Hz) and E (200 Hz). Arrows designate direction of length change where 0 is 1.4 μm shorter than L_o. The resulting figures show clear increases in energy loss 2.5 s following the PS, as indicated by increased areas circumscribed by the curves. Thus lack of an increase in viscous stiffness following the PS at low frequencies can be attributed to the inherent noisiness of the low frequency signals. Note that the 10 Hz Pre-PS loop contains a large area of seemingly negative energy loss in the upper right corner of the graph, an effect which was present in all muscles at this frequency.

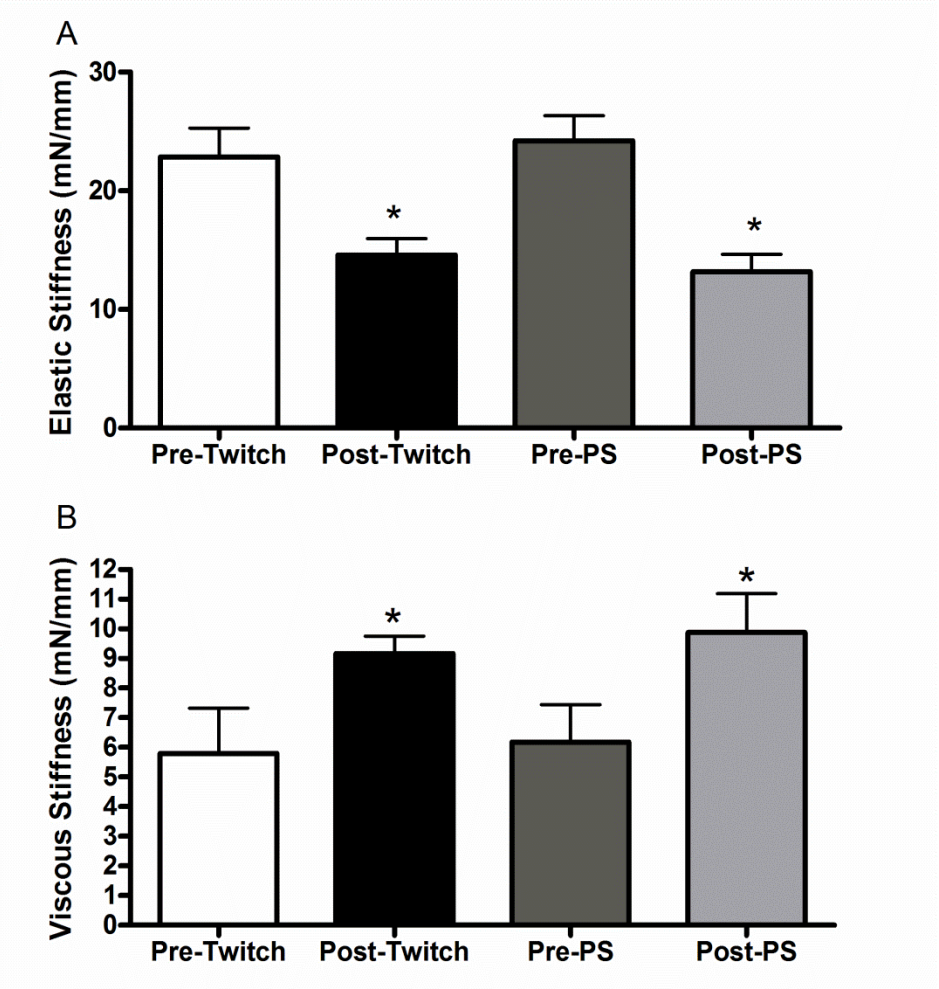

Figure V-5 - Elastic and viscous stiffness 100 ms before and 100 ms after contractions
Elastic and viscous stiffness were assessed in mouse lumbricals using 200 Hz sinusoidal length oscillations 1.4 μm in amplitude as described in the methods. Stiffness measurements were made 30 s prior (Pre) and 2.5 s following (Post) either a single twitch or a potentiating stimulus (PS) of 20 Hz for 2.5 s. Analysis was performed using a repeated measures ANOVA * Significantly different than Pre values ($P<0.05$). Values are mean ± SEM; n=8.

Effects of passive stretch on stiffness and force

Twitch and tetanic contractions were analyzed 30 s prior to and 2.5 s following sinusoidal length oscillations at 20 Hz for 2.5 s with amplitude of 33% L_o. Since muscle exhibits thixotropy, i.e. a change in behavior based on its mechanical history (Lakie *et al.*, 1984), this protocol could cause different effects depending on the final direction of length change that could affect the interpretation of the results. To account for this possibility, this test was performed four times per muscle using either lengthening or shortening as the final direction of length change, and with or without a single twitch contraction applied the moment muscle length returned to L_o to take up any slack. There were no differences in either the force or kinetics of twitch and tetanic contractions that flanked this passive stretching procedure (Figure V-2B) regardless of the final direction of the length change or the presence or absence of the stimulation immediately following the return to L_o (not shown). This stretching protocol caused similar reductions in resting stiffness as those seen during the standard PS of 20 Hz stimulation for 2.5 s (Figure V-7). This was also unaffected by the final direction of sinusoidal length change or the presence or absence of the stimulation immediately following the return to L_o (not shown).

Effects of slack/re-lengthening on stiffness and force

To determine if any of the changes in force or resting stiffness seen during potentiation could be attributed to the presence of high forces during contraction, muscles were shortened to 50% of L_o while the muscle was either stimulated at 20 Hz for 2.5 s, or left unstimulated for 3.0 s. Muscles were then returned to L_o over 1.0 s and twitch force and muscle stiffness were assessed 1.0 s later as shown in Figure V-2C1. In the absence of stimulation, the twitch force

(Figure V-2C2) was the same as that preceding the slack/re-lengthening protocol, while the force of the twitch following the condition that included the stimulation was significantly ($P<0.05$) elevated relative to the preceding twitch (Figure V-2C3). Despite the low forces (<2% of twitch force at L_o), this procedure resulted in similar declines in elastic stiffness and gains in viscous stiffness as those of the protocols described earlier (Figure V-6). Summary data regarding the changes in twitch force and stiffness caused by the various protocols used in this study are shown in Figure V-7.

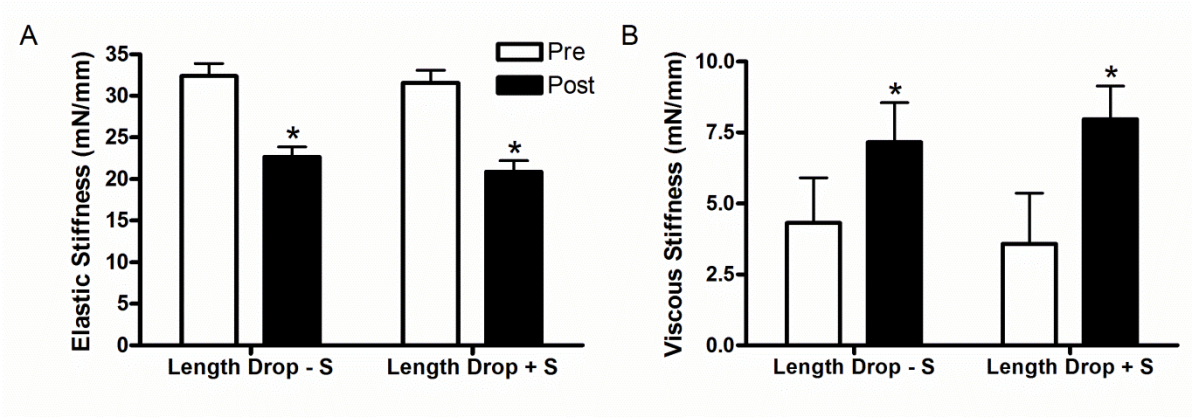

Figure V-6 - Elastic and viscous stiffness before and after slack/re-lengthen protocols
Elastic and viscous stiffness were assessed in mouse lumbricals using 200 Hz sinusoidal length oscillations 1.4 μm in amplitude as described in the methods. Stiffness measurements were made 30 s prior (Pre) to reducing muscle length to 50% of L_o over 1.0 s. While shortened, the muscle was either left unstimulated (-S) or stimulated for 2.5 s at 20 Hz (+S). 0.5 s following the end of the stimulation (3.0 s total time at 50% L_o), muscles were re-stretched to L_o and stiffness measurements were performed again 1.0 s later (Post). Changes in force and length are depicted in Figure V-2C. Analysis was performed using a repeated measures ANOVA * Significantly different than Pre values ($P<0.05$). Values are mean ± SEM; n=7.

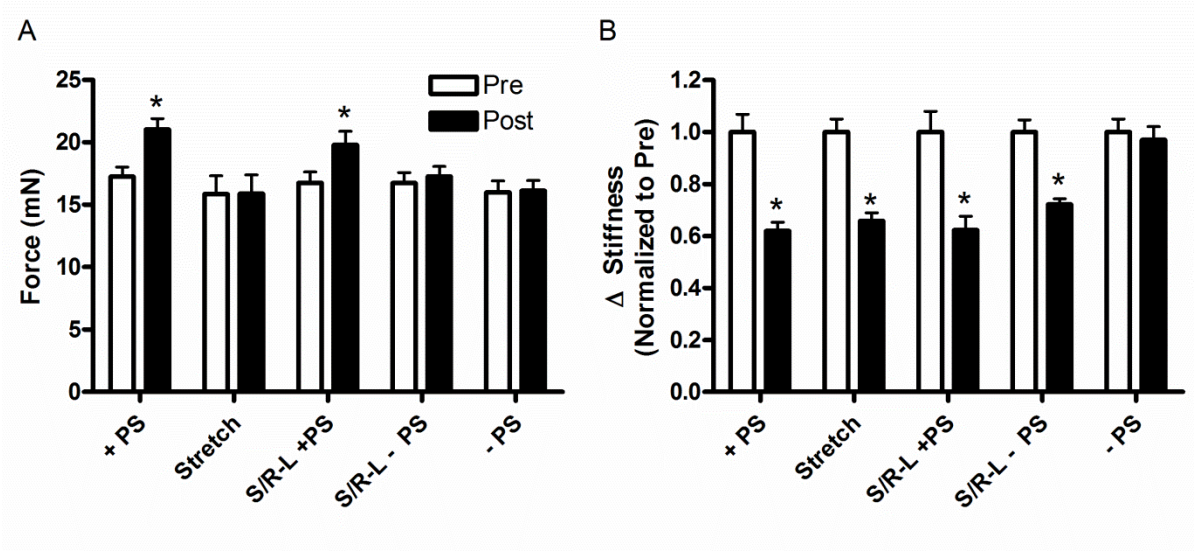

Figure V-7 - Changes in force and stiffness following electrical and mechanical perturbations

Summary data for the force (A) and stiffness (B) measurements in the various protocols used in this study, measured 30 s before (Pre) and 2.5 s after (Post) an electrical stimulation and/or a length perturbation are depicted in this figure. +PS: potentiating stimulus of 20 Hz stimulation for 2.5 s. –PS: no stimulation applied. Stretch: sinusoidal length change perturbation of 33% L_o at 20 Hz for 2.5 s. S/R-L: Slack/re-lengthening protocol where muscle was reduced to 50% L_o for 3 s either with or without the PS. Force was potentiated only in the presence of the PS, while resting stiffness was reduced following both stimulation and length changes. * Significantly different than Pre ($P<0.05$). All values are mean ± SEM. See text and prior figures for n values.

Discussion

This study was designed to determine if an increase in resting crossbridge attachment could occur following a PS, thereby providing a mechanistic explanation for elevated twitch force during potentiated contractions in the absence of myosin RLC phosphorylation as observed in both Chapter II and the current study (Figure V-3). The present data do not support this explanation. Specifically, following the slack/re-lengthening protocols there were no stimulation-dependent differences in the elastic and viscous components of stiffness (Figure V-6) which would suggest a change in crossbridge binding. It is therefore concluded that

contraction-induced increases in resting Ca^{2+} do not cause potentiation by elevating the number of crossbridges bound at rest.

Short range elastic component and latency relaxation

The predominant results in the present study were reductions in stiffness following any electrical or mechanical perturbation. These results are consistent with the short range elastic component of muscle (SREC) described by Hill (1968). The SREC manifests as a steep initial rise in tension upon lengthening which then levels off once the length exceeds a certain "breaking point" typically at ~0.2% of L_o, and once this breaking point is reached, the SREC is absent in subsequent stretches (Hill, 1968) with a recovery time of ~3 minutes (Herbst, 1976;Campbell & Lakie, 2008). This effect has been attributed to a stable population of weakly bound crossbridges in resting muscle which become detached upon a change in length (Hill, 1968;Campbell & Lakie, 1998;Campbell & Lakie, 2008;Herbst, 1976). However, it is difficult to accept that weak crossbridge binding requires minutes to be reestablished following stretch when a muscle can attain full rigor within milliseconds, thus the SREC is more likely to be caused or at least dominated by a non-crossbridge mechanism. This non-crossbridge attribution of the SREC appears to be the general, though not unanimous, accord of the scientific community (see Kellermayer *et al.*, 2008;Yagi, 2011;Campbell & Lakie, 2008). Data from Bagni *et al.* (1995) revealed that the SREC can be abolished by chemically skinning fibres, but is reestablished upon osmotic compression. Similarly, the SREC is higher during osmotic shrinkage but is unrelated to the degree of thick and thin filament overlap (Hill, 1968). Thus the SREC can be localized to the filaments, but requires proximity between the thick and thin filaments. Interesting in this regard are findings from Kellermayer et al (2001) who found that titin, which is the major determinant of tension in a resting muscle (Wang *et al.*, 1991),

exhibits discrete unfolding events of the immunoglobulin domain at molecular lengths between ~0.8-2.0 μm which effectively increases the free-spring length of titin, shifting the force-length curve to the right. Considering that titin spans the length of the half sarcomere (Wang *et al.*, 1979) and optimum sarcomere length for force production is ~2.4 μm, these unfolding events occur within a physiologically relevant range. Moreover, the recovery time of these unfolding events was in the range of 2 and 4 minutes (Kellermayer *et al.,* 2001) which is consistent with the 3 minutes SREC resolution time (Herbst, 1976;Campbell & Lakie, 1998). Thus it seems more likely that the SREC is attributable to titin unfolding. However, this conclusion is complicated by the fact that SREC is disrupted by muscle shortening as well as lengthening (Herbst, 1976;Hill, 1968) and it is difficult to reconcile titin unfolding with low forces and muscle shortening. A different perspective can be gained from the theory regarding titin as a winding filament (Nishikawa *et al.*, 2012), stating that titin binds to actin in the presence of Ca^{2+}, and active tension causes helical rotation of actin which necessitates titin winding around the thin filament. Should titin bind to or wind around the thin filament in resting muscle, new geometric possibilities may become available to explain the equivalent effects of shortening and lengthening on the SREC.

Further insights and support for the conclusion that elevations in weak crossbridge binding do not occur during potentiation can be gained from discussion of latency relaxation. Latency relaxation is the period of tension decline that follows stimulation and precedes tension development in skeletal muscle (Sandow, 1944), an effect which is inducible only at low levels of cytosolic Ca^{2+} and thin filament activation (Hill, 1968). Recent work has revealed a change in the conformation of tropomyosin that follows Ca^{2+} binding (Yagi, 2011) which in turn causes a helical twist in the actin filaments, with the magnitude of the rotation increasing with

distance from the Z-disc (Wakabayashi *et al.*, 1994). This necessitates the detachment of crossbridges prior to contraction, thereby providing an explanation for latency relaxation (Yagi, 2011). This mechanism suggests that if elevations in resting Ca^{2+} were to increase the number of crossbridges at rest, they would be unable to prime the thin filament for contraction due to the latency relaxation. Consistent with this, it has been suggested that the thin filament is regulated as a single unit due to end-to end interactions with adjacent tropomyosin filaments (Brandt *et al.*, 1987) and active tension requires a large proportion of TnC to be Ca^{2+} bound (Yagi, 2003), thus active force generation and crossbridge binding may be delayed until the twisting of the thin filament has ceased. However, it is possible that the increase in resting Ca^{2+} noted during potentiation (Smith *et al.*, 2013b) may accelerate this process, thereby enhancing the rate of force production by reducing the duration of the latency relaxation. Latency relaxation was not observed in the present study, due at least partially to the use of high temperatures (see Sandow, 1947), thus it remains unknown how potentiation affects this phenomenon.

The current study found no evidence of increased crossbridge binding at rest in potentiated muscle. When this is coupled with the crossbridge-based explanations of SREC and latency relaxation, along with the questionable existence of weak crossbridge binding in resting muscle in general (Bagni *et al.*, 1992;Bagni *et al.*, 1995;Bagni *et al.*, 1999), the likelihood of weak crossbridge attachment at the onset of force development during a potentiated contraction is very small indeed.

Changes in viscous and elastic stiffness

The use of sinusoidal length oscillations in this study permitted the separation of viscous and elastic components of stiffness. All mechanical and electrical perturbations used in this study caused reductions in elastic stiffness and increases in viscous stiffness detected at 2.5 s after completion. The declines in stiffness were not dependent on the velocity of the length change as the magnitude of the decrease in stiffness was unchanged at the different frequencies of sinusoidal oscillation. The increases in viscosity post-perturbation did exhibit some velocity-dependency, though this may be accounted for by a lower signal to noise ratio at lower velocity oscillations (Figure V-4). However, the time required for the elastic and viscous stiffness to return to baseline differed considerably from each other, with viscous stiffness requiring <5 s and elastic stiffness requiring ~20 s, thus it is possible that there are separate mechanisms causing these changes. The consistency of the stiffness response to each of the different perturbations used in this study suggests that the same events are occurring following both length changes and electrical stimulation. Future work is required to determine a definitive origin.

Effects of the SREC on force

As a byproduct of this investigation, it can also be concluded that the SREC does not grossly affect the contraction, despite the similar effect durations (Figure V-3 and Figure V-4), as neither the force nor the kinetics of twitch and tetanic contractions were affected by either the slack/re-lengthening or the passive lengthening protocols in the absence of stimulation (Figure V-2). Similarly, the passive lengthening protocol serves as a check on the procedures

used in this and previous studies, verifying that the forces involved in contraction do not induce a change in the compliance of the detection system or slippage of the muscle mounts.

Limitations and future directions

The possibility that elevated resting cytosolic Ca^{2+} can enhance weak myosin binding at rest cannot be ostensibly ruled out. Due to the dominance of titin as a determinant of resting tension (Wang *et al.*, 1991), it is possible that such an increase occurred, but is so low in magnitude that the methods employed in the current study simply failed to detect this change. However, the current rationale for latency relaxation based on myosin-detachment precludes any such increases having a direct effect on force production.

Though RLC phosphorylation was not measured in the current study, the potentiating stimulus used here was identical to that used in Chapter II. This potentiating stimulus caused similar levels of potentiation both in magnitude and duration, and the forces and kinetics of twitches were similar between these two studies. Therefore it is a safe assumption that there were no changes in the phenotype of the mice between these two studies, and no changes are attributable to myosin RLC phosphorylation in the current study. Though this is useful for the specific research question posed in the current study, it introduces a problem in the generalizability of the results of the stiffness testing. The stable order of the thick filament is disrupted by RLC phosphorylation, causing the myosin heads to extend into the cytosol, closer in proximity to the thin filament and enhancing the likelihood of their interaction (Levine *et al.*, 1996;Yang *et al.*, 1998). Thus a muscle exhibiting RLC phosphorylation would be more likely to exhibit increased weak crossbridge binding than one which does not. Thus the conclusions of this study cannot be applied to potentiated muscle in general as an elevation in

resting stiffness and weak crossbridge binding could occur in resting potentiated muscles which exhibit RLC phosphorylation, though the attribution would be to the RLC phosphorylation and not to elevations in resting cytosolic Ca^{2+} concentrations per se.

Future work regarding the potentiating mechanism of elevated resting cytosolic Ca^{2+} should focus on examining the role of Ca^{2+} binding to myosin and its light chains, and the effects of cytosolic Ca^{2+} buffer saturation on twitch force, both of which remain promising avenues of investigation. For example, though myosin heads do not change conformation in the presence of high intracellular Ca^{2+} (Yagi & Matsubara, 1980), Ca^{2+}-bound RLC is associated with reduced myosin ATPase activity (Bremel & Weber, 1975) and lower actin motility (Vikhoreva & Månsson, 2010) which could translate into higher twitch forces if myosin binding is not adversely affected. Similarly, an increase in saturation of high affinity cytosolic Ca^{2+} buffers could enhance Ca^{2+} binding to TnC, enhancing the rate of thin filament activation, leaving it activated for a longer duration, allowing greater opportunity for myosin binding.

Conclusions

The experiments performed in this study have demonstrated that potentiation of mouse lumbrical is very unlikely to be aided by increased number of crossbridges bound at rest. Disruption of the cellular milieu with either electrical stimulation or length changes induces a net decline in stiffness, consistent with the SREC previously described (Hill, 1968). Breaking the change in stiffness down into its constituent viscous and elastic components reveals it is composed of a relatively long lived decrease in elastic stiffness and a relatively short-lived increase in viscous stiffness. The differences in time course suggest two separate but

complementary mechanisms which have little to no effect on force production, as potentiation was only present following electrical stimulation. Thus the precise mechanism of potentiation of mouse lumbrical that coincides with elevations in resting cytosolic Ca^{2+} concentration remains to be determined.

Chapter VI - Summary, conclusions, and perspectives

This thesis started with four main objectives in mind. The first objective was to characterize the contractile properties, and the expression of the proteins primarily responsible for determining the contractile, relaxation, and potentiation properties of the mouse lumbrical muscle. This assessment, as performed in Chapters II and III, describes the lumbrical as a fast twitch muscle, with a predominance of type IIX fibres. It moderates the EDL and soleus in each of SERCA1a, SERCA2a, and parvalbumin expression, along with the parvalbumin to SERCA ratio. The lumbrical has low expression of skMLCK, and high expression of MYPT2, and as such did not phosphorylate its RLC in response to 2.5 s of 20 Hz stimulation. Despite this, it still exhibits both staircase and posttetanic potentiation at 37^{o}C, but not at 30^{o}C.

The second and third objectives of this thesis were to characterize the cytosolic Ca^{2+} transient and resting cytosolic Ca^{2+} during both posttetanic potentiation and staircase potentiation and determine if the changes in cytosolic Ca^{2+} can be reconciled with the enhancements in force and relaxation seen during potentiation. During posttetanic potentiation, there were increases in force and enhanced relaxation properties, though there were no changes to the Ca^{2+} transient, either in amplitude, area or duration relative to those of unpotentiated contractions. However, there was an increase in resting cytosolic Ca^{2+} that temporally matched the duration and intensity of the force potentiation. Thus it was concluded that elevations in force could be due to the higher levels of cytosolic Ca^{2+} at the onset of the contraction.

Staircase potentiation was assessed at both 30 and 37^{o}C in the lumbrical using 8 Hz stimulation for up to 8.0 s, resulting in increases in twitch force at 37^{o}C, and decreases in twitch force at 30^{o}C by 8.0 s. At both temperatures, relaxation times and rates were biphasic where they were initially enhanced and then progressively impaired. The impairments in relaxation time temporally corresponded to increases in the duration of the Ca^{2+} transient.

Likewise, the patterns of contraction force were complex, but could be explained by changes in the Ca^{2+} transient. It is unlikely that the elevation in force is caused by summation as force had returned to baseline, as did muscle stiffness (see Appendix 6) which is indicative of the absence of bound crossbridges (see Chapter V). The contraction forces in the second twitches at both 30 and 37^{o}C were higher than the force of the first twitch, which could be accounted for by the largest increase in the resting cytosolic Ca^{2+} concentration. Beyond the second twitch, force declined at both temperatures, though it declined more at 30^{o}C and did not recover, whereas at 37^{o}C, force began to increase again at twitch ~5-6. The declines in force were temporally matched to declines in both the area and the peak amplitude of the Ca^{2+} transient, and the magnitude of these declines was larger at 30^{o}C than 37^{o}C. Additionally, the peak ratio values showed a significant increase through the staircase protocol at 37^{o}C, whereas it decreased significantly at 30^{o}C. These decreases in Ca^{2+}-transient amplitude were found to be consistent with the temporal and temperature dependence of inactivation of Ca^{2+} release from the SR noted by Barclay (2012). In an effort to prevent these declines in Ca^{2+} release, 0.5 mM caffeine was administered in the bathing solution of the lumbricals. This resulted in enhanced twitch force as well as enhanced potentiation at 37^{o}C and attenuation of the force losses at 30^{o}C. Importantly, the reductions in Ca^{2+} transient amplitude and area were also attenuated. However, as caffeine has not been definitively demonstrated to overcome inactivation of Ca^{2+} release, there are two possible interpretations. The first interpretation is that the attenuation of the drop in Ca^{2+} transient amplitude and area were causative to the enhancements, while the second is that the increased Ca^{2+} released in the presence of caffeine could cause a greater increase in cytosolic resting Ca^{2+} and thereby enhance force. The results of this thesis suggest that these two mechanisms are occurring concurrently. Finally, though the early declines in the

relaxation time and enhancements in relaxation rate were temporally matched to the declines in Ca^{2+} transient amplitude and area, caffeine administration enhanced the relative decreases in relaxation time and increases in relaxation rate, despite attenuating the reductions in Ca^{2+} release and increasing the force, both of which should have caused relaxation to slow if this were a Ca^{2+}-dependent mechanism. Therefore it must be concluded that the enhanced relaxation occurs at the level of the crossbridge, and the case for Pi serving as this relaxation enhancing factor is made in Chapter IV, though much work needs to be done to either confirm or disprove this hypothesis. In summary, the degree of potentiation is the balance between factors which affect the Ca^{2+} signal (increased resting Ca^{2+}, slowing of the Ca^{2+} transient vs declining amplitude of the Ca^{2+} transient) and those which directly affect the crossbridge (RLC phosphorylation vs relaxation enhancing factor).

The fourth objective of this thesis was to determine how the changes in cytosolic Ca^{2+} may exert their influence. While many of the results in this thesis are easy to reconcile between force and Ca^{2+} data, it is not established how elevations in resting Ca^{2+} enhance force production. Three distinct possibilities were outlined in Chapter II. First, elevated resting Ca^{2+} could saturate high affinity cytosolic Ca^{2+} buffers thereby enhancing Ca^{2+} binding to TnC and enhancing thin filament activation. Second, divalent cation binding sites on myosin and its light chains may exhibit increased Ca^{2+} binding at elevated resting Ca^{2+} concentrations, thereby asserting a form of post translational modification on the structure and behavior of myosin. Third, the elevation in resting Ca^{2+} may enhance crossbridge binding in the resting state such that the crossbridges are bound, but not force-producing, but can quickly be recruited upon subsequent Ca^{2+} activation of the thin filament, serving as a primer for further thin filament activation. It was this third possibility that was assessed in Chapter V by examining resting

stiffness of the muscle using low amplitude sinusoidal length oscillations. Here it was determined that a perturbation to the muscle by either passive length change or contraction resulted in a decline in resting stiffness. This effect is consistent with the disappearance of the short range elastic component of muscle which is commonly attributed to a stable population of bound but non-force producing crossbridges in resting muscle. Should this attribution be correct, potentiation of the lumbrical occurs with a reduction in the number of crossbridges bound at rest. However, subsequent analysis determined that mechanical removal of the short range elastic component via passive length changes had no effect on the force of either twitch or tetanic contractions. Therefore it is concluded that the increases in resting Ca^{2+} concentration does not result in the formation of a population of bound crossbridges which prime the thin filament upon stimulation, and future work should focus on addressing the remaining two theories.

Appendix 1 - Protocol for loading AM indicators

Prior to initiating this process, ensure autofluorescence has been measured and recorded.

1) In the dark, add 10 μL dimethyl sulfoxide (DMSO) to the 50 μg aliquot of AM indicator.

Furaptra (722.56 g/mol) or mag-indo-1 (730.63 g/mol)
2) Add 35 μL 10% w/v pluronic in DMSO to the aliquot. Do not agitate.
3) Add 670 μL oxygenated Tyrode's experimental solution to the aliquot. Vortex.
4) Add entire contents of aliquot to a beaker covered in aluminum foil.
5) Repeat steps 3 and 4 a total of 5 times

Fura-2 (1001.85 g/mol) or indo-1 (1009.93 g/mol)
2) Add 25 μL 10% w/v pluronic in DMSO to the aliquot. Do not agitate.
3) Add 670 μL oxygenated Tyrode's experimental solution to the aliquot. Vortex.
4) Add entire contents of aliquot to a beaker covered in aluminum foil.
5) Repeat steps 3 and 4 a total of 4 times

Final concentration ~20μM indicator, 0.1% pluronic

6) Stop circulation of Tyrode's experimental solution. Adjust temperature of muscle to 32^{o}C. DO NOT STOP CIRCULATION OF WATER THROUGH PELTIER HEATER: IT CAN BURN OUT IN SECONDS WITHOUT CONTINUOUS FLOW DURING OPERATION.

7) With a Teflon tipped syringe, remove the contents of the chamber from the filling well (separate from, but connected to the muscle well). 7) Add half the contents of the beaker containing the indicator solution to the muscle chamber using the filling well.

8) After 30 minutes, drain the muscle chamber as in step 6. Add the remainder of the indicator solution to the filling well. Wait 30 min.

9) Drain the muscle chamber as in step 6. Wash the chamber with fresh oxygenated Tyrode's solution a minimum of 5 times. Restart circulation and adjust temperature on Peltier to desired experimental settings. Wait ~10 minutes for muscle to equilibrate.

Muscles loaded with the lower molecular weight indicators mag-indo-1 and furaptra exhibit >10 000 fold higher fluorescence at 380 nm than unloaded muscles (depending on PMT and light settings), while for indo-1 and fura-2 the fluorescence signal is only 3-4 times higher following indicator loading, reflecting the differences in molecular weight.

Appendix 2 - Alternate figure for SERCA1a, SERCA2a and parvalbumin expression

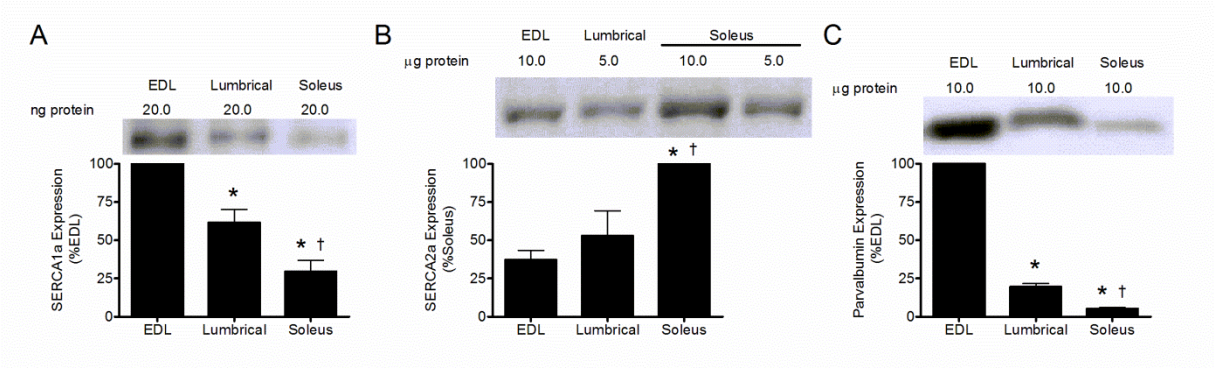

Figure VI-1 - Protein expression of Ca^{2+}-sequestering proteins (simplified version)
This figure depicts sample Western blots and summarized densitometric analysis for SERCA1a (A), SERCA2a (B) and parvalbumin (C). All values are expressed relative to a linear protein gradient established with either extensor digitorum longus (EDL) (SERCA1a and parvalbumin) or soleus (sol) (SERCA2a). N=8 for all muscles and proteins. * Significantly different than EDL. †Significantly different than lumbrical (lum). Significance was taken at $P<0.05$. Notes: Two lumbricals from the same animal (one from each hind foot) are pooled, whereas soleus and EDL are unpooled (due to size differences).

Appendix 3 - Extended twitch kinetic parameters

Table VI-1 - Extended twitch kinetic parameters before, during and after posttetanic potentiation

Time (s)	TPT (ms)	½ RT (ms)	+df/dt (mN/ms)	-df/dt (mN/ms)	90% RT (ms)	FWHM (ms)
-150	12.46±0.70	11.50±0.41	3.36±0.30	-1.12±0.10	25.59±1.21	19.62±0.98
-120	12.32±0.69	11.48±0.41	3.37±0.30	-1.12±0.09	25.47±1.24	19.46±0.98
-90	12.22±0.68	11.45±0.43	3.35±0.30	-1.13±0.10	25.30±1.24	19.34±0.98
-60	12.15±0.69	11.39±0.39	3.37±0.30	-1.14±0.11	25.18±1.24	19.23±0.96
-30	12.16±0.69	11.33±0.40	3.41±0.31	-1.14±0.10	25.16±1.25	19.18±0.96
2.5	*11.41±0.73*	*10.00±0.32*	*4.57±0.42*	*-1.40±0.13*	*23.23±1.47*	*17.61±0.97*
5	*11.01±0.71*	*10.01±0.33*	*4.39±0.41*	*-1.39±0.12*	*22.78±1.43*	*17.14±0.95*
7.5	*10.82±0.70*	*10.03±0.34*	*4.22±0.39*	*-1.39±0.12*	*22.57±1.39*	*16.91±0.95*
10	*10.68±0.69*	*10.08±0.35*	*4.15±0.37*	*-1.37±0.13*	*22.47±1.37*	*16.79±0.95*
20	*10.82±0.71*	*10.34±0.39*	*3.81±0.36*	*-1.30±0.12*	*23.31±1.45*	*17.05±0.99*
30	*11.25±0.72*	*10.70±0.41*	3.60±0.33	*-1.23±0.11*	24.44±1.48	*17.74±1.02*
60	*12.79±0.80*	11.55±0.44	3.31±0.30	-1.09±0.09	*26.94±1.51*	*19.96±1.12*
90	*13.14±0.77*	*11.82±0.43*	3.26±0.30	-1.06±0.09	*27.05±1.34*	*20.55±1.07*
120	*13.05±0.76*	*11.71±0.41*	3.23±0.28	-1.06±0.09	*26.61±1.27*	*20.38±1.03*
150	12.61±0.69	11.64±0.41	3.23±0.29	-1.08±0.09	25.89±1.18	*19.89±0.97*

Summary of the twitch kinetic parameters for all twitches measured during the course of study in Chapter II (n=10 muscles, 8-10 cyclic repetitions per muscle per data point, values are mean ± SEM). Times listed with a negative value denote that they occur before the potentiating stimulus and times without the negative sign occurred after the potentiating stimulus. Note the cyclic nature of these data (i.e. -150 s occurred ~30 s after 150 s and therefore could accurately be labeled 180 s). TPT: Time to peak tension. ½ RT: Time for force to relax from peak to 50% peak. +dF/dt: Maximum rate of force production. -dF/dt: Maximum rate of force relaxation. 90% RT: Time for force to relax from peak to 10% peak. FWHM: Full width at half maximum. Italicized values are significantly different from the -30 s time point (i.e. the last twitch before the potentiating stimulus; $P<0.05$).

Appendix 4 - A brief note on the contribution of the cytosolic Ca^{2+} transient to post tetanic potentiation in lumbrical muscle in the phospholamban null line

This study was intended to investigate the effects of phospholamban (PLN) ablation on Ca^{2+} transients during post tetanic potentiation using PLN null mice and their wildtype littermates. Western blotting data of the lumbrical of mice used in Chapter II revealed the presence of PLN in C57BL/6 mouse lumbrical (Figure VI-2), but assessment of the wildtype mice used in this appendix revealed that there were very small, virtually undetectable, amounts of PLN present in the lumbrical of the PLN null/PLN wildtype mice – an impure C57 strain (Figure VI-3). Moreover, contractile data revealed that these mice were of a faster phenotype than the mice used in Chapter II. Thus the lumbricals of the mice used here likely would display a predominantly type IIB fibre type profile rather than predominantly type IIX profile characterized in Chapter II. Moreover, genotyping errors occurred and some mice heterozygous for the PLN KO gene were incorrectly identified as homozygous for the PLN KO gene, and due to the very low amounts of PLN in any lumbrical used for this study, the heterozygous and homozygous PLN KO mice could not be distinguished with confidence using Western blotting.

Due to the low expression of PLN, the lack of functional differences between the WT and mixed $PLNKO^{+/+,+/-}$ groups, and no individual muscles exhibited obviously different force or Ca^{2+} characteristics from any other muscle, it was deemed valid to group all mice (n=6 WT; 10 $PLNKO^{+/+,+/-}$) in order to gain insights into how Ca^{2+} transients may behave in a faster phenotype of muscle. The force and fluorescence methods used in this study were identical to those described in Chapter II using AM-furaptra. The results are virtually identical to those of Chapter II with the following notable exceptions: 1) In addition to the faster kinetics noted

above, the degree of PTP was ~40% higher in these mice than in Chapter II and lasted for 30 s, but was absent at 60 s. 2) The amplitude of the peak change in cytosolic Ca^{2+} was lower in early PTP than control (P=0.07), but no differences were found between Con and Late PTP or Early and Late PTP.

These results support the findings of the earlier Chapters of this thesis, but cannot offer insight into either the role or the regulation of PLN during brief muscle activation.

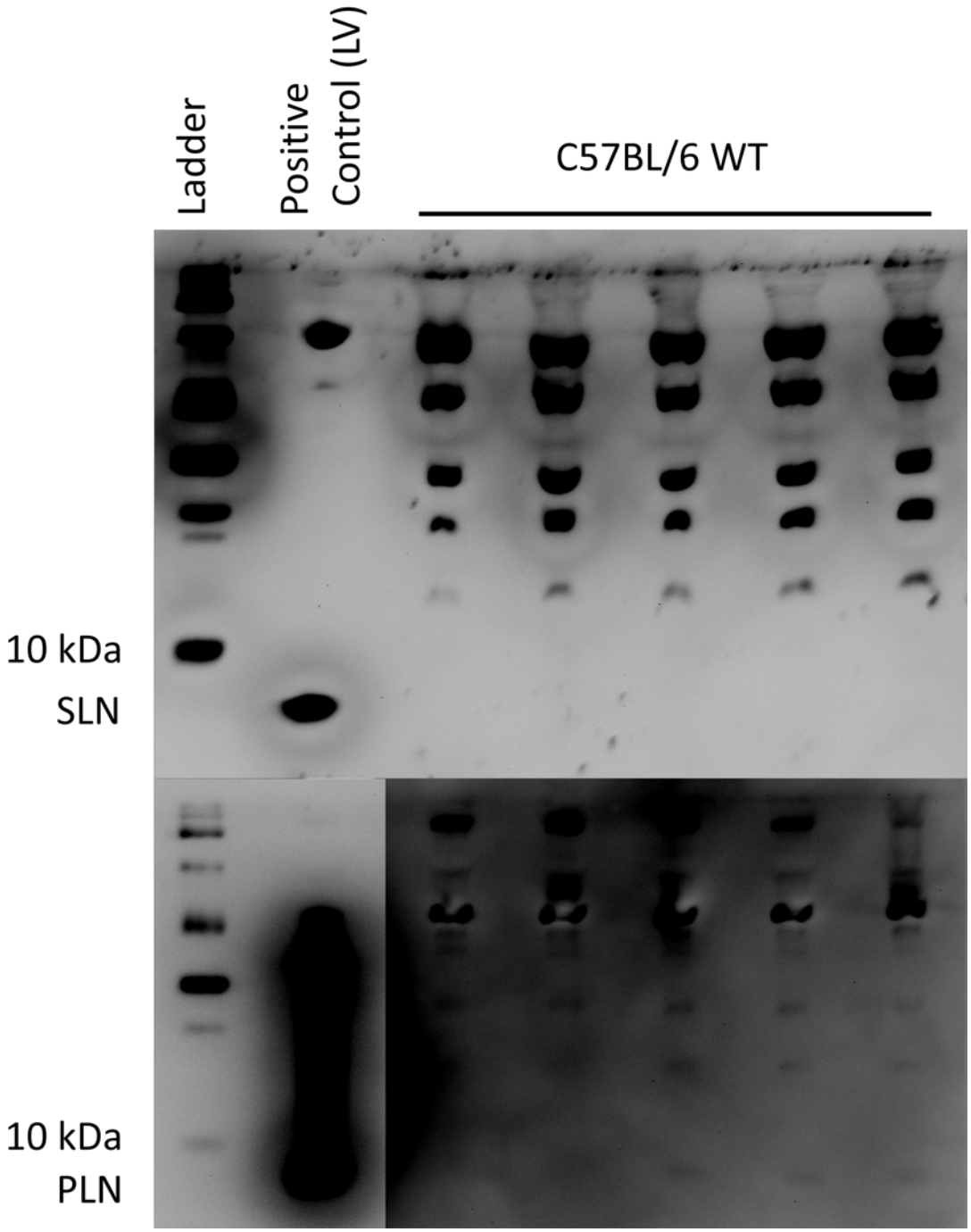

Figure VI-2 - Western blots for sarcolipin and phospholamban in C56BL/6 mouse lumbrical muscle

Sample blots for sarcolipin (SLN; top panel) and phospholamban (PLN; bottom panel). Lane 1 is a molecular weight protein ladder. Lane 2 is a positive control for SLN and PLN respectively (mouse left ventricle). Subsequent lanes are homogenates from male C57BL/6 mouse lumbrical. No SLN and only low levels of PLN were detected in the lumbrical. Single lumbrical muscles were homogenized in 50 μL of PMSF buffer and 30 μL of the resulting homogenate was loaded into wells.

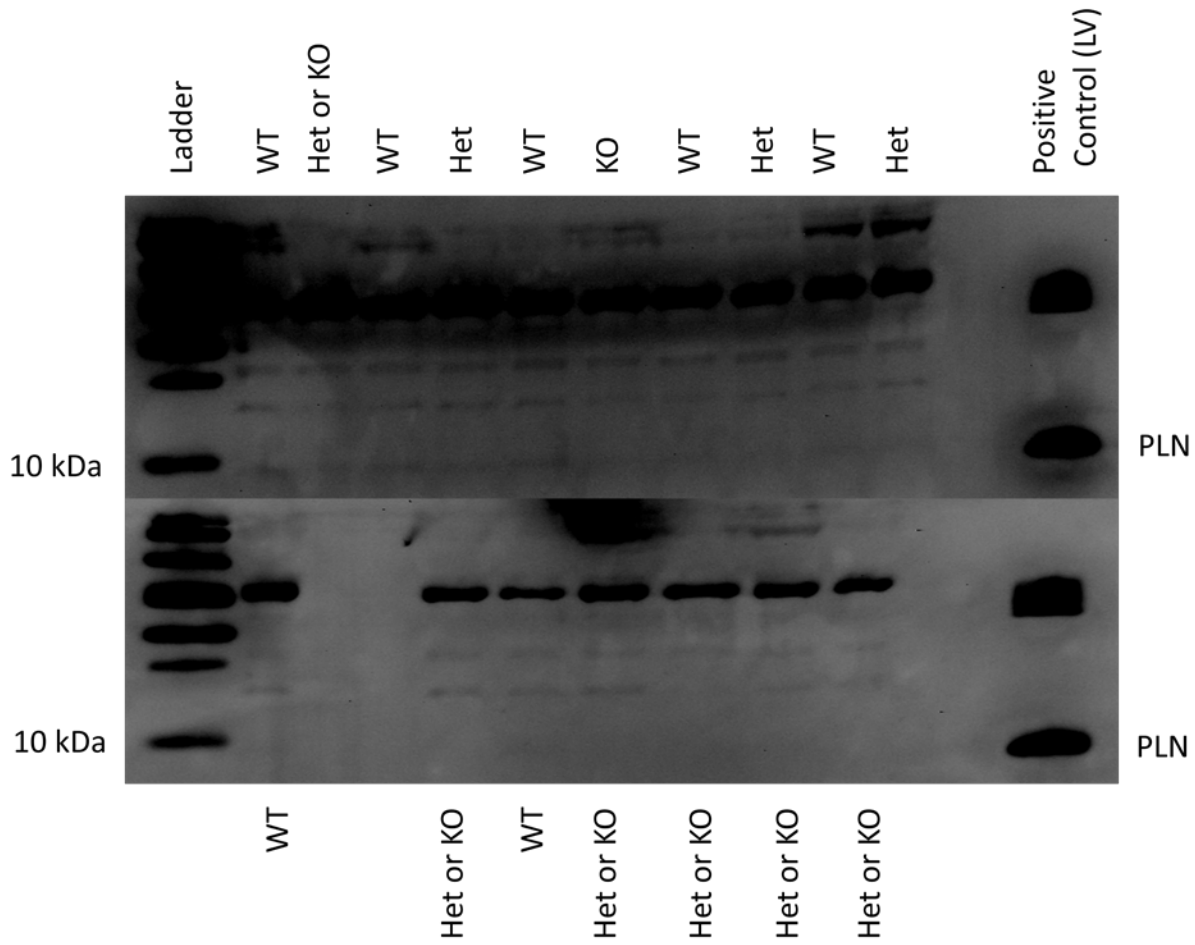

Figure VI-3 - Phospholamban expression in lumbricals from the phospholamban transgenic mouse line

Phospholamban was nearly undetectable in lumbrical muscles from the phospholamban (PLN) transgenic line, regardless of whether the genotype of the mouse was wild type (WT), phospholamban null (KO) or heterozygous (Het) for the PLN gene. Samples were run opposite a mouse left ventricle positive control for comparison. Due to errors in the initial genotyping of the PLN KO gene, some mice are marked as “Het or KO” to identify the ambiguity. Single lumbrical muscles were homogenized in 50 μL of PMSF buffer and 30 μL of the resulting homogenate was loaded into wells.

Appendix 5 - The resolution of relaxation properties following potentiating contractions

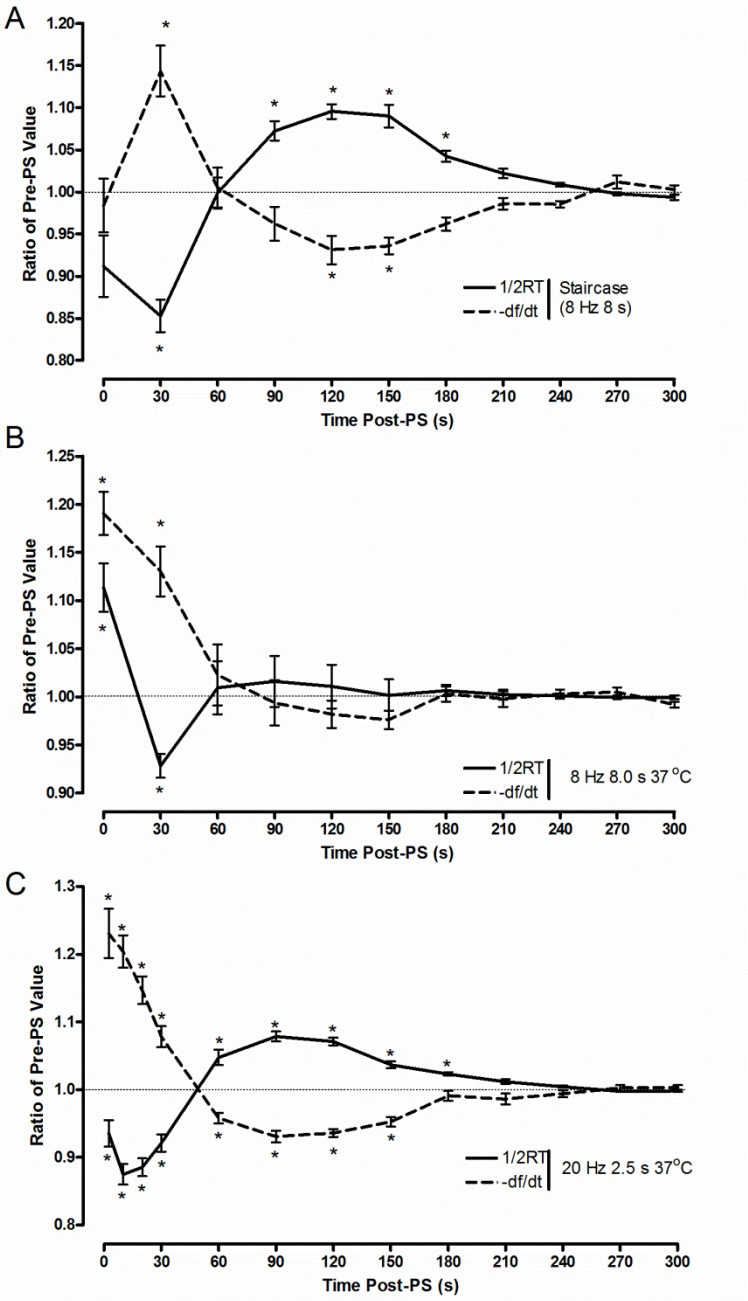

Figure VI-4 - Biphasic responses of twitch relaxation following a potentiating stimulus
Changes in time to reach 50% relaxation following peak twitch force (1/2RT) and the peak rate of relaxation (-df/dt) were measured at 30 s intervals following potentiating stimulations (PS), either staircase potentiation (8 Hz for 8.0 s at either 30 (A) or 37^{o}C (B)) or posttetanic potentiation (20 Hz for 2.5 s (C)). * Different from pre-potentiated levels ($P<0.05$). Time zero corresponds to the final twitch in the staircase protocol in panels A and B while the first data point in panel C falls 2.5 s after the end of the conditioning stimulus. Peak force returned to stable baseline 20-60 s post-PS in all conditions. The biphasic changes in relaxation properties highlight the complexity of the recovery process.

Appendix 6 - Resolution of force and muscle stiffness following twitch contraction

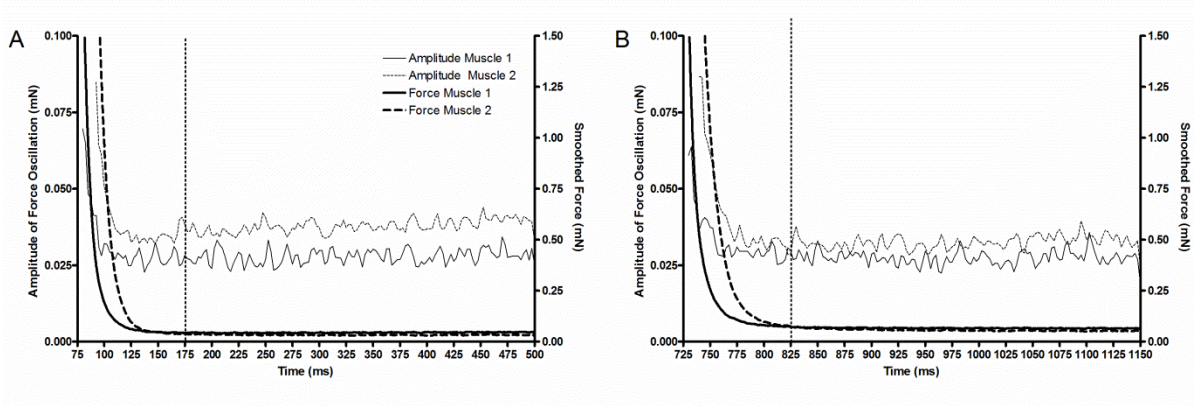

Figure VI-5 - Resolution of force and stiffness following unpotentiated and potentiated twitch contractions

Muscle stiffness was assessed using low amplitude (1.4 μM), 200 Hz sinusoidal length oscillations during twitch contractions applied 30 s before (A) and 2.5 s after (B) a potentiating stimulus of 20 Hz for 2.5 s. Force records were smoothed using a 49 point filter, to minimize contribution from the sinusoidal oscillations (based on 10000 Hz collection frequency / 200 Hz oscillation = 50 point smooth) and plotted. The difference between the unsmoothed record and the smoothed record was used to determine the amplitude of the force oscillations caused by the length changes. This was performed by calculating the difference in force between consecutive peaks and valleys, and converting these values to amplitude by dividing by two. This amplitude is proportional to stiffness, though only late in relaxation due to the rapid changes in force at the onset of contraction which introduce artifact into the smoothed records. Similar results were found using both band pass and high pass filters. Stimulation was applied at 50 ms in A and at 700 ms in B. Vertical dashed lines are presented at 125 ms post stimulus to demonstrate that both force and stiffness have resolved before the onset of a twitch contraction during staircase potentiation at 8 Hz. Therefore the increases in force seen in twitch 2 of staircase protocols (see Chapters III and IV) cannot be attributed to summation of force or an increase in the number of bound crossbridges at rest.

Appendix 7 - The Journal of General Physiology provisional license to publish

Please send this completed form with your original manuscript submission

The Journal of General Physiology
Manuscript content verification and provisional license to publish

Article Title
(in full): _____

Authors
(all names): _____

In recognition of the author(s)' desire to publish this manuscript and any supplemental material in *The Journal of General Physiology*, and The Rockefeller University Press' (RUP) desire to publish the article as quickly as possible should it be accepted, this manuscript will be considered for publication provided the following criteria are met.

Contribution Warranty: The undersigned (all contributing authors) warrant that the Work is original and that it contains no matter that is defamatory or otherwise unlawful or that invades individual privacy or infringes on any proprietary right or any statutory copyright; and the undersigned agree to indemnify and hold the Journal and The Rockefeller University harmless against any claim to the contrary. The undersigned further warrant they have contributed significantly to the content and preparation of the Work, and that they have seen and approve the content, authorship, order of author representation, and any listing of author contributions. It is the responsibility of the contributors to review subsequent revisions of the Work should there be any. Except in the case of employees of the United States Government, and certain foreign governments, the undersigned warrant that they have the authority to license publication rights to RUP and that no portion of the copyright to the Work has been assigned or licensed previously.

Prior Publication: All contributing authors agree that the content of the Work has not been published in any article listed in a public citation database or in a book identified with an ISBN. The authors further agree that the Work is not currently under consideration for publication elsewhere. If accepted, it will be not be submitted elsewhere.

Competing Financial Interests: All contributing authors confirm that all commercial affiliations, stock or equity interests, or patent-licensing arrangements that could be considered to pose a financial conflict of interest regarding the submitted article have been disclosed.

Permission: The contributing authors are responsible for obtaining permission for the use of any material in the Work that may be under copyright to others, and this permission shall be obtained by the authors and submitted to the editorial office at the time of submission. Uncopyrighted or unpublished material that is provided by others and included in the Work must be accompanied by a signed permission letter from the provider of such information.

Copyright:

1. Ownership of copyright in the Work remains with the Authors.

2. The Authors retain the non-exclusive right to do anything they want with the Work, so long as the Authors provide attribution to the place of original publication. The retained right specifically includes the right to post the Work on the authors' or their institutions' web sites.

3. The Authors grant RUP a license (a) to publish, reproduce, distribute, display and store the Work in all forms, (b) to translate the Work into other languages, create adaptations, summaries or extracts of the Work or other derivative works based on the Work and exercise all of the rights set forth in (a) above in such translations, adaptations, summaries, extracts and derivative works, and (c) to license others to do any or all of the above. For the first six months after publication, this license will be exclusive to RUP (except as RUP may grant sublicenses). Beginning six months after publication, the Work will be made freely available to the public on RUP's website, and RUP's license will be non-exclusive. The Authors acknowledge that RUP will submit all Works to PubMed Central in accordance with PubMed Central's requirements, where they will be released to the public six months after the publication date.

4. For the first six months after publication, RUP grants the public the non-exclusive right to copy, distribute, or display the Work, under the following conditions:

a. **Attribution.** The user must attribute the Work as being copyright of the Authors and published in *The Journal of General Physiology*, but not in any way that suggests that the Authors or RUP endorse the user or the user's use of the Work.

b. **Noncommercial.** The user must not use the Work for commercial purposes.

c. **Share Alike.** If the user shares, alters, transforms, or builds upon the Work, the user may distribute the resulting work only under the same license the user received from RUP.

d. **No Mirror Sites.** The user may not create, compile, publish, host, enable, or otherwise make available a mirror site of the RUP web site, any of its constituent journal web sites (*The Journal of Cell Biology*, *The Journal of Experimental Medicine*, and *The Journal of General Physiology*), or any subset of the RUP or journal web sites. A "mirror site" is a web site that contains the same content as a parent web site but is located at a different geographic location from the parent site. This prohibition applies regardless of the commercial or non-commercial nature of the mirror site.

The full legal text of the license is available at http://http://www.rupress.org/site/subscriptions/RUP_license.xhtml

5. Beginning six months after publication, RUP grants the public the non-exclusive right to copy, distribute, or display the Work under a Creative Commons Attribution-Noncommercial-Share Alike 3.0 Unported license, as described at http://creativecommons.org/licenses/by-nc-sa/3.0/ and http://creativecommons.org/licenses/by-nc-sa/3.0/legalcode.

6. "Work" is defined as the final published article appearing in an RUP journal, including all forms of supplemental material and any images used for cover art or for any other journal feature.

The University recognizes that works prepared under United States Government contract or by employees of a foreign government or its instrumentalities are subject to the government's prior non-exclusive, royalty-free license to publish, translate, reproduce, use, or dispose of the published form of their work or to allow others to do so for non-commercial government purposes.

In cases where a manuscript is NOT accepted, the portions of this agreement regarding licensing shall be null and void.

Corresponding
Author: _____ (please print or type) **Date:** _____ **Signature:** _____

Author: _____ (please print or type) **Date:** _____ **Signature:** _____

Author: _____ (please print or type) **Date:** _____ **Signature:** _____

Author: _____ (please print or type) **Date:** _____ **Signature:** _____

Author: _____ (please print or type) **Date:** _____ **Signature:** _____

Please send this completed form as a PDF file with your original manuscript submission or by fax to the editorial office at:
212-327-8996

FOR OFFICIAL USE ONLY VOL _____ NO _____ ISSUE _____ YEAR _____

References

Abbate, F., Sargeant, A. J., Verdijk, P. W. L., & de Haan, A. (2000). Effects of high-frequency initial pulses and posttetanic potentiation on power output of skeletal muscle. *J Appl Physiol* **88**, 35-40.

Abbate, F., Van Der Velden, J., Stienen, G. J. M., & de Haan, A. (2001). Post-tetanic potentiation increases energy cost to a higher extent than work in rat test muscle. *Journal of Muscle Research and Cell Motility* **22**, 703-710.

Adachi, T., Weisbrod, R. M., Pimentel, D. R., Ying, J., Sharov, V. S., Schöneich, C., & Cohen, R. A. (2004). S-Glutathiolation by peroxynitrite activates SERCA during arterial relaxation by nitric oxide. *Nat Med* **10**, 1200-1207.

Allen, D. G., Lamb, G. D., & Westerblad, H. (2008). Skeletal muscle fatigue: Cellular mechanisms. *Physiol Rev* **88**, 287-332.

Allen, D. G., Lee, J. A., & Westerblad, H. (1989). Intracellular calcium and tension during fatigue in isolated single muscle fibres from Xenopus Laevis. *Journal of Physiology* **415**, 433-458.

Allen, D. G. & Trajanovska, S. (2012). The multiple roles of phosphate in muscle fatigue. *Front Physiol* **3**, doi:10.3389/fphys.2012.00463.

Allen, D. G. & Westerblad, H. (1995). The effects of caffeine on intracellular calcium, force and the rate of relaxation of mouse skeletal muscle. *J Physiol* **487**, 331-342.

Arvanitis, D. A., Vafiadaki, A., Sanoudou, D., & Kranias, E. G. (2011). Histidine-rich calcium binding protein: the new regulator of sarcoplasmic reticulum calcium cycling. *J Mol Cell Cardiol* **50**, 43-49.

Augusto, V., Padovani, C. R., & Campos, G. E. R. (2004). Skeletal muscle fiber types in C57BL6J mice. *Braz J Morphol Sci* **21**, 89-94.

Aydin, J., Korhonen, T., Tavi, P., Allen, D. G., Westerblad, H., & Bruton, J. D. (2007). Activation of Ca^{2+}-dependent protein kinase II during repeated contractions in single mouse fibres from mouse is dependent on the frequency of sarcoplasmic Ca^{2+} release. *Acta Physiol* **191**, 131-137.

Bagni, M. A., Cecchi, G., Colombini, B., & Colomo, F. (1999). Mechanical properties of frog muscle fibres at rest and during twitch contraction. *J Electromyogr Kinesiol* **9**, 77-86.

Bagni, M. A., Cecchi, G., Colomo, F., & Garzella, P. (1992). Are weakly binding bridges present in resting intact muscle fibers? *Biophys J* **63**, 1412-1415.

Bagni, M. A., Cecchi, G., Colomo, F., & Garzella, P. (1995). Absence of mechanical evidence for attached weakly binding cross-bridges in frog relaxed muscle fibres. *J Physiol* **482**, 391-400.

Bagshaw, C. R. & Reed, G. H. (1977). The significance of the slow dissociation of divalent metal ions from myosin 'regulatory' light chains. *FEBS Lett* **81**, 386-390.

Bal, N. C., Maurya, S. K., Sopariwala, D. H., Sahoo, S. K., Gupta, S. C., Shaikh, S. A., Pant, M., Rowland, L. A., Bombardier, E., Goonasekera, S. A., Tupling, A. R., Molkentin, J. D., & Periasamy, M. (2012). Sarcolipin is a newly identified regulator of muscle-based thermogenesis in mammals. *Nat Med* **18**, 1575-1579.

Balog, E. M., Fruen, B. R., Kane, P. K., & Louis, C. F. (2000). Mechanisms of P_i regulation of the skeletal muscle SR Ca^{2+} release channel. *Am J Physiol Cell Physiol* **278**, C601-C611.

Bandyopadhyay, A., Shin, D. W., Ahn, J. O., & Kim, D. H. (2000). Calcineurin regulates ryanodine receptor/Ca^{2+}-release channels in rat heart. *Biochem J* **352**, 61-70.

Barclay, C. J. (1992). Effect of fatigue on rate of isometric force development in mouse fast- and slow-twitch muscle. *Am J Physiol* **263**, C1065-C1072.

Barclay, C. J. (2005). Modelling diffusive O_2 supply to isolated preparations of mammalian skeletal and cardiac muscle . *J Muscle Res Cell Motil* **26**, 225-235.

Barclay, C. J. (2012). Quantifying Ca^{2+} release and inactivation of Ca^{2+} release in fast- and slow-twitch muscles. *J Physiol* **590**, 6199-6212.

Baylor, S. M. & Hollingworth, S. (2000). Measurement and interpretation of cytoplasmic calcium levels. *News Physiol Sci* **15**, 19-26.

Baylor, S. M. & Hollingworth, S. (2003). Sarcoplasmic reticulum calcium release compared in slow-twitch and fast-twitch fibres of mouse muscle. *J Physiol* **551**, 125-138.

Baylor, S. M. & Hollingworth, S. (2011). Calcium indicators and calcium signalling in skeletal muscle fibres during excitation-contraction coupling. *Prog Biophys Mol Biol* **105**, 162-179.

Baylor, S. M. & Hollingworth, S. (2012). Intracellular calcium movements during excitation-contraction coupling in mammalilan slow-twitch and fast-twitch muscle fibers. *J Gen Physiol* **139**, 261-272.

Beard, N. A., Wei, L., & Dulhunty, A. F. (2008). Control of muscle ryanodine receptor calcium release channels by proteins in the sarcoplasmic reticulum lumen. *Clin Exp Pharmacol Physiol* **36**, 340-345.

Bennett, A. F. (1985). Temperature and muscle. *J Exp Biol* **115**, 333-344.

Bhupathy, P., Babu, G. J., Ito, M., & Periasamy, M. (2009). Threonine-5 at the N-terminus can modulate sarcolipin function in cardiac myocytes. *J Mol Cell Cardiol* **47**, 723-729.

Blazev, R. & Lamb, G. D. (1999a). Adenosine inhibits depolarization-induced Ca^{2+}-release in mammalian skeletal muscle. *Muscle Nerve* **22**, 1674-1683.

Blazev, R. & Lamb, G. D. (1999b). Low [ATP] and elevated [Mg^{2+}] reduce depolarization-induced Ca^{2+} release in mammalian skeletal muscle. *J Physiol* **520**, 203-215.

Bloemberg, D. & Quadrilatero, J. (2012). Rapid determination of myosin heavy chain expression in rat, mouse, and human skeletal muscle using multicolor immunofluorescence analysis. *PLoS One* **7**, e35273.

Bombardier, E., Smith, I. C., Gamu, D., Fajardo, V. A., Vigna, C., Sayer, R. A., Gupta, S. C., Bal, N. C., Periasamy, M., & Tupling, A. R. (2013a). Sarcolipin trumps β-adrenergic receptor signaling as the favored mechanism for muscle-based diet-induced thermogenesis. *FASEB J* **27**, 3871-3878.

Bombardier, E., Smith, I. C., Vigna, C., Fajardo, V. A., & Tupling, A. R. (2013b). Ablation of sarcolipin decreases the energy requirements for Ca^{2+} transport by sarco(endo)plasmic reticulum Ca^{2+}-ATPases in resting skeletal muscle. *FEBS Lett* **587**, 1687-1692.

Brandt, P. W., Diamond, M. S., Rutchik, J. S., & Schachat, F. H. (1987). Co-operative interactions between troponin-tropomyosin units extend the length of the thin filament in skeletal muscle. *J Mol Biol* **195**, 885-896.

Braz, J., Gregory, K., Pathak, A., Zhao, W., Sahin, B., Klevitsky, R., Kimball, T. F., Lorenz, J. N., Nairn, A. C., Liggett, S. B., Bodi, I., Wang, S., Schwartz, A., Lakatta, E. G., DePauoli-Roach, A. A., Robbins, J., Hewett, T. E., Bibb, J. A., Westfall, M. V., Kranias, E. G., & Molkentin, J. D. (2004). PKC-α regulates cardiac contractility and propensity toward heart failure. *Nat Med* **10**, 248-254.

Bremel, R. D. & Weber, A. (1975). Calcium binding to rabbit skeletal myosin under physiological conditions. *Biochim Biophys Acta* **376**, 366-374.

Brenner, B. (1988). Effect of Ca^{2+} on cross-bridge turnover kinetics in skinned single rabbit psoas fibers: implications for regulation of muscle contraction. *Proc Natl Acad Sci U S A* **85**, 3265-3269.

Brenner, B. (1990). Muscle mechanism and biochemical kinetics. In *Molecular mechanisms in muscular contraction*, ed. Squire, J. M., pp. 77-149. Macmillan Press Ltd, Southampton.

Brenner, B. & Eisenberg, E. (1986). Rate of force generation in muscle: correlation with actomyosin ATPase activity in solution. *Proc Natl Acad Sci U S A* **83**, 3542-3546.

Brenner, B., Schoenberg, M., Chalovich, J. M., Greene, L. E., & Eisenberg, E. (1982). Evidence for cross-bridge attachment in relaxed muscle at low ionic strength. *Proc Natl Acad Sci USA* **79**, 7288-7291.

Brito, R., Alamo, L., Lundberg, U., Guerrero, J. R., Pinto, A., Sulbarán, G., Gawinowicz, M. A., Craig, R., & Padrón, R. (2011). A molecular model of phosphorylation-based activation and potentiation of tarantula muscle thick filaments. *J Mol Biol* **414**, 44-61.

Brown, I. E. & Loeb, G. E. (1999). Measured and modeled properties of mammalian skeletal muscle. I. The effects of post-activation potentiation on the time course and velocity dependencies of force production. *J Mus Res Cell Motil* **20**, 443-456.

Bruton, J., Tavi, P., Aydin, J., Westerblad, H., & Lännergren, J. (2003). Mitochondrial and myoplasmic [Ca^{2+}] in single fibres from mouse limb muscles during repeated tetanic contractions. *J Physiol* **551**, 179-190.

Buller, A. J., Kean, C. J. C., Ranatunga, K. W., & Smith, J. M. (1981). Post-tetanic depression of twitch tension in the cat soleus muscle. *Exp Neurol* **73**, 78-89.

Campbell, K. S. & Lakie, M. (1998). A cross-bridge mechanism can explain the thixotropic short-range elastic component of relaxed frog skeletal muscle. *J Physiol* **510**, 941-962.

Campbell, K. S. & Lakie, M. (2008). Response to Bianco *et al.*: interaction forces between F-actin and titin PEVK domain measured with optical tweezers. *Biophys J* **94**, 327-328.

Capogrossi, M. C., Kaku, T., Filburn, C. R., Pelto, D. J., Hansford, R. G., Spurgeon, H. A., & Lakatta, E. G. (1990). Phorbol ester and dioctanoylglycerol stimulate membrane association of protein kinase C and have a negative inotropic effect mediated by changes in cytosolic Ca^{2+} in adult rat cardiac myocytes. *Circ Res* **66**, 1143-1155.

Caputo, C., Bolaños, P., & Gonzalez, A. (2004). Inactivation of Ca^{2+} release in amphibian and mammalian muscle fibres. *J Mus Res Cell Motil* **25**, 315-328.

Carroll, S. L., Klein, M. G., & Schneider, M. F. (1997). Decay of calcium transients after electrical stimulation in rat fast- and slow- twitch skeletal fibres. *J Physiol* **501**, 573-588.

Caterini, D., Gittings, W., Huang, J., & Vandenboom, R. (2011). The effect of work cycle frequency on the potentiation of dynamic force in mouse fast twitch skeletal muscle. *J Exp Biol* **214**, 3915-3923.

Chalovich, J. M., Chock, P. B., & Eisenberg, E. (1981). Mechanism of action of troponin•tropomyosin inhibition of actomyosin ATPase activity without inhibition of myosin binding to actin. *J Biol Chem* **256**, 575-578.

Chin, E. R. (2005). Role of Ca^{2+}/calmodulin-dependent kinases in skeletal muscle plasticity. *J Appl Physiol* **99**, 414-423.

Claflin, D. R. & Brooks, S. V. (2008). Direct observation of filing fibers in muscles of dystrophic mice provides mechanistic insight into muscular dystrophy. *Am J Physiol Cell Physiol* **294**, C651-C658.

Claflin, D. R., Morgan, D. L., & Julian, F. J. (1998). The effect of length on the relationship between tension and intracellular [Ca^{2+}] in intact frog skeletal muscle fibres. *J Physiol* **508**, 179-186.

Claflin, D. R., Morgan, D. L., Stephenson, D. G., & Julian, F. J. (1994). The intracellular Ca^{2+} transient and tension in frog skeletal muscle fibres measured with high temporal resolution. *J Physiol* **475**, 319-325.

Close, R. & Hoh, J. F. Y. (1968). Influence of temperature on isometric contractions of rat skeletal muscle. *Nature* **217**, 1179-1180.

Colpo, P., Nori, A., Sacchetto, R., Damiani, E., & Margreth, A. (2001). Phosphorylation of the triadin cytoplasmic domain by CaM protein kinase in rabbit fast-twitch muscle sarcoplasmic reticulum. *Mol Cell Biochem* **223**, 139-145.

Colyer, J. (1998). Phosphorylation states of phospholamban. *Ann N Y Acad Sci* **853**, 79-91.

Cooke, R. & Pate, E. (1985). The effects of ADP and phosphate on the contraction of muscle fibers. *Biophys J* **48**, 789-798.

Cornea, R. L., Nitu, F., Gruber, S., Kohler, K., Satzer, M., Thomas, D. D., & Fruen, B. R. (2009). FRET-based mapping of calmodulin bound to the RyR1 Ca^{2+} release channel. *Proc Natl Acad Sci U S A* **106**, 6128-6133.

Coupland, M. E., Puchert, E., & Ranatunga, K. W. (2001). Temperature dependence of active tension in mammalian (rabbit psoas) muscle fibres: effect of inorganic phosphate. *J Physiol* **536**, 879-891.

Crow, M. T. & Kushmerick, M. J. (1982). Chemical energetics of slow and fast twitch muscles of the mouse. *Journal of General Physiology* **79**, 147-166.

Curran, J., Hinton, M. J., Ríos, E., Bers, D. M., & Shannon, T. R. (2007). β-adrenergic enhancement of sarcoplasmic reticulum calcium leaks in cardiac myocytes is mediated by calcium/calmodulin-dependent protein kinase. *Circ Res* **100**, 391-398.

Dahlstedt, A. J., Katz, A., Wieringa, B., & Westerblad, H. (2000). Is creatine kinase responsible for fatigue? Studies of isolated skeletal muscle deficient in creatine kinase. *FASEB J* **14**, 982-990.

Dantzig, J. A., Goldman, Y. E., Millar, N. C., Lacktis, J., & Homsher, E. (1992). Reversal of the cross-bridge force-generating transition by photo-generation of phosphate in rabbit psoas muscle fibres. *J Physiol* **451**, 247-278.

Dawson, M. J., Gadian, D. G., & Wilkie, D. R. (1980). Mechanical relaxation rate and metabolism studied in fatiguing muscle by phosphorous nuclear magnetic resonance. *J Physiol* **299**, 465-484.

Debold, E. P. (2012). Recent insights into muscle fatigue at the cross-bridge level. *Front Physiol* **3**, 151.

Debold, E. P., Dave, H., & Fitts, R. H. (2004). Fiber type and temperature dependence of inorganic phosphate: implications for fatigue. *Am J Physiol Cell Physiol* **287**, C673-C681.

Debold, E. P., Romatowski, J., & Fitts, R. H. (2006). The depressive effect of P_i on the force-pCa relationship in skinned single muscle fibers is temperature dependent. *Am J Physiol Cell Physiol* **290**, C1041-C1050.

Decostre, V., Gillis, J. M., & Gailly, P. (2000). Effect of adrenaline on the post-tetanic potentiation in mouse skeletal muscle. *J Muscle Res Cell Motil* **21**, 254.

Diffee, G. M., Greaser, M. L., Reinach, F. C., & Moss, R. L. (1995). Effects of a non-divalent cation binding mutant of myosin regulatory light chain on tension generation in skinned skeletal muscle fibers. *Biophys J* **68**, 1443-1452.

Diffee, G. M., Patel, J. R., Reinach, F. C., Greaser, M. L., & Moss, R. L. (1996). Altered kinetics of contraction in skeletal muscle fibers containing a mutant myosin regulatory light chain with reduced divalent cation binding. *Biophys J* **71**, 341-350.

Duhamel, T. A. Role of second messenger signaling pathways in the regulation of sarcoplasmic reticulum Ca^{2+}-handling properties in the left ventricle and skeletal muscles of different fibre type composition. 2007. University of Waterloo.

Duke, A. M. & Steele, D. S. (2001a). Interdependent effects of inorganic phosphate and creatine phosphate on sarcoplasmic reticulum Ca^{2+} regulation in mechanically skinned rat skeletal muscle. *J Physiol* **531**, 729-742.

Duke, A. M. & Steele, D. S. (2001b). Mechanisms of reduced SR Ca^{2+} release induced by inorganic phosphate in rat skeletal muscle fibers. *Am J Physiol Cell Physiol* **276**, 67-82.

Dutka, T. L. & Lamb, G. D. (2004). Effect of low cytoplasmic [ATP] on excitation-contraction coupling in fast-twitch muscle fibres of the rat. *J Physiol* **560**, 451-468.

Ebashi, S. & Endo, M. (1968). Calcium ion and muscle contraction. *Prog Biophys Mol Biol* **18**, 123-183.

Endo, M. (1972). Stretch-induced increase in activation of skinned muscle fibres by calcium. *Nat New Biol* **237**, 211-213.

Fajardo, V. A., Bombardier, E., Vigna, C., Devji, T., Bloemberg, D., Gamu, D., Gramolini, A. O., Quadrilatero, J., & Tupling, A. R. (2013). Co-expression of SERCA isoforms, phospholamban and sarcolipin in human skeletal muscle fibers. *PLoS One* **8**, e84304.

Fields, R. W. (1970). Mechanical properties of the frog sarcolemma. *Biophys J* **10**, 462-479.

Fowles, J. R. & Green, H. J. (2003). Coexistence of potentiation and low-frequency fatigue during voluntary exercise in human skeletal muscle. *Can J Physiol Pharmacol* **181**, 1092-1100.

Franzini-Armstrong, C. & Protasi, F. (1997). Ryanodine receptors of striated muscles: a complex channel capable of multiple interactions. *Physiological Reviews* **77**, 699-729.

Fruen, B. R., Mickelson, J. R., Shomer, N. H., Roghair, T. J., & Louis, C. F. (1994). Regulation of the sarcoplasmic reticulum ryanodine receptor by inorganic phosphate. *J Biol Chem* **269**, 192-198.

Fryer, M. W., Owen, V. J., Lamb, G. D., & Stephenson, D. G. (1995). Effects of creating phosphate and P_i on Ca^{2+} movements and tension development in rat skinned skeletal muscle fibres. *J Physiol* **482**, 123-140.

Füchtbauer, E. M., Rowlerson, A. M., Götz, K., Friedrich, G., Mabuchi, K., Gergely, J., & Jockusch, H. (1991). Direct correlation of parvalbumin levels with myosin isoforms and succinate dehydrogenase activity on frozen sections of rodent muscle. *J Histochem Cytochem* **39**, 355-361.

Fuentes, O., Valvida, C., Vaughan, D., Coronado, R., & Valdivia, H. H. (1994). Calcium-dependent block of ryanodine receptor channel of swine skeletal muscle by direct binding of calmodulin. *Cell Calcium* **15**, 305-316.

Fujii, J., Ueno, A., Kitano, K., Tanaka, S., Kadoma, M., & Tada, M. (1987). Complete complementary DNA-derived amino acid sequence of canine cardiac phospholamban. *J Clin Invest* **79**, 301-304.

Gao, Z. H., Zhi, G., Herring, B. P., Moomaw, C., Deogny, L., Slaughter, C. A., & Stull, J. T. (1995). Photoaffinity labeling of a peptide substrate to myosin light chain kinase. *J Biol Chem* **270**, 10125-10135.

Gittings, W., Huang, J., Smith, I. C., Quadrilatero, J., & Vandenboom, R. (2011). The effect of skeletal myosin light chain kinase gene ablation on the fatigability of mouse fast muscle. *J Muscle Res Cell Motil* **31**, 337-348.

Gittings, W., Huang, J., & Vandenboom, R. (2012). Tetanic force potentiation of mouse EDL muscle is shortening speed dependent. *J Mus Res Cell Motil* **33**, 359-368.

Godt, R. E. & Lindley, B. D. (1982). Influence of temperature upon contractile activation and isometric force production in mechanically skinned muscle fibers of the frog. *J Gen Physiol* **80**, 279-297.

Goldman, Y. E. (1987). Kinetics of the actomyosin ATPase in muscle fibers. *Ann Rev Physiol* **49**, 637-654.

Gordon, A. M., Homsher, E., & Regnier, M. (2000). Regulation of contraction in striated muscle. *Physiol Rev* **80**, 853-924.

Gordon, A. M., Homsher, E., & Regnier, M. (2001). Skeletal and cardiac muscle contractile activation: Tropomyosin "Rocks and Rolls". *News Physiol Sci* **16**, 49-55.

Gordon, D. A., Enoka, R. M., & Stuart, D. G. (1990). Motor-unit force potentiation in adult cats during a standard fatigue test. *J Physiol* **421**, 569-582.

Gramolini, A., Trivieri, M. G., Oudit, G. Y., Kislinger, T., Li, W., Patel, M. M., Emili, A., Kranias, E. G., Backx, P. H., & MacLennan, D. H. (2006). Cardiac-specific overexpression of sarcolipin in phospholamban null mice impairs myocyte function that is restored by phosphorylation. *Proc Natl Acad Sc USA* **103**, 2446-2451.

Grange, R. W., Vandenboom, R., & Houston, M. E. (1993). Physiological significance of myosin phosphorylation in skeletal muscle. *Can J Appl Physiol* **18**, 229-242.

Grassie, M. E., Moffatt, L. D., Walsh, M. P., & MacDonald, J. A. (2011). The myosin phosphatase targeting protein (MYPT) family: a regulated mechanism for achieving substrate specificity of the catalytic subunit of protein phosphatase type 1σ. *Arch Biochem Biophys* **510**, 147-159.

Grynkiewicz, G., Poenie, M., & Tsien, R. Y. (1985). A new generation of Ca^{2+}-indicators with greatly improved fluorescence properties. *Journal of Biological Chemistry* **260**, 3440-3450.

Gulati, J. & Babu, A. (1985). Contraction kinetics of intact and skinned frog muscle fibers and degree of activation. *J Gen Physiol* **86**, 479-500.

Györke, I., Hester, N., Jones, L. R., & Györke, S. (2004). The role of calsequestrin, triadin, and junctin in conferring cardiac ryanodine receptor responsiveness to luminal calcium. *Biophys J* **86**, 2121-2128.

Hagemann, D., Kuschel, M., Kuramochi, T., Zhu, W., Cheng, H., & Xiao, R. P. (2000). Frequency-encoding Thr^{17} phospholamban phosphorylation is independent of Ser^{16} phosphorylation in cardiac myocytes. *J Biol Chem* **275**, 22532-22536.

Haiech, J., Derancourt, J., Pechère, J. F., & Demaille, J. G. (1979). Magnesium and calcium binding to parvalbumins: evidence for difference between parvalbumins and an explanation of their relaxing function. *Biochemistry* **18**, 2252-2258.

Hain, J., Nath, S., Maryleitner, M., Fleischer, S., & Schindler, H. (1994). Phosphorylation modulates the function of the calcium release channel of sarcoplasmic reticulum from skeletal muscle. *Biophys J* **67**, 1823-1833.

Hamada, T., Sale, D. G., MacDougall, J. D., & Tarnopolsky, M. A. (2000). Postactivation potentiation, fiber type, and twitch contraction time in human knee extensor muscles. *J.Appl.Physiol* **88**, 2131-2137.

Hanson, J. (1974). The effects of repetitive stimulation on the action potentiatl and the twitch of rat muscle. *Acta Physiol Scand* **90**, 387-400.

Hawkins, C., Xu, A., & Narayan, N. (1994). Sarcoplasmic reticulum calcium pump in cardiac and slow twitch skeletal muscle but not fast twitch skeletal muscle undergoes phosphorylation by endogenous and exogenous Ca^{2+}/calmodulin-dependent protein kinase. *Journal of Biological Chemistry* **269**, 31198-31206.

Herbst, M. (1976). Studies on the relation between latency relaxation and resting cross-bridges of frog skeletal muscle. *Pflügers Arch* **364**, 71-76.

Herrmann-Frank, A. & Varsánya, M. (1993). Enhancement of Ca^{2+} release channel activity by phosphorylation of the skeletal muscle ryanodine receptor. *FEBS Lett* **332**, 237-242.

Herzog, W., Leonard, T., Journaa, V., DuVall, M., & Panchangam, A. (2012). The three filament model of skeletal muscle stability and force production. *Mol Cell Biomech* **9**, 175-191.

Hibberd, M. G., Dantzig, J. A., Trentham, D. R., & Goldman, Y. E. (1985a). Phosphate release and force generation in skeletal muscle fibers. *Science* **228**, 1317-1319.

Hibberd, M. G., Webb, M. R., Goldman, Y. E., & Trentham, D. R. (1985b). Oxygen exchange between phosphate and water accompanies calcium-regulated ATPase activity of skinned fibers from rabbit skeletal muscle. *J Biol Chem* **260**, 3496-3500.

Hill, D. K. (1968). Tension due to interaction between sliding filaments in resting striated muscle. The effect of stimulation. *J Physiol* **199**, 637-684.

Hollingworth, S. & Baylor, S. M. (2013). Return of myoplasmic calcium (Ca) to resting levels following stimulation of fast- and slow-twitch mouse muscle fibers. *Biophys J* **104**, 291a-292a.

Hollingworth, S., Kim, M. M., & Baylor, S. M. (2012). Measurement and simulation of myoplasmic calcium transients in mouse slow-twitch muscle fibres. *J Physiol* **590**, 575-594.

Hollingworth, S., Zhao, M., & Baylor, S. M. (1996). The amplitude and time course of the myoplasmic free Ca^{2+} transient in fast-twitch fibers of mouse muscle. *J Gen Physiol* **108**, 455-469.

Holroyde, M. J., Potter, J. D., & Solaro, R. J. (1979). The calcium binding properties of phosphorylated and unphosphorylated cardiac and skeletal myosins. *J Biol Chem* **254**, 6478-6482.

Hou, T. T., Johnson, J. D., & Rall, J. A. (1992). Effect of temperature on relaxation rate and Ca^{2+}, Mg^{2+} dissociation rates from parvalbumin of frog muscle fibres. *J Physiol* **449**, 399-410.

Hou, T. T., Johnson, J. D., & Rall, J. A. (1993). Role of parvalbumin in relaxation of frog skeletal muscle. *Adv Exp Med Biol* **332**, 141-151.

Huxley, A. F. (1957). Muscle structure and theories of contraction. *Prog Biophys* **7**, 255-318.

Isaacson, A. (1969). Post-staircase potentiation, a long-lasting twitch potentiation of muscles induced by previous activity. *Life Sci* **8**, 337-342.

James, P., Inui, M., Tada, M., Chiesi, M., & Carafoli, E. (1989). Nature and site of phospholamban regulation of the Ca^{2+} pump of sarcoplasmic reticulum. *Nature* **342**, 90-92.

Kellermayer, M. S. Z., Bianco, P., Mártonfalvi, Z., Nagy, A., Kengyel, A., Szatmári, D., Huber, T., Linari, M., Caremani, M., & Lombardi, V. (2008). Muscle thixotropy: more than just cross-bridges? Response to comment by Campbell and Lakie. *Biophys J* **94**, 329-330.

Kellermayer, M. S. Z., Smith, S. B., Bustamante, C., & Granzier, H. L. (2001). Mechanical fatigue in repetitively stretched single molecules of titin. *Biophys J* **80**, 852-863.

Kerrick, W. G. L. & Xu, Y. (2004). Inorganic phosphate affects the pCa-force relationship more than the pCa-ATPase by increasing the rate of dissociation of force generating cross-bridges in skinned fibers from both EDL and soleus muscles of the rat. *J Mus Res Cell Motil* **25**, 107-117.

Klug, G. A., Botterman, B. R., & Stull, J. T. (1982). The effect of low frequency stimulation on myosin light chain phosphorylation in skeletal muscle. *J Biol Chem* **257**, 4688-4690.

Konishi, M., Hollingworth, S., Harkins, A. B., & Baylor, S. M. (1991). Myoplasmic calcium transients in intact frog skeletal muscle fibers monitored with the fluorescent indicator furaptra. *J Gen Physiol* **97**, 271-301.

Konishi, M., Suda, N., & Kurihara, S. (1993). Fluorescence signals from the Mg^{2+}/Ca^{2+} indicator furaptra in frog skeletal muscle fibers. *Biophys J* **64**, 223-239.

Koss, K. L. & Kranias, E. G. (1996). Phospholamban: A prominent regulator of myocardial contractility. *Circ Res* **79**, 1059-1063.

Kovacs, R. J. & Szucs, G. (1983). Effect of caffeine on intramembrane charge movement and calcium transients in cut skeletal muscle fibres of the frog. *J Physiol* **341**, 559-578.

Krarup, C. (1981). Temperature dependence of enhancement and diminution of tension evoked by staircase and by tetanus in rat muscle. *J Physiol* **311**, 373-387.

Laemmli, U. K. (1970). Cleavage of structural proteins during the assembly of the head of the bacteriophage. *Nature* **227**, 680-685.

Lakie, M., Walsh, E. G., & Wright, G. W. (1984). Resonance at the wrist demonstrated by the use of a torque motor: an instrumental analysis of muscle tone in man. *J Physiol* **353**, 265-285.

Lamb, G. D., Junankar, P. R., & Stephenson, D. G. (1995). Raised intracellular $[Ca^{2+}]$ abolishes excitatino-contraction coupling in skeletal muscle fibres of rat and toad. *489* **(Pt 2)**, 362.

Lancel, S., Zhang, J., Evangelista, A., Trucillo, M. P., Tong, X., Siwik, D. A., Cohen, R. A., & Colucci, W. S. (2009). Nitroxyl activates SERCA in cardiac myocytes via glutathiolation of cysteine 674. *Circ Res* **104**, 720-723.

Laver, D. R., Lenz, G. K., & Lamb, G. D. (2001). Regulation of the calcium release channel from rabbit skeletal muscle by the nucleotides ATP, AMP, IMP and adenosine. *J Physiol* **537**, 763-778.

Lednev, V. V. & Malinchik, S. B. (1981). Partial activation of thin filaments in resting frog skeletal muscle fibers. *Biofizika* **26**, 366-368.

Lee, R. S., Tikunova, S. B., Kline, K. P., Zot, H. G., Hasbun, J. E., Minh, N. V., Swartz, D. R., Rall, J. A., & Davis, J. P. (2010). Effect of Ca^{2+} binding properties of troponin C on rate of skeletal muscle force redevelopment. *Am J Physiol Cell Physiol* **299**, C1091-C1099.

Lehrer, SS. (2011). The 3-state model of muscle regulation revisited: is a fourth state involved? *J Mus Res Cell Motil* **32**, 203-208.

Levine, R. J., Kensler, R. W., Yang, Z., Stull, J. T., & Sweeney, H. L. (1996). Myosin light chain phosphorylation affects the structure of rabbit skeletal muscle thick filaments. *Biophys J* **71**, 898-907.

Ma, J., Gutiérrez, L. M., Hosey, M. M., & Ríos, E. (1992). Dihydropyridine-sensitive skeletal muscle Ca channels in polarized planar bilayers 3. Effects of phosphorylation by protein kinase C. *Biophys J* **63**, 639-647.

MacDonald, W. A. & Stephenson, D. G. (2001). Effect of ADP on sarcoplasmic reticulum function in mechanically skinned skeletal muscle fibres of the rat. *J Physiol* **532**, 499-508.

MacIntosh, B. R. & Gardiner, P. F. (1987). Posttetanic potentiation and skeletal muscle fatigue: interactions with caffeine. *Can J Physiol Pharmacol* **65**, 260-268.

MacIntosh, B. R. & Kupsh, C. C. (1987). Staircase, fatigue, and caffeine in skeletal muscle in situ. *Muscle Nerve* **10**, 717-722.

MacIntosh, B. R., Smith, M. J., & Rassier, D. E. (2008). Staircase but not posttetanic potentiation in rat muscle after spinal cord hemisection. *Muscle Nerve* **38**, 1455-1465.

MacLennan, D. H. & Kranias, E. G. (2003). Phospholamban: A crucial regulator of cardiac contractility. *Nature Rev Mol Cell Biol* **4**, 566-577.

MacLennan, D. H., Rice, W. J., & Green, N. M. (1997). The mechanism of Ca^{2+} transport by sarco(endo) plasmic reticulum Ca^{2+}-ATPases. *Journal of Biological Chemistry* **272**, 28815-28818.

Mahaney, J. E., Autry, J. M., & Jones, L. R. (2000). Kinetic studies of the cardiac Ca-ATPase expressed in Sf21 cells: New insights on Ca-ATPase regulation by phospholamban. *Biophys J* **78**, 1306-1323.

Manning, D. R. & Stull, J. T. (1982). Myosin light chain phosphorylation-dephosphorylation in mammalian skeletal muscle. *Am J Physiol Cell Physiol* **242**, C234-C241.

Månsson, A., Mörner, J., & Edman, K. A. (1989). Effects of amrinone on twitch, tetanus and shortening kinetics in mammalian skeletal muscle. *Acta Physiol Scand* **136**, 37-45.

Martyn, D. A. & Gordon, A. M. (1992). Force and stiffness in glycerinated rabbit psoas fibers. Effects of calcium and elevated phosphate. *J Gen Physiol* **99**, 795-816.

Maruyama, K. (1997). Connectin/titin, giant elastic protein of muscle. *FASEB J* **11**, 341-345.

Mason, P. (1977). Dynamic stiffness and crossbridge action in muscle. *Biophys Struct Mech* **4**, 15-25.

Masuda, H. & De Meis, L. (1977). Effect of temperature on the Ca^{2+} transport ATPase of sarcoplasmic reticulum. *J Biol Chem* **252**, 8567-8571.

Maytum, R., Lehrer, SS., & Geeves, M. A. (1999). Cooperativity and switching within the three-state model of muscle regulation. *Biochemistry* **38**, 1102-1110.

McKillop, D. F. & Geeves, M. A. (1993). Regulation of the interaction between actin and myosin subfragment 1: evidence for three states of the thin filament. *Biophys J* **65**, 693-701.

Meissner, G. (1984). Adenine nucleotide stimulation of Ca^{2+}-induced Ca^{2+} release in sarcoplasmic reticulum. *Journal of the Biological Society* **259**, 2365-2374.

Meissner, G. (2004). NADH, a new player in the cardiac ryanodine receptor. *Circ Res* **94**, 418-419.

Meissner, G., Darling, E., & Eveleth, J. (1986). Kinetics of rapid Ca^{2+} release by sarcoplasmic reticulum. Effects of Ca^{2+}, Mg^{2+}, adenine nucleotides. *Biochemistry* **25**, 236-244.

Meissner, G. & Lu, X. (1995). Dihydropyrdine receptor-ryanodine receptor interactions in skeletal muscle excitation-contraction coupling. *Biosci Rep* **15**, 399-408.

Metzger, J. M. & Fitts, R. H. (1987). Role of intracellular pH in muscle fatigue. *J Appl Physiol* **62**, 1392-1397.

Millar, N. C. & Homsher, E. (1990). The effect of phosphate and calcium on force generation in glycerinated rabbit skeletal muscle fibers; a steady-state and transient kinetic study. *J Biol Chem* **265**, 20234-20240.

Millman, B. M. (1998). The filament lattice of striated muscle. *Physiol Rev* **78**, 359-391.

Moore, R. L., Houston, M. E., Iwamoto, G. A., & Stull, J. T. (1985). Phosphorylation of rabbit skeletal muscle myosin in situ. *J Cell Physiol* **125**, 301-305.

Moore, R. L., Palmer, B. M., Williams, S. L., Tanabe, H., Grange, R. W., & Houston, M. E. (1990). Effect of temperature on myosin phosphorylation in mouse skeletal muscle. *Am J Physiol* **259**, C432-C438.

Moore, R. L. & Stull, J. T. (1984). Myosin light chain phosphorylation in fast and slow skeletal muscles in situ. *Am J Physiol* **247**, C462-C471.

Moorhead, G., Johnson, D., Morrice, N., & Cohen, P. (1998). The major myosin phosphatase in skeletal muscle is a complex between the β–isoform of protein phosphatase 1 and the MYPT2 gene product. *FEBS Lett* **438**, 141-144.

Morgan, D. L., Claflin, D. R., & Julian, F. J. (1997). The relationship between tension and slowly varying intracellular calcium concentratino in intact frog skeletal muscle. *J Physiol* **500**, 177-192.

Morgan, M., Perry, V. S., & Ottaway, J. (1976). Myosin light-chain phosphatase. *Biochem J* **157**, 687-697.

Movsesian, M. A., Nishikawa, M., & Adelstein, R. S. (1984). Phosphorylation of phospholamban by calcium-activated, phospholipid-dependent protein kinase. *J Biol Chem* **259**, 8029-8032.

Mundiña-Weilenmann, C., Chang, C. F., Gutierrez, L. M., & Hosey, M. M. (1991). Demonstration of the phosphorylation of dihydropyridine-sensitive calcium channels in chick skeletal muscle and the resultant activation of the channels after reconstitution. *J Biol Chem* **266**, 4067-4073.

Murphy, R. M., Larkins, N. T., Mollica, J. P., Beard, N. A., & Lamb, G. D. (2009). Calsequestrin content and SERCA determine normal and maximal Ca^{2+} storage levels in sarcoplasmic reticulum of fast- and slow-twitch fibres of the rat. *J Physiol* **587**, 443-460.

Nishikawa, K. C., Monroy, J. A., Uyeno, T. E., Yeo, S. H., Pai, D. K., & Linstedt, S. L. (2012). Is titin a 'winding filament'? A new twist on muscle contraction. *Proc Biol Sci* **279**, 981-990.

O'Callahan, C. M., Ptasienski, J., & Hosey, M. M. (1988). Phosphorylation of the 165-kDa dihydropyridine/phenylalkylamine receptor from skeletal muscle by protein kinase c. *J Biol Chem* **263**, 17342-17349.

Odermatt, A., Becker, S., Khanna, V. K., Kuryzydlowski, K., Leisner, E., Pette, D., & MacLennan, D. H. (1998). Sarolipin regulates the activity of SERCA 1, the fast twitch skeletal muscle sarcoplasmic reticulum Ca^{2+}-ATPase. *Journal of Biological Chemistry* **273**, 12360-12369.

Odermatt, A., Kurzydlowski, K., & MacLennan, D. H. (1996). The Vmax of the Ca^{2+}-ATPase of cardiac sarcoplasmic reticulum (SERCA 2a) is not altered by Ca^{2+}/calmodulin-dependent phosphorylation or by interaction with phospholamban. *Journal of Biological Chemistry* **271**, 14206-14213.

Odermatt, A., Taschner, P. E. M., Scherer, S. W., Beatty, B., Khanna, V.-K., Cornblath, D. R., Chaudhry, D. R., Lee, W. C., Schrank, B., Karpati, G., & et al (1997). Characterization of the gene encoding human sarcolipin (SLN), a proteolipid associated with SERCA 1: absence of structural mutations in five patients with Brody disease. *Genomics* **45**, 541-553.

Oliver, A. E., Baker, G. A., Fugate, R. D., Tablin, F., & Crowe, J. H. (2000). Effects of temperature on calcium-sensitive fluorescent probes. *Biophys J* **78**, 2116-2126.

Palmer, S. & Kentish, J. C. (1994). The role of troponin C in modulating the Ca^{2+} sensitivity of mammalian skinned cardiac and skeletal muscle fibres. *J Physiol* **480**, 45-60.

Parry, D. J. & DiCori, S. (1990). The relationship between post-tetanic potentiation of motor units and myosin isoforms in mouse soleus muscle. *Can J Physiol Pharmacol* **68**, 51-56.

Patel, J. R., Diffee, G. M., Huang, X. P., & Moss, R. L. (1998). Phosphorylation of myosin regulatory light chain eliminates force-dependent changes in relaxation rates in skeletal muscle. *Biophys J* **74**, 360-368.

Persechini, A., Stull, J. T., & Cooke, R. (1985). The effect of myosin phosphorylation on the contractile properties of skinned rabbit skeletal muscle fibers. *J Biol Chem* **260**, 7951-7954.

Podolsky, R. J. (1964). The maximum sarcomere legnth for contraction of isolated myofibrils. *J Physiol (London)* **170**, 110-123.

Poledna, J. & Morad, M. (1983). Effect of caffeine on the birefringence signal in single skeletal muscle fibers and mammalian heart. *Pfluegers Arch* **397**, 184-189.

Posterino, G. S., Cellini, M. A., & Lamb, G. D. (2003). Effects of oxidation and cytosolic redox conditions on excitation-contraction coupling in rat skeletal muscle. *J Physiol* **547**, 807-823.

Posterino, G. S. & Lamb, G. D. (2003). Effect of sarcoplasmic reticulum Ca^{2+} content on action potential-induced Ca^{2+} release in rat skeletal muscle fibres. *J Physiol* **551**, 219-237.

Potter, J. D. & Gergely, J. (1975). The calcium and magnesium binding sites on troponin and their role in the regulation of myofibrillar adenosine triphosphatase. *J Biol Chem* **250**, 4628-4633.

Prosser, B. L., Hernández-Ochoa, E. O., & Schneider, M. F. (2011). S100A1 and calmodulin regulation of ryanodine receptor in striated muscle. *Cell Calcium* **50**, 323-331.

Puglisi, J. L., Bassani, R. A., Bassani, J. W. M., Amin, J. M., & Bers, D. M. (1996). Temperature and relative contributions of Ca transport systems in cardiac myocyte relaxation. *Am J Physiol* **270**, H1772-H1778.

Qin, F., Siwik, D. A., Lancel, S., Zhang, J., Kuster, G. M., Luptak, I., Wang, L., Tong, X., Kang, J., Cohen, R. A., & Colucci, W. S. (2013). Hydrogen peroxide-mediated SERCA cysteine 674 oxidation contributes to impaired cardiac myocyte relaxation in senescent mouse heart. *J Am Heart Assoc* **2**, e000184.

Raju, B., Murphy, E., Levy, L. A., Hall, R. D., & London, R. E. (1989). A fluorescent indicator for measuring cytosolic free magnesium. *Am J Physiol* **256**, C540-C548.

Rapoport, S. I. (1972). Mechanical properties of the sarcolemma and myoplasm in frog muscle as a function of sarcomere length. *J Gen Physiol* **59**, 559-585.

Rassier, D. E. & MacIntosh, B. R. (1999). Length dependence of staircase potentiation: interactions with caffeine and dantrolene sodium. *Can J Physiol Pharmacol* **78**, 350-357.

Rassier, D. E. & MacIntosh, B. R. (2000). Co-existence of potentiation and fatigue in skeletal muscle. *Braz.J.Med.Biol.* **33**, 499-508.

Rassier, D. E. & MacIntosh, B. R. (2002). Sarcomere length-dependence of activity-dependent twitch potentiation in mouse skeletal muscle. *BMC Physiol* **10**, 19.

Rassier, D. E., Tubman, L. A., & MacIntosh, B. R. (1997). Inhibition of Ca^{2+} release in rat atrophied gastrocnemius muscle. *Exp Physiol* **82**, 665-676.

Rassier, D. E., Tubman, L. A., & MacIntosh, B. R. (1998). Caffeine and length dependence of staircase potentiation in skeletal muscle. *Can J Physiol Pharmacol* **76**, 975-982.

Rassier, D. E., Tubman, L. A., & MacIntosh, B. R. (1999). Staircase in mammalian muscle without light chain phosphorylation. *Braz J Med Biol Res* **32**, 121-129.

Ratkevicius, A., Skurvydas, A., & Lexell, J. (1995). Submaximal-exercise-induced impairment of human muscle to develop and maintain force at low frequencies of electrical stimulation. *Eur J Physiol* **70**, 294-300.

Richter, E. A., Nielsen, J. N., Jørgensen, S. B., Frøsig, C., Birk, J. B., & Wojtaszewski, J. F. P. (2004). Exercise signalling to glucose transport in skeletal muscle. *Proc Nutr Soc* **63**, 211-216.

Robertson, S. P., Johnson, J. D., & Potter, J. D. (1981). The time-course of Ca^{2+}-exchange with calmodulin, troponin, parvalbumin and myosin in response to transient increases in Ca^{2+}. *Biophys J* **34**, 559-569.

Roof, S. R., Shannon, T. R., Janssen, P. M. L., & Ziolo, M. T. (2011). Effects of increased systolic Ca^{2+} and phospholamban phosphorylation during β-adrenergic stimulation on Ca^{2+} transients kinetics in cardiac myocytes. *Am J Physiol Heart Circ Physiol* **301**, H1570-H1578.

Rose, A. J., Kiens, B., & Richter, E. A. (2006). Ca^{2+}-calmodulin-dependent protein kinase expression and signalling in skeletal muscle during exercise. *J Physiol* **574**, 889-903.

Rosser, J. I., Walsh, B., & Hogan, M. C. (2009). Effect of physiological levels of caffeine on Ca^{2+} handling and fatigue development in *Xenopus* isolated single myofibers. *Am J Physiol Regul Integr Comp Physiol* **296**, R1512-R1517.

Ryder, J. W., Lau, K. S., Kamm, K. E., & Stull, J. T. (2007). Enhanced skeletal muscle contraction with myosin light chain phosphorylation by a calmodulin-sensing kinase. *J Biol Chem* **282**, 20447-20454.

Sacchetto, R., Bovo, E., & Damiani, E. (2005). The Ca^{2+}-calmodulin dependent protein kinase II system of skeletal muscle sarcoplasmic reticulum. *Basic Appl Myol* **15**, 5-17.

Sacchetto, R., Turcato, F., Damiani, E., & Margreth, A. (1999). Interaction of triadin with the histidine-rich Ca^{2+}-binding protein at the triadic junction in skeletal muscle fibers. *J Mus Res Cell Motil* **20**, 403-415.

Sahin, B., Shu, H., Fernandez, J., El-Armouche, A., Molkentin, J. D., Nairn, A. C., & Bibb, J. A. (2006). Phosphorylation of protein phosphatase inhibitor-1 by protein kinase c. *J Biol Chem* **281**, 24322-24335.

Sahoo, S. K., Shaikh, S. A., Sopariwala, D. H., Bal, N. C., & Periasamy, M. (2013). Sarcolipin protein interaction with sarco(endo)plasmic reticulum Ca^{2+} ATPase (SERCA) is distinct from phospholamban protein and only sarcolipin can promote uncoupling of the SERCA pump. *J Biol Chem* **288**, 6881-6889.

Sandow, A. (1944). Studies on the latent period of muscular contraction. Method. General properties of latency relaxation. *J Cell Comp Physiol* **24**, 221-256.

Sandow, A. (1947). Latency relaxation and a theory of muscular mechano-chemical coupling. *Annals of the New York Academy of Sciences* **47**, 895-929.

Schiaffino, S. & Reggiani, C. (2011). Fiber types in mammalian skeletal muscles. *Physiol Rev* **91**, 1447-1531.

Schneider, J. S., Shanmugam, M., Gonzalez, J. P., Lopez, H., Gordon, R., Fraidenraich, D., & Babu, G. J. (2013). Increased sarcolipin expression and decreased sarco(endo)plasmic reticulum Ca^{2+} uptake in skeletal muscles of mouse models of Duchenne muscular dystrophy. *J Mus Res Cell Motil* **34**, 349-356.

Schneider, M. F. & Simon, B. J. (1988). Inactivation of calcium release from the sarcoplasmic reticulum in frog skeletal muscle. *J Physiol* **405**, 727-745.

Schoenberg, M. (1988). Characterization of the myosin adenosine triphosphate (M•ATP) crossbridge in rabbit and frog skeletal muscle fibers. *Biophys J* **54**, 135-148.

Shirokova, N. & Ríos, E. (1996). Activation of Ca^{2+} release by cafffeine and voltage in frog skeletal muscle. *J Physiol* **493**, 317-339.

Siemankowski, R. F., Wiseman, M. O., & White, H. D. (1985). ADP dissociation from actomyosin subfragment 1 is sufficiently slow to limit the unloaded shortening velocity in vertebrate muscle. *Proc Natl Acad Sci U S A* **82**, 662.

Simon, B. J., Klein, M. G., & Schneider, M. F. (1989). Caffeine slows turn-off of calcium release in voltage clamped skeletal muscle fibers. *Biophys J* **55**, 793-797.

Simon, B. J., Klein, M. G., & Schneider, M. F. (1991). Calcium dependent inactivation of calcium release from sarcoplasmic reticulum in skeletal muscle fibers. *Journal of General Physiology* **97**, 437-471.

Slack, J. P., Grupp, I. L., Ferguson, D. G., Rosenthal, N., & Kranias, E. G. (1997). Ectopic expression of phospholamban in fast-twitch skeletal muscle alters sarcoplasmic reticulum Ca^{2+}transport and muscle relaxation. *J Biol Chem* **272**, 18862-18868.

Smith, I. C., Bombardier, E., Vigna, C., & Tupling, A. R. (2013a). ATP consumption by sarcoplasmic reticulum Ca^{2+} pumps accounts for 40-50% of resting metabolic rate in mouse fast and slow twitch muscle. *PLoS One* **8**, e68924.

Smith, I. C., Gittings, W., Huang, J., McMillan, E. M., Quadrilatero, J., Tupling, A. R., & Vandenboom, R. (2013b). Potentiation in mouse lumbrical muscle without myosin light chain phosphorylation: is resting calcium responsible? *J Gen Physiol* **141**, 297-308.

Smith, I. C., Huang, J., Quadrilatero, J., Tupling, A. R., & Vandenboom, R. (2010). Posttetanic potentiation in *mdx* muscle. *J Mus Res Cell Motil* **31**, 267-277.

Steeghs, K., Benders, A., Oerlemans, F., de Haan, A., Heerschap, A., Ruitenbeek, W., Jost, C., Van Deursen, J., Perryman, D., Pette, D., Bruckwilder, M., Koudijs, J., Jap, P., Veerkamp, J., & Weiringa, B. (1997). Altered Ca^{2+} responses in muscles with combined mitochondrial and cytosolic creatine kinase deficiencies. *Cell* **89**, 93-103.

Steele, D. S. & Duke, A. M. (2003). Metabolic factors contributing to altered Ca^{2+} regulation in skeletal muscle fatigue. *Acta Physiol Scand* **179**, 39-48.

Stein, R. B., Gordon, T., & Shriver, J. (1982). Temperature dependence of mammalian muscle contractions and ATPase activities. *Biophys J* **40**, 97-107.

Stienen, G. J., van Graas, I. A., & Elzinga, G. (1993). Uptake and caffeine-induced release of calcium in fast muscle fibers of Xenopus laevis: effects of MgATP and P_i. *Am J Physiol* **265**, C650-C657.

Stull, J. T., Kamm, K. E., & Vandenboom, R. (2011). Myosin light chain kinase and the role of myosin light chain phosphorylation in skeletal muscle. *Arch Biochem Biophys* **510**, 120-128.

Stull, J. T., Krueger, J. K., Kamm, K. E., Gao, Z., Zhi, G., & Padre, R. (1996). Myosin light chain kinase. In *Biochemistry of Smooth Muscle Contraction*, ed. Bárany, M., pp. 119-130. Elselvier.

Sun, Q. A., Hess, D. T., Nogueira, L., Yong, S., Bowles, D. E., Eu, J., Laurita, K. R., Meissner, G., & Stamler, J. S. (2011). Oxygen-coupled redox regulation of the skeletal muscle ryanodine receptor-Ca^{2+} release channel by NADPH oxidase 4. *Proc Natl Acad Sci U S A* **108**, 16098-16103.

Sweeney, H. L., Bowman, B. M., & Stull, J. T. (1993). Myosin light chain phosphorylation in vertebrate striated muscle: regulation and function. *Am J Physiol* **264**, C1085-C1095.

Sweeney, H. L. & Kushmerick, M. J. (1985). Myosin phosphorylation in permeablized rabbit psoas fibers. *Am J Physiol* **249**, C362-C365.

Sweeney, H. L. & Stull, J. T. (1986). Phosphorylation of myosin in permeablized mammalian cardiac and skeletal muscle cells. *Am J Physiol* **250**, C657-C660.

Sweeney, H. L. & Stull, J. T. (1990). Alteration of cross-bridge kinetics by myosin light chain phosphorylation in rabbit skeletal muscle: implications for regulation of actin-myosin interaction. *Proc Natl Acad Sci U S A* **87**, 414-418.

Takagi, Y., Shuman, H., & Goldman, Y. E. (2004). Coupling between phosphate release and force generation in muscle actomyosin. *Philos Trans R Soc Lond B Biol Sci* **359**, 1913-1920.

Tidball, J. G. (1986). Energy stored and dissipated in skeletal muscle basement membranes during sinusoidal oscillations. *Biophys J* **50**, 1127-1138.

Tohtong, R., Yamashita, H., Graham, M., Haeberle, J., Simcox, A., & Maughan, D. (1995). Impairment of muscle function caused by mutations of phosphorylation sites in myosin regulatory light chain. *Nature* **374**, 650-653.

Toyofuku, T., Kurzydlowski, K., Tada, M., & MacLennan, D. H. (1993). Identifications of regions in the Ca^{2+}-ATPase of sarcoplasmic reticulum that affect functional association with phospholamban. *J Biol Chem* **268**, 2809-2815.

Toyoshima, C., Asahi, M., Sugita, Y., Khanna, R., Tsuda, T., & MacLennan, D. H. (2003). Modeling of the inhibitory interaction of phospholamban with the Ca^{2+} ATPase. *Proc Natl Acad Sci U S A* **100**, 467-472.

Tripathy, A., Xu, L., Mann, G., & Meissner, G. (1995). Calmodulin activation and inhibition of skeletal muscle Ca^{2+} release channel (ryanodine receptor). *Biophys J* **69**, 106-119.

Tubman, L. A., Rassier, D. E., & MacIntosh, B. R. (1996). Absence of myosin light chain phosphorylation and twitch potentiation in atrophied skeletal muscle. *Can J Physiol Pharmacol* **74**, 723-728.

Tubman, L. A., Rassier, D. E., & MacIntosh, B. R. (1997). Attenuation of myosin light chain phosphorylation and posttetanic potentiation in atrophied skeletal muscle. *Pfluegers Arch* **434**, 848-851.

Tupling, A. R. (2004). The sarcoplasmic reticulum in muscle fatigue adn disease: Role of the sarco(endo)plasmic reticulum Ca^{2+}-ATPase. *Can J Appl Physiol* **29**, 308-329.

Tupling, A. R. (2009). The decay phase of Ca^{2+}-transients in skeletal muscle: regulation and physiology. *Appl Physiol Nutr Metab* **34**, 368-372.

Tupling, A. R., Asahi, M., & MacLennan, D. H. (2002). Sarcolipin overexpression in rat slow twitch muscle inhibits sarcoplasmic reticulum Ca^{2+}-uptake and impairs contractile function. *J Biol Chem* **277**, 44740-44746.

Tupling, A. R., Bombardier, E., Gupta, S. C., Hussain, D., Vigna, C., Bloemberg, D., Quadrilatero, J., Trivieri, M. G., Babu, G. J., Backx, P. H., Periasamy, M., MacLennan, D. H.,

& Gramolini, A. O. (2011). Enhanced Ca^{2+} transport and muscle relaxation in skeletal muscle from sarcolipin-null mice. *Am J Physiol Cell Physiol* **301**, C841-C849.

Tupling, A. R., Vigna, C., Ford, R. J., Tsuchiya, S. C., Graham, D. A., Denniss, S. G., & Rush, J. W. E. (2007). Effects of buthionine sulfoximine treatment on diaphragm contractility and SR Ca^{2+} pump function in rats. *J Appl Physiol* **103**, 1921-1928.

Vandenboom, R., Claflin, D. R., & Julian, F. J. (1998). Effects of rapid shortening on rate of force regeneration and myoplasmic [Ca^{2+}] in intact frog skeletal muscle fibers. *J Physiol* **511**, 171-180.

Vandenboom, R., Gittings, W., Smith, I. C., Grange, R. W., & Stull, J. T. (2013). Myosin phosphorylation and force potentiation in skeletal muscle: evidence from animal models. *J Mus Res Cell Motil* **34**, 317-332.

Vandenboom, R., Grange, R. W., & Houston, M. E. (1995). Myosin phosphorylation enhances rate of force development in fast-twitch skeletal muscle. *Am J Physiol* **268**, C596-C603.

Vandenboom, R., Hannon, J. D., & Sieck, G. C. (2002). Isotonic Force Modulates Force Redevelopment Rate of Intact Frog Skeletal Muscle Fibers: Evidence for Cross-Bridge Induced Thin Filament Activation. *Journal of Physiology* **543**, 555-566.

Vandenboom, R. & Houston, M. E. (1996). Phosphorylation of myosin and twitch potentiation in fatigued skeletal muscle. *Can J Physiol Pharmacol* **74**, 1315-1321.

Vandenboom, R., Xeni, J., Bestic, N. M., & Houston, M. E. (1997). Increased force development rates of fatigued mouse skeletal muscle are graded to myosin light chain phosphate content. *Am J Physiol Regul Integr Comp Physiol* **272**, 1980-1984.

Vangheluwe, P., Schuermans, M., Zador, E., Waelkens, E., Raeymakers, L., & Wuytack, F. (2005). Sarcolipin and phospholamban mRNA and protein expression in cardiac and skeletal muscle of different species. *Biochem J* **389**, 151-159.

Vikhoreva, N. N. & Månsson, A. (2010). Regulatory light chains modulate in vitro actin motility driven by skeletal heavy meromyosin. *Biochem Biophys Res Commun* **403**, 1-6.

Vøllestad, N. K., Sejersted, I., & Saugen, E. (1997). Mechanical behavior of skeletal muscle during intermittent voluntary isometric contractions in humans. *J Appl Physiol* **83**, 1557-1565.

Wakabayashi, K., Sugimoto, Y., Tanaka, H., Ueno, Y., Takezawa, Y., & Amemiya, Y. (1994). X-ray diffraction evidence for the extensibility of actin and myosin filaments during muscle contraction. *Biophys J* **67**, 2422-2435.

Walker, S. M. (1951). Failure of potentiation in successive, posttetanic, and summated twitches in cooled skeletal muscle of the rat. *Am J Physiol* **166**, 480-484.

Wang, J. & Best, P. M. (1992). Inactivation of the sarcoplasmic reticulum calcium channel by protein kinase. *Nature* **359**, 739-741.

Wang, K., McCarter, R., Wright, J., Beverly, J., & Ramirez-Mitchell, R. (1991). Regulation of skeletal muscle stiffness and elasticity by titin isoforms: a test of segmental extension model of resting tension. *Proc Natl Acad Sci U S A* **88**, 7101-7105.

Wang, K., McClure, J., & Tu, A. (1979). Titin: major myofibrillar components of striated muscle. *76* **8**, 3702.

Wang, Y. & Kerrick, W. G. (2002). The off rate of Ca^{2+} from troponin C is regulated by force-generating cross bridges in skeletal muscle. *J Appl Physiol* **92**, 2409-2418.

Weber, A. (1968). The mechanism of the action of caffeine on sarcoplasmic reticulum. *J Gen Physiol* **52**, 760-772.

Wegener, A. D., Simmerman, H. K., Lindemann, J. P., & Jones, L. R. (1989). Phospholamban phosphorylation in intact ventricles. Phosphorylation of serine 16 and threonine 17 in response to beta-adrenergic stimulation. *J Biol Chem* **264**, 11468-11474.

Wendt, I. R. & Stephenson, D. G. (1983). Effects of caffeine on Ca-activated force production in skinned cardiac and skeletal muscle fibres of the rat. *Pfluegers Arch* **398**, 210-216.

Westerblad, H. & Allen, D. (1993). The contribution of $[Ca^{2+}]_i$ to the slowing of relaxation in fatigued single fibres from mouse skeletal muscle. *Journal of Physiology* **468**, 729-740.

Westerblad, H. & Allen, D. G. (1991). Changes in myoplasmic calcium concentration during fatigue in single mouse muscle fibers. *Journal of General Physiology* **98**, 615-635.

Westerblad, H. & Allen, D. G. (1992a). Changes of intracellular pH due to repetitive stimulation of single fibres from mouse skeletal muscle. *J Physiol* **453**, 413-434.

Westerblad, H. & Allen, D. G. (1992b). Myoplasmic free Mg^{2+} concentration during repetitive stimulation of single fibres from mouse skeletal muscle. *J Physiol* **453**, 413-434.

Westerblad, H. & Allen, D. G. (1996). The effects of intracellular injections of phosphate on intracellular calcium and force in single muscle fibres of mouse skeletal muscle. *Pflügers Arch* **431**, 964-970.

Westerblad, H., Dahlstedt, A. J., & Lännergren, J. (1998). Mechanisms underlying reduced maximum shortening velocity during fatigue of intact, single fibres of mouse muscle. *J Physiol* **510**, 269-277.

Wu, K. D. & Lytton, J. (1993). Molecular cloning and quantification of sarcoplasmic reticulum Ca^{2+}-ATPase isoforms in rat muscles. *Am J Physiol Cell Physiol* **238**, C56-C61.

Xeni, J., Gittings, W., Caterini, D., Huang, J., Houston, M. E., Grange, R. W., & Vandenboom, R. (2011). Myosin light-chain phosphorylation and potentiation of dynamic function in mouse fast muscle. *Pflügers Arch* **462**, 349-358.

Yagi, N. (2003). An X-ray diffraction study on early structural changes in skeletal muscle contraction. *Biophys J* **92**, 162-171.

Yagi, N. (2011). Mechanism of latency relaxation in frog skeletal muscle. *Prog Biophys Mol Biol* **105**, 180-186.

Yagi, N. & Matsubara, I. (1980). Myosin heads do not move on activation in highly stretched vertebrate striated muscle. *Science* **207**, 307-308.

Yang, Z., Stull, J. T., Levine, R. J., & Sweeney, H. L. (1998). Changes in interfilament spacing mimic the effects of myosin regulatory light chain phosphorylation in rabbit psoas fibers. *J Struct Biol* **122**, 139-148.

Zhang, H., Zhang, J. Z., Danila, C. I., & Hamilton, S. L. (2003). A noncontiguous, intersubunit binding site for calmodulin on the skeletal muscle Ca^{2+} release channel. *J Biol Chem* **278**, 8348-8355.

Zhao, F. Q. & Craig, R. (2003). Ca^{2+}causes release of myosin heads from the thick filament surface on the milliseconds time scale. *J Mol Biol* **327**, 145-158.

Zhao, F. Q. & Craig, R. (2008). Millisecond time-resolved changes occurring in Ca^{2+}-regualted myosin filaments upon relaxation. *J Mol Biol* **381**, 256-260.

Zhao, M., Hollingworth, S., & Baylor, S. M. (1996). Properties of tri- and tetracarboxylate Ca^{2+} indicators in frog skeletal muscle. *Biophys J* **70**, 896-916.

Zhao, M., Hollingworth, S., & Baylor, S. M. (1997). AM-loading of fluorescent Ca^{2+} indicators into intact singel fibers of frog muscle. *Biophys J* **72**, 2736-2747.

Zhao, Y. & Kawai, M. (1994). Kinetic and thermodynamic studies of the cross-bridge cycle in rabbit psoas muscle fibers. *Biophys J* **67**, 1655-1668.

Zhi, G., Ryder, J. W., Huang, J., Ding, P., Chen, Y., Zhao, Y., Kamm, K. E., & Stull, J. T. (2005). Myosin light chain kinase and myosin phosphorylation effect frequency-dependent potentiation of skeletal muscle contraction. *Proc Natl Acad Sci U S A* **102**, 17519-17524.